INTEGRATION OF GRID CONNECTED PHOTOVOLTAIC SYSTEM WITH ACTIVE POWER FILTERING FUNCTIONALITY

Thesis

submitted in partial fulfillment of the requirements for the degree of

DOCTOR OF PHILOSOPHY

by

NAIK ANANT JAIVANT

DEPARTMENT OF ELECTRICAL AND ELECTRONICS ENGINEERING

NATIONAL INSTITUTE OF TECHNOLOGY KARNATAKA

SURATHKAL, MANGALORE INDIA-575 025

OCTOBER 2014

D E C L A R A T I O N

by the Ph.D. Research Scholar

I hereby *declare* that the Research Thesis entitled **Integration of Grid Connected Photovoltaic System with Active Power Filtering Functionality** which is being submitted to the **National Institute of Technology Karnataka, Surathkal** in partial fulfilment of the requirements for the award of the Degree of **Doctor of Philosophy** in department of Electrical and Electronics Engineering is a *bonafide report of the research work carried out by me*. The material contained in this Research Thesis has not been submitted to any University or Institution for the award of any degree.

NAIK ANANT JAIVANT

(100682EE10F02)

(Register Number, Name & signature of the Research Scholar)

Department of Electrical and Electronics Engineering

Place: NITK-Surathkal

Date:

C E R T I F I C A T E

This is to certify that the Research Thesis entitled **Integration of Grid Connected Photovoltaic System with Active Power Filtering Functionality** submitted by **NAIK ANANT JAIVANT** (Register Number, 100682EE10F02) as the record of the research work carried out by him, is *accepted as the Research Thesis submission* in partial fulfilment of the requirements for the award of degree of **Doctor of Philosophy.**

(Prof. Udaykumar R. Y.)
Research Guide
(Name and Signature with Date and Seal)

Chairman-DRPC

(Signature with Date and Seal)

ACKNOWLEDGEMENTS

It gives me immense pleasure and great sense of satisfaction to express my heartfelt gratitude to those who made this dissertation possible.

I take this opportunity to sincerely thank my research supervisor Dr. Udaykumar R.Y. for all his invaluable guidance, patience, encouragement, timely advice and support. He has been a constant source of inspiration throughout this journey. I feel proud to have worked under his guidance.

I wish to thank my research progress assessment committee (RPAC) members Dr. D. N. Gaonkar and Dr. Ajith K. M., for their constructive feedback and guidance from research problem definition stage to thesis submission stage. Without their help the thesis would not have taken this shape.

I would like to thank Dr. K.P.Vittal, former HOD and Chairman, DRPC for providing the necessary resources in the department to carry out my research. Also, I would like to thank HOD, Prof. Jora M. Gonda for encouragement and providing valuable suggestions.

My special thanks to Dr. R.D. Patidar, Mandsaur Instituite of Technology, Mandsaur, M.P., India and Dr. K.N. Shubhanga, NITK Surathkal for enlightening me in the areas of power quality and power systems respectively.

I take this opportunity to thank all teaching and non-teaching staff of EEE Department, NITK Surathkal.

I express my gratitude and thanks to Principal and Director, Government of Goa, for deputing and sponsoring me to pursue Doctoral studies NITK Surathkal.

My stay at NITK Surathkal was a sweet and memorable in the company of my fellow researchers who never let me knew that I am away from home. Big thanks to Mr.Sham, Kappali sir, Santoshkumar, Sanjeev, Sreenivasappa, Shivarudraswamy, Joshi, Raghu, Vijay, Sravankumar, Santosh, Ansal, Shashidhar, Basavraj, Chetanraj, Ramesh & Swapna to name few.

Finally, I would like to thank my family members for their patience, care and love which drew me with inspiration to carry out my research.

NAIK ANANT JAIVANT

ABSTRACT

The development in the field of power electronics has led to its optimum and efficient use in domestic and industrial arena especially in control and automation processes. In turn this has created a threat in terms of power quality issues. The main issue with such devices and the associated circuits is that they act as non linear loads on the system. Due to this the source/grid current in which they are connected gets polluted. The solution for such problems is the use of power filters. Passive filters have certain drawbacks and hence active filters are predominantly used. To some extent, solution to power quality issues is obtained again using power electronic devices in the form of active power filtering.

On the other hand, due to social and environmental issues, there is a rising awareness among masses to use renewable sources of energy. In many places renewable sources like photovoltaic systems are being connected to the grid. Renewable sources such as photovoltaic cells and fuel cells need conversion stage before connecting to the utility grid. Normally a DC-AC inverter is used for this purpose. Hence the performance of such system considerably depends upon the type of inverter used. In order to avail better performance, a multilevel inverter is preferred. But the complexity of control circuitry and the number of devices required are the issues of concern with this type of inverters.

Here, an attempt is being made to address these two aspects in a common domain. The features of active filtering can be combined with the PV source connected to the grid so that active and reactive power transfer takes place at the point of common coupling (PCC). In this work a PV source is connected to the grid through a dual inverter which also acts as active power filter. A dual inverter topology is simple three level inverter topology compared to existing multi level topologies. A grid connected photovoltaic system is integrated with active power filtering functionality to address both issues of real power injection and harmonic filtering. The performance of such system is enhanced by using multilevel inverters. A transformer fed from both ends at its primary terminals with two independent voltage source inverters is used to replace a filter inductance of a conventional system.

In this dissertation firstly a grid connected PV system through a dual inverter topology is modeled and simulated. The system performance is verified under different load and solar cell operating conditions. Secondly, in a power distribution system with nonlinear loads an active power filter is developed with three level (dual inverter) inverter. The source current THD and the source displacement power factor are improved at different loads. Finally, two systems are integrated such that grid connected PV system with active power filter functionality is obtained. This system is tested for different atmospheric as well as load conditions.

CONTENTS

LIST OF FIGURES

LIST OF TABLES

NOMENCLATURE

I_{ph} - Light generated current

I_c - Cell output current

V_c - Cell output voltage

I_d - Reverse saturation current of the diode;

T_c - Cell temperature at standard test conditions (STC) in ^0C;

k - Boltzmann's constant in $J/^0C$;

e - Electronic charge;

A - Ideality factor;

R_{se} - Series resistance.

N_s - Cells connected in series,

N_p - Cells connected in parallel,

S_c - Solar insolation level

C_{TV} - Temperature coefficients for cell output voltage

C_{TI} - temperature coefficients for cell photocurrent

C_{SV} – Solar insolation coefficients for cell output voltage

C_{SI} – Solar insolation coefficients for cell photocurrent

I_{SC} – Short circuit current of solar cell

V_{OC} – Open circuit voltage of solar cell

I_m – Maximum current of solar cell

V_m – Maximum voltage of solar cell

P_m – Maximum power output of solar cell

ABBREVIATIONS

MPPT- Maximum power point tracking

THDi - Current total harmonic distortion

PCC - Point of common coupling

APF - Active Power Filter

APLC - Active Power Line Compensators

IRPC - Instantaneous Reactive Power Compensators

APQC - Active Power Quality Conditioners

UPQC - Unified Power Quality Compensator

IRPT - Instantaneous reactive power theory

SRF - Synchronous reference frame

PLL - Phase locked loop

MLI - Multilevel inverter

NSHC - Nearest Sub Hexagonal Center

DC-MLI - Diode clamped multilevel inverter

FC-MLI - Flying capacitor multilevel inverter

CHB-MLI - Cascaded H-bridge multilevel inverter

Chapter 1 : INTRODUCTION

1.1 PHOTOVOLTAIC (PV) SYSTEM

Energy resources and their utilization is a prominent issue all over the world. As the conventional natural resources of energy are exhaustible in nature and also there is exponential rise in demand for the power, the man is forced to explore the new sources of energy. The solar energy is available abundant in nature. Also it is free of cost. Hence, there lies a challenge to extract this energy effectively and efficiently. Major advantages of solar cells over conventional methods of power system are:

(i) Solar cells convert the solar radiation directly into electricity using photovoltaic effect without going through a thermal process.

(ii) Solar cells are reliable, modular, durable and generally maintenance free and therefore suitable for isolated and remote places.

(iii) Solar cells are quiet and have an expected life time of 20 or more years.

(iv) Solar cells can be located at the place of use and hence no distribution network is required.

Like other devices, solar cells also suffer from disadvantages, such as:

(i) The conversion efficiency of solar cells is limited to 17-20%. Since solar intensity is generally low, large areas of solar cell modules are required to generate sufficient useful power.

(ii) The present costs of solar cells are comparatively high, making them economically uncompetitive with other conventional power generation methods.

(iii) Solar energy is intermittent and solar cells produce electricity only when sun shines and in proportion to solar intensity, hence some kind of electric storage is required making the whole system more costly. However in large installations, the electricity generated by solar cells can be fed directly into the electric grid system. Grid-tied PV systems are very promising. In many countries like Germany, Japan, USA, Korea etc national solar roof programs have been launched successfully.

A grid connected solar system requires an effective Inverter circuit which injects harmonic free currents into the grid system. The current waveform injected by

PV source into the grid contains ripple as it is the integral of the applied voltage. The magnitude of the ripple is a function of interconnecting inductor, switching frequency and the number of discrete input voltage levels. The number of levels that exists in a power circuit topology can reduce output current ripple. The ripple is less when the levels are more because the voltage differential placed across the inductor is reduced. With more number of levels, switching frequency can be reduced so also the filter effect is significantly reduced. Hence obvious choice is to use multilevel inverters to integrate PV system to the grid. However the complexity in the control of this type of converters increases as number of levels increases.

1.1.1 PV modeling and characteristics

The electrical output from the PV cell is described by the I-V characteristics whose parameters can be linked to the material properties of the semiconductor. These I-V characteristics of solar cell can be obtained by drawing an equivalent circuit of the device as shown in the Figure 1-1.(Koutroulis *et al*., 2001; Femia *et al*., 2005).

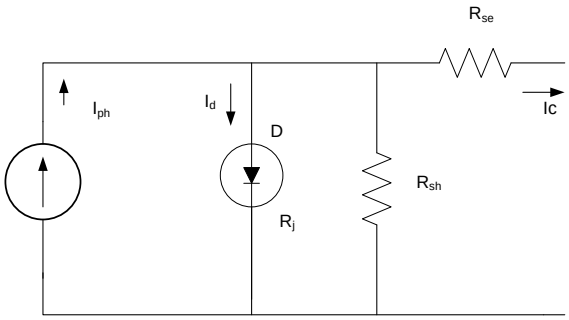

Figure 1-1: Equivalent circuit of PV module.

The generation of current I_{ph} by light is represented by a current generator in parallel with a diode which represents the p-n junction. The output current I_c is then equal to the difference between the light generated current I_{ph} and the diode current $I_{d.}$ In practice, solar cells do not operate under standard conditions. The two most important aspects to be accounted for are the effects due to variable temperature and irradiance. Usually, the PV cells in a module are interconnected in series. The number of cells in a module is governed by the voltage of the module. The three most important electrical characteristics of a module are the short circuit current, open circuit voltage and the maximum power point as function of temperature and

irradiance. To simulate PV array, the mathematical model neglecting shunt resistance R_{sh} is used according to the following set of equations:

The output voltage of PV cell is a function of photo current and it depends upon solar insolation level.

$$V_c = \frac{AkT_c}{e}\ln\left(\frac{I_{ph} + I_d - I_c}{I_d}\right) - R_{se}I_c \qquad (1.1)$$

where, I_c and V_c: cell output current and voltage, respectively; I_d: reverse saturation current of the diode; T_c: cell temperature at standard test conditions (STC) in ^{0}C; k: Boltzmann's constant in J/^{0}C; e: electron charge; I_{ph}: light-generated current; A=1.92: ideality factor; R_{se}: series resistance. The array voltage is obtained by multiplying equation (1.1) by the number of the cells connected in series, N_s. The array current is obtained by multiplying the cell current by the number of the cells connected in parallel, N_p. This value of current is valid for a certain cell operating temperature T_c and its corresponding solar insolation level S_c. A method to include the effects of the changes in temperature and solar insolation levels is given in (Buresch, 1983). According to this, a model is obtained for known temperature (T_a) and solar insolation (S_a). The solar cell operating temperature varies as a function of solar insolation level and ambient temperature. The cell output voltage and cell photocurrent are affected by ambient temperature. These effects are represented by temperature coefficients C_{TV} and C_{TI} for cell output voltage and cell photocurrent respectively.

$$C_{TV} = 1 + \beta_T(T_a - T_x) \qquad (1.2)$$

$$C_{TI} = 1 + \frac{\gamma_T}{S_a}(T_x - T_a) \qquad (1.3)$$

where T_a and S_a are ambient temperature and cell solar insolation level at STC, respectively. T_x is any other temperature. β_T and γ_T are constants specified by the manufacturers. Similarly, the change in solar insolation level causes a change in the cell photocurrent and operating temperature. Therefore, the change in the cell output voltage and the cell photocurrent are corrected by the two factors,

$$C_{SV} = 1 + \beta_T \alpha_S (S_x - S_a) \qquad (1.4)$$

$$C_{SI} = 1 + \frac{1}{S_a}(S_x - S_a) \qquad (1.5)$$

where, S_x is the new level of solar insolation. α_s represents the slope of the change in the solar insolation level. Using correction factors given in equations (1.2)-(1.5), the new values of cell output voltage V_{cx} and photocurrent I_{phx} are given for any temperature T_x and solar insolation S_x as

$$V_{cx} = C_{TV} C_{SV} V_c \qquad (1.6)$$

$$I_{phx} = C_{TI} C_{SI} I_{ph} \qquad (1.7)$$

where, V_c and I_{ph} are the cell output voltage and photocurrent at STC, respectively.

The rating of a PV module is estimated by the maximum power at STC which corresponds to an insolation level of 1000 W/m^2 and a cell temperature of 25^{0}C. The PV cell manufacturers provide its characteristics by specifying the parameters given in Table 1-1.

Module: Solarex MSX60, 60 W PV module at STC irradiance: 1000W/sq.m, ambient temp: 25^{0}C

Table 1-1: Specifications for solar array at STC

I_{sc}	3.74 A
V_{oc}	21 V
P_m	61.85 W
I_m	3.5 A
V_m	17.1 V

Using equations (3.1)-(3.7) and the parameters at STC, the I-V and P-V characteristics of above PV module at different solar insolation and cell temperatures can be obtained as shown in Figure 1-2 and Figure 1-3.

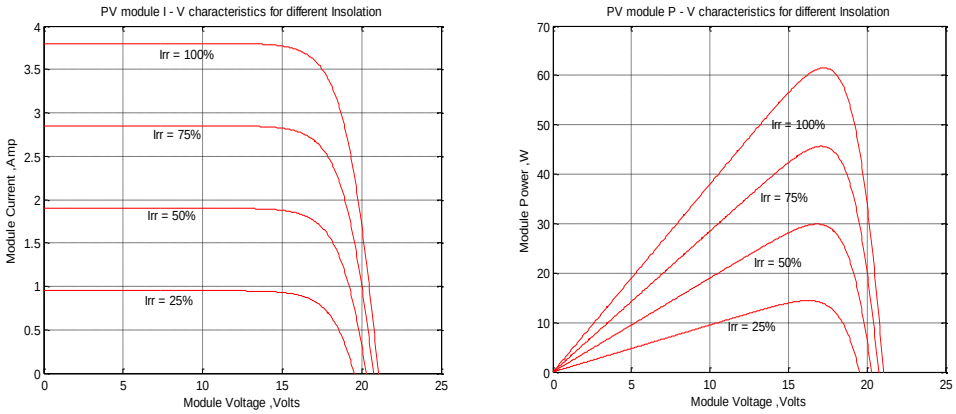

Figure 1-2 : The I-V and P-V characteristics at different solar insolation at 25^0C temperature.

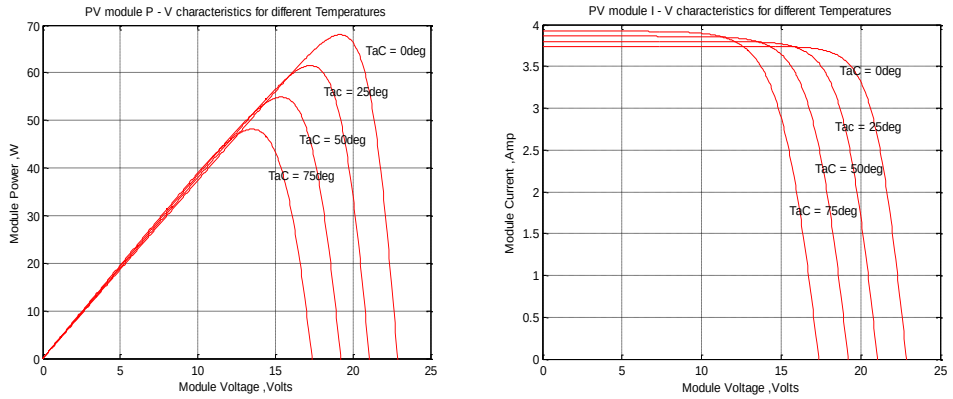

Figure 1-3: The I-V and P-V characteristics at different cell temperature at 1000W/m^2 solar insolation.

1.1.2 Maximum Power Point Tracking (MPPT)

A solar cell array consists of many solar cells connected in series/parallel fashion. The array has I-V characteristics similar to those of a single solar cell. The I-V characteristics change in response to the variations in isolation. Each I-V curve has a maximum power point at which the product of the array voltage and current is maximized. It is clearly advantageous always to operate the array at its maximum power point, hence the desire for maximum power point tracking.

Maximum power point tracking is not always employed nor is it always cost-effective. Consider a common type of load, the constant voltage load such as battery (or a connection to the utility grid through an inverter). A battery voltage is chosen such that the array operates at its maximum-power point at noon on a clear day. At

other times of the day or when the sky is not clear, the chosen battery voltage would cause the array to deliver less, but not far less, than the maximum possible power. This observation raises the question of whether the increased energy output can justify the cost of a maximum power point tracker.

An exact analysis of the benefit of tracking would be difficult because the maximum power point also varies as a result of temperature changes and, possibly, aging of the array. Further, a battery is not an ideal constant voltage load. Its terminal voltage can vary by 30 % depending on the state of charge and the charging or discharging current. Consequently, a maximum power point may boost the annual energy output by 5 to 20 percent depending on the overall design and location of the solar cell system and the efficiency of the tracker.

Assuming that the maximum power point is at a lower voltage than the voltage of the battery load, what can be done about the mismatch? Obviously a dc "transformer" is needed. The function of dc voltage transformation is performed by a group of circuits known as choppers, or dc-dc converters.

The maximum power point operation of a PV array is achieved by maximizing its output power to load. To obtain a maximized output power, controllers are used to minimize the error between the operating power and the reference, Maximum power must be determined for the changing temperature and solar irradiation level before it is compared with the operating power.

In distributed generation (DG) system, PV system is interfaced to the utility grid with the help of VSI's. The DC input of this inverter is fed from a maximum power output of a PV array. The maximum power from the PV array is extracted either using intermediate converter like buck/boost or single stage conversion system. Many MPPT algorithms are specified in the literature like

1) Perturbation and Observation (P&O) Method
   (a) Conventional P&O Method
   (b) Incremental Conductance Method
2) Linearity-based Methods:
   (a) Short-circuit current method

(b) Open Circuit Voltage Method

3) Artificial Intelligence methods

(a) Fuzzy logic control

(b) Neural network control

Here, in this work P&O method of MPPT is used. According to this method a DC-DC converter is used to adjust the PV voltage corresponding to the maximum power output. P&O algorithm as shown in Figure 1-4 is very popular because of its simplicity and ease of implementation. Basically, the module current is perturbed by a small increment, and the resulting change in the power is observed. If the change in power is positive, the current is adjusted by the same increment, and the power is again observed. This continues until the change in power is negative, at which point the direction of the change in current is reversed.

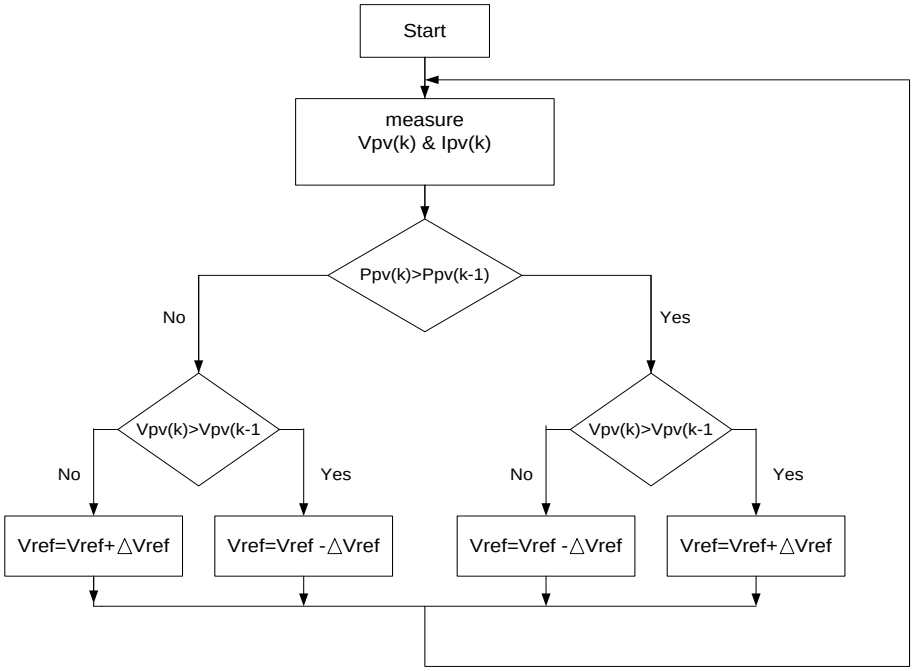

Figure 1-4: Perturb and Observe algorithm

The MPPT controller takes V_{pv} and I_{pv} as inputs to detect power slope and generates V_{ref} to track the maximum power point. This V_{ref} is then used to generate firing pulses for the DC-DC converter in closed loop system as shown in Figure 1-5.

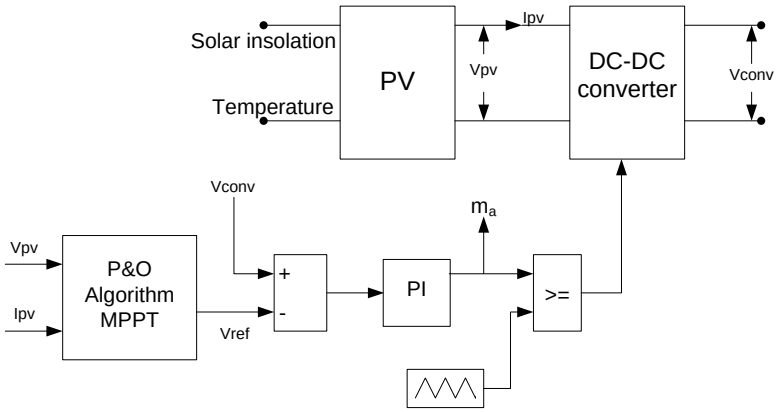

Figure 1-5: Control of DC-DC converter to obtain maximum power from PV system

1.2 ACTIVE POWER FILTERING

With the developments of power electronics devices, the non linear loads that consume non sinusoidal current have increased significantly e.g. VFD, electronic fan regulator, UPS, electronic choke fitted fluorescent lamps etc. These modern equipments behave as non linear loads and draw harmonic current from the power network. Current harmonics drawn by non linear loads disturb the waveform of the voltage at the point of common coupling (PCC) and lead to the voltage harmonics. The other linear loads and sensitive loads connected to this PCC then suffer from these distorted voltages. The non sinusoidal voltage and/or current have adverse effect on the utilities and the load connected to it. The current harmonics cause poor power factor and increase of losses in the AC network, transformers & rotating machines. It also causes mechanical stresses due to oscillatory torque, malfunctioning in protective/sensible equipments and significant interferences with communication circuits.

Hence it has become very essential to pay attention to the power quality issues. Several power quality standards are defined in order to keep the harmonic distortion within the limits like IEEE-519-1992/IEC 61000.

Conventionally, to eliminate harmonics and to improve power factor, passive filters were used. But due to their large size, resonance and fixed compensation they posed difficulties in their use.

The power quality distortion is due to the power electronics devices and solution to this problem is also derived from the same power electronic devices. Active power filtering (APF) uses either a current source inverter or a voltage source inverter which acts as a harmonic source to compensate for the load harmonics. APF's can compensate not only for current harmonics produced by non-linear loads but also for reactive power and unbalance of non linear and fluctuating loads.

Multilevel pulse width modulation inverters can be used as APF for high power applications. Multilevel topologies are able to generate better output quality while operating at lower switching frequency. With the use of multilevel inverter topology in the APF, the switching losses are reduced and the higher order harmonics are suppressed. Compared to conventional two level inverters working as APF, multilevel inverters have received more attention due to their capability of high voltage operation, high efficiency and low electromagnetic interference (EMI). It also reduces the dv/dt stress across each of the inverter switches. In general, a greater number of switches in multilevel converters can be justified since the semiconductor cost decreases at a much greater rate than the filter components cost.

1.2.1 Power Quality

The definition of power quality as per IEEE: "Power quality is the concept of powering and grounding sensitive equipment in a matter that is suitable to the operation of that equipment". IEEE recommended practice for monitoring electrical power quality**,** defines disturbances as: interruptions, sags and swells, long duration variations, impulsive transients, oscillatory transients, harmonic distortion, voltage fluctuations and noise. The ultimate reason that both utility and customer are interested in power quality is economic value. Extensive analysis on the estimation, measurement of harmonics and uncompensated load generated power quality problems are reported to precipitate main causes and their impacts on the utility and other equipments.

Previously, equipment was generally simpler and therefore more robust and insensitive to minor variations in supply voltage. The mechanical design was aimed at the performance rather than the cost aspect. Voltage fluctuations coming from the public supply network were therefore not even noticed. Now equipment is used which

depends on a higher level of power quality and consumers expect disruption-free operation. The ultimate reason that we are interested in power quality is economic value. There are economic impacts due to power quality on utilities, their customers and the load equipment suppliers. The industrial customers recently started using more automated electronically controlled, energy efficient equipments which are more sensitive to deviations in the supply voltage. The electric utility is concerned about power quality issues as well. Meeting customer expectations and maintaining customer confidence are strong motivations. Residential customers do not suffer direct financial loss or the inability to earn income as a result of poor power quality problems, but they can be an important force when they perceive that the utility is providing poor service. Load equipment suppliers generally find themselves in a very competitive market with most customers buying on lowest cost. Thus there is a general disincentive to add features to the equipment to withstand common disturbances.

1.2.1.1Types of power quality disturbances

Any significant deviation in the magnitude of the voltage, current and frequency, or their waveform purity may result in a potential power quality problem. Power quality problems arise when these deviations exceed beyond the tolerable limit, and can occur in three different ways: -

1. Power Frequency Variations

Power Frequency variations can be defined as any deviation of the power system fundamental frequency from its specified nominal value (50Hz or 60Hz). The most important causes of this are faults on the bulk power transmission system, a large block of loads being disconnected or a large source of generation going off-line.

Figure 1-6: Frequency Variation Waveform

2. Voltage Variations

Change of the voltage amplitude beyond its normal range. These can be long-term variations, short-term variations, unbalance, continuous or random fluctuations (flickers) or complete interruption.

Short-term variations are of duration less than one minute. These are called sags (voltage between 10% and 90% of nominal) or swells (voltage greater than 110% of nominal). Short duration voltage variations are caused by fault conditions, the energization of heavy loads, which require high starting currents, or intermittent loose connections in power wiring. Depending on the fault location and the system conditions, the fault can cause.

- Temporary voltage dip (Sags)
- Temporary over Voltage (Swells)
- Complete loss of Voltage (Interruptions)

Voltage Sags: Voltage sags are the most common power problems encountered in power system. Sags are a short-term reduction in voltage (that is 10-90% of normal voltage) and can cause interruptions to sensitive equipment such as adjustable speed drives, relays, robots etc. Sags are most often caused by fuse or breaker operation, starting of high rating motors, capacitors switching etc. Voltage sags typically are non-repetitive or repeat only a few times due to recloser operation. Sags can occur on multiple phases or a single phase and can be accompanied by voltage swells on other phase.

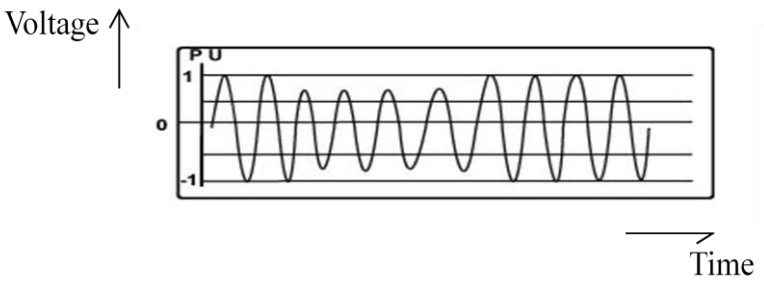

Figure 1-7: Voltage sag waveform

Voltage Swells: Swell is an rms increase in the AC voltage, at the power frequency, for durations from a half-cycle to a few seconds, which occurs on the healthy phases of a three-phase system during a single line-to-ground fault. The magnitude of swell is related to system grounding. Voltage swells are almost always caused by an abrupt reduction in load on a circuit with a poor or damaged voltage regulator, although they can also be caused by a damaged or loose neutral connection and also due to over reactive power compensation.

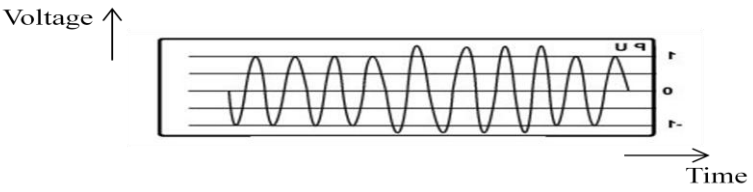

Figure 1-8: Voltage swell waveform

Power Interruption (Momentary): Power interruptions are zero-voltage events that can be caused by equipment malfunctions, recloser operation or transmission outages. Interruptions can occur on one or more phases and are typically short duration events. Vast majority of power interruptions are of duration less than 30 second.

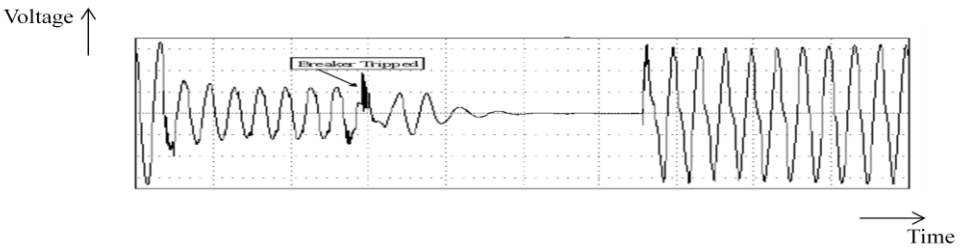

Figure 1-9: Power interruption waveform

Long Duration Voltage Variations: Long-term variations sustain for more than one minute, and are called undervoltages (*if less than 90% of the nominal value*) or over voltages (*if greater than 110% of nominal voltage*). Overvoltages may cause loss of life of the equipment due to over stressed insulation. While due to undervoltage, load would draw more current in an attempt to take the same power from the source. This would increase the motor temperature and leads to the loss of service life. Long duration variations can be: -

- Undervoltages
- Overvoltages
- Sustained Interruptions

Over voltages and under voltages generally are not the results of system faults, but are caused by load variations on the system and system switching operations.

Overvoltage: An overvoltage is an increase in the voltage greater than 110% at the power frequency for duration longer than 1 minute. An overvoltage is usually the

result of load switching (e.g., switching of a large load), or energizing a capacitor bank. The over voltages result because the system is either too weak for the desired voltages regulation or voltage controls are inadequate. Incorrect tap settings on transformers can also result in system overvoltages.

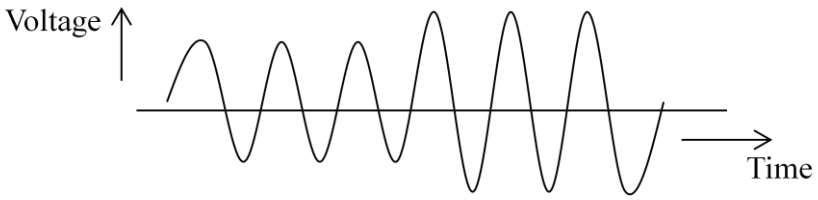

Figure 1-10: Overvoltage waveform

Undervoltage: An undervoltage is a decrease in the ac voltage to less than 90% at the power frequency for duration longer than 1 minute. Undervoltages are the results of the events, which are the reverse of the overvoltages events. A load switching on or a capacitor bank switching off can cause an under voltage until voltage regulation equipment on the system can bring the voltage back to within tolerances also.

Figure 1-11: Undervoltage waveform

Sustained Interruptions: When the supply voltage has been zero for a period of time in excess of one minute, the long duration voltage variation is considered a sustained interruption. Voltage interruptions longer than one minute are often permanent and require human intervention to repair the system for restoration.

Voltage Imbalance: Voltage unbalance is sometimes defined as the maximum deviation from the average of the three phase voltages or currents, divided by the average of the three phase voltages or currents, expressed in percent. Imbalance can also be defined using symmetrical components. The ratio of either the negative or zero sequence components to the positive sequence component can be used to specify the percentage of unbalance. The primary source of voltage imbalance less than two

percent is single-phase loads on a three-phase circuit. Voltage imbalance can also be the result of blown fuses in one phase of a three-phase capacitor bank.

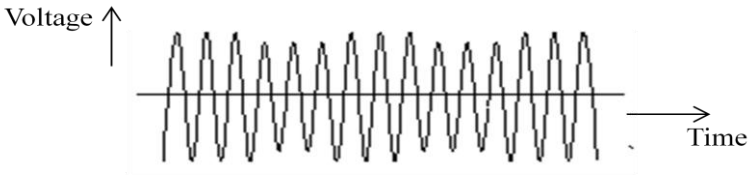

Figure 1-12: Unbalance voltage waveform

Voltage Fluctuations: Voltage fluctuation is a repeatable fluctuating load that causes changes in the supply voltage, which in turn causes flicker. They are rapid changes in voltage within the allowable limits of voltage magnitude of 0.95 to 1.05 of nominal voltage. Devices that usually have continuous and rapid change in the load current causes voltage fluctuations that are often referred to as flicker and any load that has significant current variations, especially in the reactive component, such as arc furnaces can also cause voltage fluctuations.

3. Waveform Events

Distortion of the voltage/current waveforms from the normal sinusoidal wave shape are considered as waveform events and can be identified as steady state distortions and transient distortions.

Steady-State Distortion

DC Offset: The presence of a DC voltage or current in an AC power system is termed DC offset. This can occur as the result of a geomagnetic disturbance or due to the effect of half-wave rectification. Direct current in alternating current networks can have a detrimental effect by biasing transformer cores so they saturate in normal operation. This causes additional heating and reduction in transformer life. DC may also cause the electrolytic erosion of grounding electrodes and other connectors.

Harmonics: These are due to additional frequency components present in the mains voltage or current, which are integral multiples of the mains frequency. In case of harmonic distortion, each cycle is distorted but identical as shown in Figure 1-13. Harmonic distortion originates due to the nonlinear characteristics of the devices and loads on the power system. Harmonic distortion levels are described by the complete harmonic spectrum with magnitudes and phase angles of each individual harmonic

component. It is also common to use a single quantity, the total Harmonic Distortion (THD), as a measure of the effective value of harmonic distortion.

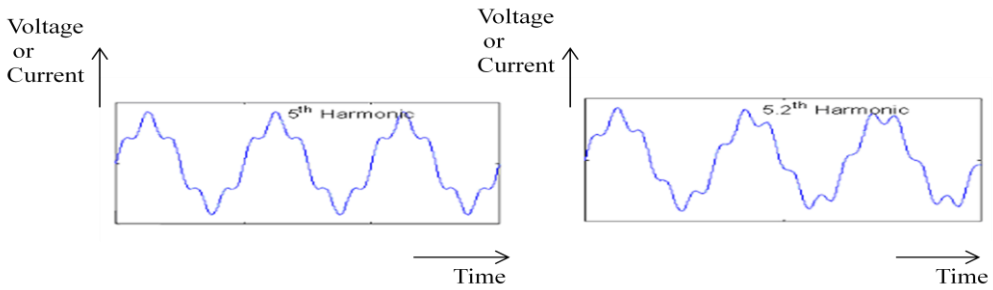

Figure 1-13: Harmonic current waves

Interharmonics: Voltages or currents having frequency components that are not integer multiples of the frequency at which the supply system is designed to operate (e.g., 50 Hz) are called inter harmonics. They can appear as discrete frequencies or as a wide-band spectrum. The most important cause of inter harmonics is the transformer inrush current shown in Figure 1-14. The main sources of inter harmonic waveform distortion are static frequency converters, cyclo-converters, induction motors and arcing devices. Power line carrier signals can also be considered as interharmonics.

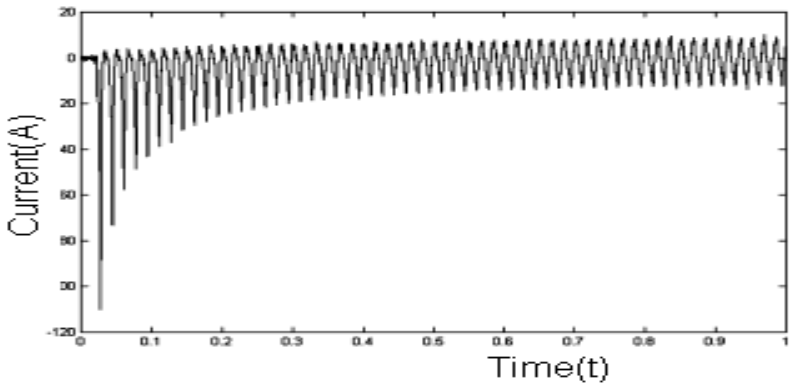

Figure 1-14: Inrush current of a transformer

The effect of Interharmonics is not well known. They have been shown to affect power line carrier signaling, and induce visual flicker in display devices such as CRTs.

Notching: Notching is a periodic voltage disturbance caused by the normal operation of power electronics devices when current is commutated from one phase to another. The effect of notching on the waveform is shown in Figure 1-15.

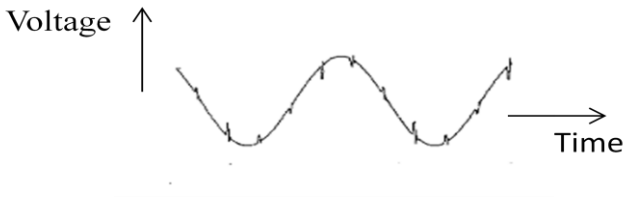

Figure 1-15: Notching effect

Noise: Noise is defined as unwanted electrical signals with broadband spectral content lower than 200 kHz superimposed upon the power system voltage or current in phase conductors, or found on neutral conductors or signal lines. Noise in power systems can be caused by power electronic devices, control circuits, arcing equipment, loads with solid-state rectifiers, and switching power supplies. Improper grounding that fails to conduct noise away from the power system often exacerbates noise problems. Noise consists of any unwanted distortion of the power signal that cannot be classified as harmonic distortion or transients. Noise disturbs electronic devices such as microcomputer and programmable controllers. Using filters, isolation transformers, and line conditioners can mitigate the problem.

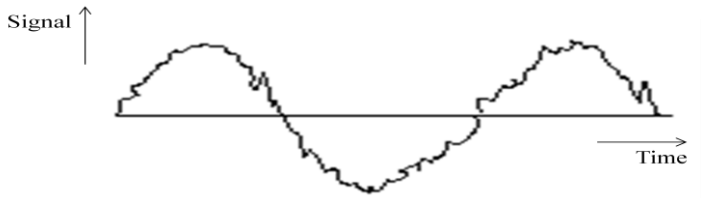

Figure 1-16: Noise effect

Transient Distortion: The term transients have been long used in the analysis of power system variations to denote an event that is undesirable but momentary in nature. Broadly speaking, transients can be classified into two categories. Figure 1-17 shows both the voltage and current transients.

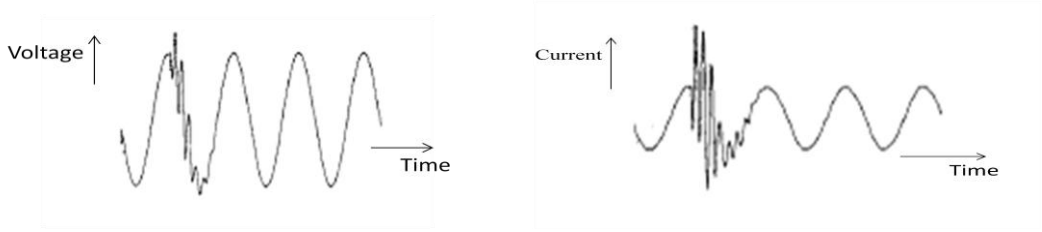

Figure 1-17: Voltage and current transients

Impulsive Transient: An impulsive transient is a sudden, non-power frequency change in the steady state condition of voltage/current, or both, that is unidirectional in polarity (primarily either positive or negative). Impulsive transients are normally characterized by their rise and decay times, which can also be revealed by their spectral content. For example, a 1.2 x 50μsec 2000V impulsive transient nominally rises from zero to its peak value of 200 V in 1.2-μsec then decays to half its peak value in 50-μsec.

Oscillatory Transient: An oscillatory transient is a sudden, non-power frequency change in the steady state condition of voltage/current, or both, that includes both positive and negative polarity values. It consists of a voltage or current whose instantaneous value changes polarity rapidly. It is described by its spectral content (predominate frequency), duration, and magnitude.

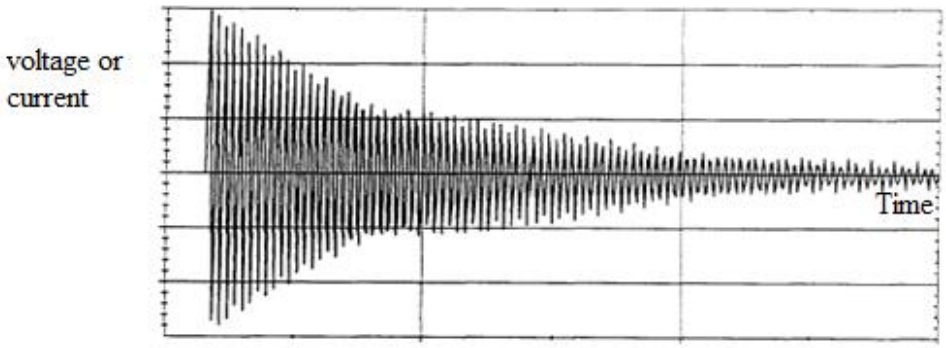

Figure 1-18: Oscillatory transients

Oscillatory transients with a primary frequency component greater than 500 kHz and a typical duration measured in microseconds (or several cycles of the principal frequency) are considered high frequency oscillatory transients. These transients are often the result of a local system response to an impulsive transient. A transient with a primary frequency component between 5 and 500 kHz with duration measured in the tens of microseconds (or several cycles of the principle frequency) is termed a medium frequency transient. Back-to-Back capacitor energization results in oscillatory transient currents in the tens of kilohertz.

1.2.1.2 Harmonic distortion

In power system, the deviation of voltage and current waveforms from sinusoidal waveforms is known as harmonic distortion. Harmonic distortions are mainly caused by the nonlinear devices. Generally, it is desired to draw purely sinusoidal current from the distribution network, but this is no longer the case with the new generation of loads, consisting of power electronic converters. Current harmonics generated by these nonlinear loads are propagated throughout the network; add further distortion to the ideal sinusoidal voltage waveform. Voltage distortion is the result of distorted currents passing through the linear, series impedance of the system.

Recently, with the significant development of the power electronics and microelectronics technology, the proliferation of nonlinear loads such as static power converters has deteriorated power quality in power transmission/distribution systems. These power converters utilizing switching devices are being increasingly used in industrial as well as in the domestic applications, ranging from few watts to MWs. Some applications that are increasingly being dominated by power electronics are variable speed motor drives, switched mode power supplies, efficient control of heating and lighting, efficient interface for photovoltaic, modern domestic appliances, fuel cell and high voltage dc system for efficient transmission of power. Advancements in power semiconductor technology have made earlier predictions true and these days substantial electrical power is being processed through solid-state methods.

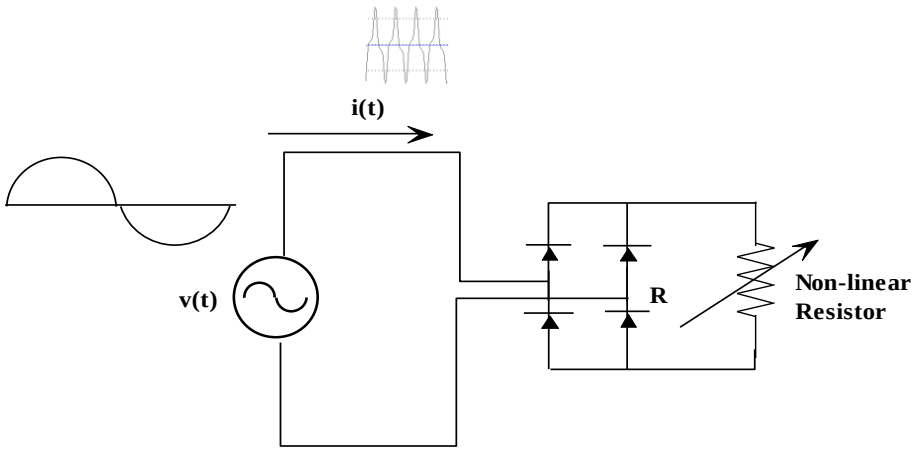

Figure 1-19: Distorted current produced by a non-linear load

Generally, it is desired to draw purely sinusoidal current from the distribution network, but this is no longer the case with the new generation of loads, consisting of power electronic converters. In addition to the numerous advantages offered by these power electronic converters, they offer highly nonlinear characteristics and suffer from the problem of drawing non-sinusoidal current and reactive power from the AC mains. Current harmonics generated by these nonlinear loads are propagated throughout the network; add further distortion to the ideal sinusoidal voltage waveform. Voltage distortion is the result of distorted currents passing through the linear, series impedance of the system, as shown in Figure 1-20. Harmonic currents passing through the system impedance causes a voltage drop for each harmonic, and results in voltage harmonics appearing at the load bus and leads to other power quality problems. These problems led to implementation of standards and guidelines such as IEEE-519, for controlling harmonics on the power system along with the recommended limits. Hence, mitigation of current waveform distortions due to harmonics, and compensation of reactive power requirements of nonlinear loads, is considered among the major remedies for the power quality deteriorations.

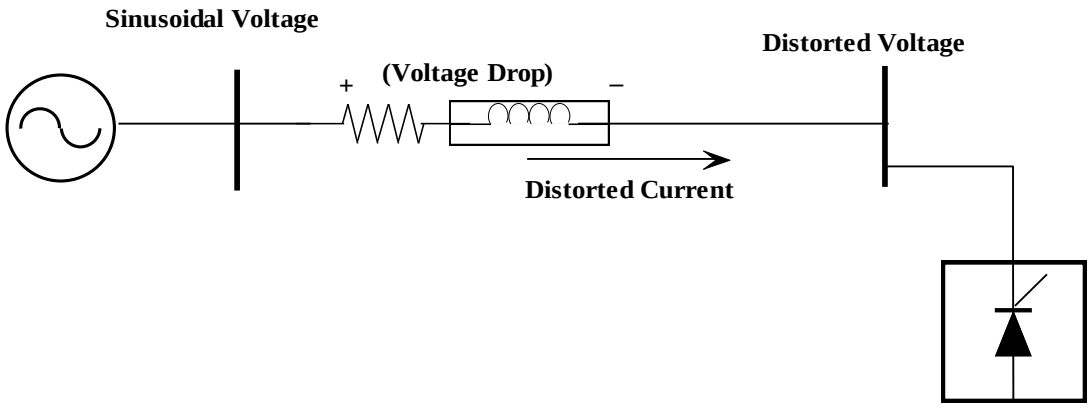

Figure 1-20: Voltage distortion caused by distorted current at load centers

1.2.1.3 Harmonic sources

The main sources of voltage and current harmonics within the power system are: -

Single-Phase: -

- Computers, fax machines, photocopiers, UPS's, TV's, VCR's, etc.
- Lighting dimmers & electronic ballasts for high efficiency lighting.

- Single-phase AC & DC drives.
- Ultra-violet disinfections systems.

Three- Phase: -

- Variable speed AC & DC drives.
- UPS systems.
- Arc furnaces & SCR temperature controllers.
- Battery chargers.
- In general, any single or three- phase electrical power conversion equipment, which converts from AC to DC.

1.2.1.4 Harmonic effects

The main effects of voltage and current harmonics within the power system are: -

- Amplification of harmonic levels resulting from series and parallel resonance.
- Reduction of efficiency of power generation, transmission, and utilization.
- Aging of the installation of electrical plant components and as a consequence the shortening of their useful life.
- Plant mal-operation.
- Malfunctioning and failure of electronic equipment.
- Overheating and failure of electric motors.
- Overloading, overheating and failure of power factor correction capacitors.
- Overloading and overheating of distribution transformers and neutral conductors.
- Excessive measurement errors in metering equipment.
- Spurious operation of fuses, circuit breakers and other protective equipment.
- Voltage glitches in computers systems resulting in lost data. Excessive flicker on Video Display Units (VDU).
- Electromagnetic interference with TV, radio, communication & telephone systems.

- Damage and disruption to standby generators and associated AVR control equipment.
- Interference with ripple control systems.

1.2.1.4.1 Effects of harmonics on power factor

To analyze the effect of voltage distortion on the system power factor, let us assume that the supply voltage consists of the set of harmonic components *H* and *N*. The corresponding load current have a set of common harmonic component *H*, and another set of uncommon harmonic component *P*. Based on this, the instantaneous value of voltage and current are represented by (1.8) and (1.9), respectively (Sankaran, 2002; Dugan *et al*., 2004).

$$v = \sum_{h\in H} \sqrt{2} V_h \sin(h\omega t + \alpha_h) + \sum_{n\in N} \sqrt{2} V_n \sin(n\omega t + \alpha_n) \qquad (1.8)$$

$$i = \sum_{h\in H} \sqrt{2} I_h \sin(h\omega t + \phi_h + \alpha_h) + \sum_{p\in P} \sqrt{2} I_p \sin(p\omega t + \alpha_p) \qquad (1.9)$$

The system power factor is calculated as

$$PF = \frac{\frac{1}{T}\int_0^T vidt}{V_{rms} I_{rms}} = \frac{\sum_{h\in H} V_h I_h \cos(\phi_h)}{\left\{\left(\sum_{h\in H} V_h^2 + \sum_{n\in N} V_n^2\right)\left(\sum_{h\in H} I_h^2 + \sum_{p\in P} I_p^2\right)\right\}^{1/2}} \qquad (1.10)$$

This factor represents the figure of merit for the character of the power consumption. A low value indicates a poor utilization of the source-power capacity needed by the load. If the voltage waveform is sinusoidal, equation (1.10) is reduced to

$$PF = \frac{V_1 I_1 \cos(\phi_1)}{V_1 I_{rms}} = \frac{I_1}{I_{rms}} \cos(\phi_1) \qquad (1.11)$$

= distortion factor X displacement factor

where, I_1 is the rms value of fundamental component, I_{rms} is the rms value of source current, and ϕ_1 is the phase angle between the fundamental components of voltage and current, $\cos\varphi_1$ is the displacement power factor of fundamental components of voltage and current, and I_1/I_{rms} is current distortion factor. It is inferred that real power is transferred by similar harmonic components present in the voltage and current,

under distorted supply conditions. Thus, the voltage and current affect the power factor of the system.

1.2.1.4.2 Effect of harmonics on power system equipment

This section provides an overview of the effect of harmonics on some of the very commonly used power system equipments.

1. Effects on Rotating Machines

Distorted voltage and current have an impact on the entire spectrum of rotating electrical machines. Induction motors form the largest numbers among all rotating electrical machines in power systems. The distortion present in the supply voltages at motor terminals is translated into harmonic flux within the motor. The distorted flux rotates at a frequency other than the synchronous frequency, and induces high frequency current in the rotor conductor (Sankaran, 2002). The positive sequence components of distorted currents produce magneto-motive force (mmf) and torque in the forward direction (direction of the fundamental mmf and torque), while the negative sequence components produce counter mmf and torque. The resultant torque consequently increases vibration and reduces bearing life. The harmonic pairs, such as the fifth and the seventh, can also produce transitional harmonic current in the rotor. These also create mechanical oscillations in a turbine-generator or a motor-load system. Also, under non-sinusoidal voltage conditions, non-oriented core materials used in the rotating machines produce higher magnetic losses (Lancarotte and Penteado, 2001). The losses in the motor conductors are greater than the losses associated with DC resistance, because of eddy current and skin effects. Decreased efficiency, increased heating, increased vibration and excessive noise, are some common symptoms of harmonics on rotating machines (Lee and Lee, 1999).

2. Effects on Transformers

The primary effect of power system harmonics on transformers is the additional heat generated due to the losses caused by the harmonic content of the load current. This adds up to the ageing effect in transformers. Losses in a transformer are categorized as magnetizing or no load losses and load losses. No load losses mainly comprise of hysteresis and eddy current losses. These losses are related to the design of the core and magnetic material. The presence of harmonic voltage increases hysteresis and

eddy current losses in the laminations and increases insulation stresses (Lancarotte and Penteado, 2001). The core loss can be represented as:

$$P_{coreL} = k_e \sum_{h \in H} B_{\max h}^2 (hf_1)^2 + k_h \sum_{h \in H} B_{\max h}^{\sigma} (hf_1) \qquad (1.12)$$

where k_e and k_h are constants, B_{maxh} is the maximum flux density corresponding to harmonic order h, σ is Steinmetz coefficient, and f_1 is the fundamental frequency. Second, but a more serious effect of harmonics is caused due to harmonic frequency currents in transformer windings. The harmonic currents increase the net rms current flowing in the transformer windings, which results in additional I^2R losses. Copper loss, which is due to the rms value of the current and resistance of the winding, could be higher at harmonic frequencies, if the rms value of load current is increased due to harmonics.

$$P_{CL} = \sum_{h \in H} I_{Lh}^2 (R_p + R_s^{'}) \qquad (1.13)$$

where, P_{CL} is the copper loss, I_{Lh} is the rms value of h^{th} order harmonic component of load current with respect to the primary, R_p is the primary winding resistance, and R_s' is the equivalent secondary winding resistance with respect to the primary.

Winding eddy current losses also increase due to the presence of harmonics. Winding eddy currents are circulating currents induced in the conductors by the leakage magnetic flux. Eddy current concentrations are higher at the ends of the windings due to the crowding effect of the leakage magnetic field at the coil extremities. The winding eddy current losses increase as the square of harmonic current and the square of harmonic frequency. Thus, eddy losses are proportional to $I_h^2 \times h^2$, where, I_h is the rms value of the harmonic current of order h, and is expressed as (Sankaran, 2002; Dugan *et al*., 2004):

$$P_{EC} = P_{EC-R} \sum_{h \in H} \left[\frac{I_{Lh}}{I_R} \right]^2 h^2 = P_{EC-R} K \qquad (1.14)$$

where, P_{EC} is the winding eddy current loss, $P_{EC\text{-}R}$ is the winding eddy current loss under rated conditions, I_R is the rated rms fundamental current, and K is the multiplication factor, called the K-factor (IEEE std.C57.110-1998). The K-factor is

equal to the sum of the square of the harmonic frequency currents multiplied by the square of the harmonic frequency numbers,

$$K = \sum I_h^2 n^2 \text{ (n=1,2,3,....h)} \qquad (1.15)$$

Other stray losses P_{OSL} in the core, clamps and structural parts also increase as a result of harmonic current. However, temperature rise in these regions will be less critical than in the windings. Adding all the above equations, the total loss P_{TL} is given by,

$$P_{TL} = P_{coreL} + P_{CL} + P_{EC} + P_{OSL} \qquad (1.16)$$

Thus, it can be concluded that the most important effect of waveform distortion on transformer is the additional loss and possibly higher operating temperature. Other problems include possible resonances between the transformer inductance and system capacitance, mechanical insulation stress (winding and lamination) due to temperature cycling, and possible small core vibrations.

3. Effects on Power Capacitors

Capacitor banks are commonly installed in the commercial and industrial power systems for reactive power compensation and voltage control. Usually the capacitor banks are designed to operate at a maximum voltage of 110% of their rated voltages and at 135% of their rated kVARs (Singh, 2007; IEEE std. 1036-1992; IEEE Working Group on Power System Harmonics; Dugan *et al*., 2004). When significant levels of voltage and current harmonics are present in the system, the ratings of the capacitor banks are relatively exceeded. This happens because the reactance of a capacitor bank is inversely proportional to the frequency. The capacitor bank acts as a sink, absorbing stray harmonic currents and causing overloads and subsequent failure of the bank. The presence of voltage distortion increases the dielectric loss in the capacitors, the total loss being expressed as (Sankaran, 2002):

$$P_{loss} = \sum_{h=1}^{\infty} C(\tan\delta)\omega_h V_h^2 \qquad (1.17)$$

where, $\tan\delta = \omega C\mathrm{R}$ is the loss factor, $\omega_h = 2\pi fh$, and V_h is the rms voltage of the h^{th} harmonic.

A more serious condition, having the potential of substantial damage occur due to a phenomenon called harmonic resonance. Resonance conditions are created when the inductive and capacitive reactance become equal at one of the harmonic frequencies, and are termed as series or parallel resonance. In general, parallel resonance produces current multiplication and series resonance results in voltage amplification (Dugan *et al*., 2004). In parallel resonance, looking from the harmonic current source, the capacitor bank used for power factor correction appears in parallel with the system short-circuit impedance. The combined impedance of the capacitor bank and short-circuit reactance appear to be large.

Harmonic current of a frequency similar to the resonance frequency, if injected into the circuit, results in a high voltage distortion due to this large impedance. This high harmonic voltage produces a high harmonic current, in both the capacitor bank and the short-circuit impedance. The net effect of parallel resonance is the magnification of harmonic currents injected by the primary harmonic source. In power systems, series resonance conditions occur as a result of series combination of capacitor banks and line or transformer inductance. The series resonance offers low impedance path for the harmonic current to which it is tuned. This results in high voltage distortion between inductive and capacitive element of the circuit (IEEE std. 1036-1992).

4. Effects on Measuring Instruments.

Measuring instruments are generally calibrated on purely sinusoidal currents and voltages. When they are used for distorted supply, they are error prone. An expression for total power as seen by a meter under distorted supply is represented as (IEEE std.141-1993):

$$\underbrace{Total\ power}_{=P_T} = \underbrace{V_{dc}I_{dc}}_{=P_{dc}} + \underbrace{V_F I_F \cos\phi_F}_{=P_F} + \underbrace{V_H I_H \cos\phi_H}_{=P_H} \qquad (1.18)$$

The meters do not measure P_{dc} but are sensitive to presence of P_{dc}. The meters measure P_F accurately and P_H inaccurately, the error being frequency based.

Harmonics create serious problems in the measurement of VAR, since VAR is a quantity, defined with respect to sinusoidal waveforms.

5. Interference with Power System Protection

Digital relays are used nowadays for almost all kinds of power system protection. The digital relays and their control algorithms depend on the sampled data and zero crossing, and are particularly prone to error when harmonic distortion is present (Singh, 2007). Due to presence of harmonics in voltage and current waveforms, there is a possibility of mal-operation of the digital relays. Also, increase in use of single-phase nonlinear loads like computers, results in the presence of triplen harmonics in the neutral current, which may affect the operating characteristics of the conventional ground-fault relays. Current harmonic distortion can also have an effect on the interruption capability of the circuit breakers and fuses (Phipps *et al*., 1994).

6. Effects on Power System Neutral

In case of a three-phase four-wire (3P4W) system with balanced nonlinear loads, fundamental and harmonics (including triplen harmonics) are present in the phase currents. Summing these currents at the neutral point, the fundamental and non-triplen harmonic components are found to be zero (Packebush and Enjeti, 1994). However, the triplen harmonic components in neutral are three times the triplen harmonic phase currents, because they coincide in phase and time. Triplens become an important issue for grounded wye-system, as they are added in the neutral and produce a substantial neutral current. The current may exceed the rating of the neutral conductors, resulting in the overheating of power system equipments. The excessive neutral current may cause other adverse effects, such as overloading of power feeders, overloading of distribution transformers, voltage distortion and common mode noise (IEEE std.1100-1992).

7. Interference with Communications

Noise in communication circuits degrades the quality of the signals. At low levels, noise causes annoyance, while at high levels, it causes information loss. The continuously changing power transmission environment requires regular reconsideration of the interference issues, when telephone lines are laid in the vicinity

of the power system. This factor should be given due consideration when sizing protective devices for use in a harmonic environment (Dugan et al., 2004)]. The electromechanical relays are also affected by harmonics.

The harmonics can be reduced or eliminated by the use of passive and/or active filters.

1.2.2 Passive Filter

Classically, shunt passive filters, which consist of tuned LC filters, and/or high pass filters are used to suppress the harmonics, and power capacitors are employed to improve the power factor of the utility/mains. The shunt passive filters are tuned most of the time on a particular harmonic frequency to be eliminated. So that it exhibits low impedance at the tuned frequency than the source impedance, to reduce the harmonic current flowing into the source (i.e. the filtering characteristics are determined by the impedance ratio of the source and passive filter). In (Steeper and Stratford, 1976) the conventional methods for reactive power compensation like use of fixed capacitors, synchronous motors, synchronous condensers etc. are discussed. (Gyugyi, 1988; Gyugyi, 1979; Gyugyi *et al*., 1978) have analyzed the important theoretical foundations to compensate large fluctuating unbalanced industrial loads by using variable reactance. In (Chu *et al*., 1994) the optimization of capacitors and tuned filters based on costs, harmonic constraints and fundamental frequency consideration in distribution networks is investigated. These shunt passive filters have following problems.

- Passive filters are not suitable for changing system conditions. Once installed these are rigidly in place.
- Neither the tuned frequency not the size of the filter can be changed so easily.
- The source impedance, which is not accurately known and varies with the system configuration, strongly influences the filtering characteristics of the shunt passive filter.
- The shunt passive filter acts as a sink to the harmonic current flowing from the source. In the worst case, the shunt passive filter may fall in series resonance with the source impedance.

- At a specific frequency, an anti-resonance or parallel resonance may occur between the source impedance and the shunt passive filter, which is the called harmonic amplification.
- As both the harmonics and the fundamental current component flow into the filter, the capacity of the filter must be rated by taking into account both the currents.
- Increase in harmonic current component can overload the filter.
- Special protective and monitoring devices are required.
- Also, if a good level of correction is targeted, one needs as many filters as the number of harmonics to be eliminated.

1.2.3 Active Power Filter

The sensitivity of these problems has attracted the attention of researchers to develop techniques with adjustable and dynamic components. Extensive research is being carried out in the field of harmonics and reactive power compensation, to overcome all these limitations. Recently, Active Power Filters (APFs) are seen as a viable alternative over the classical passive filters and static var compensators to compensate harmonics and reactive power requirement of nonlinear loads. Such equipments generally known as Active Power Filters are also called Active Filters (AFs), Active Power Line Compensators (APLCs), Instantaneous Reactive Power Compensators (IRPCs) and Active Power Quality Conditioners (APQCs). The objectives of the active filtering are to solve these problems by combining the advantages of regulated systems with much reduced rating of the necessary passive components.

In addition to the harmonics and reactive power compensation, APFs are also used to eliminate voltage harmonics, for load balancing, to regulate terminal voltage, to suppress voltage flickers etc. These wide range of objectives are achieved either individually or in combination, depending upon the requirements, control strategy and configuration, which is to be selected appropriately.

Also, as no energy storage passive elements are required theoretically, the size and projected cost is significantly reduced. It results in low losses and high efficiency. Remarkable progress in the capacity and switching speed of the self commutating devices such as Insulated Gate Bipolar Transistors (IGBTs), and Gate Turn-off

Thyristors (GTOs) have eliminated the drawback of their implementation for medium and high power applications up to some extent. Due to all these advantages, APFs have generated tremendous interest among the researchers to solve increasing power quality problems.

1.2.3.1 Basic compensation principle

The basic compensation principle of shunt active filter is explained with the help of Figure 1-21. The instantaneous current of the non-linear load can be represented by

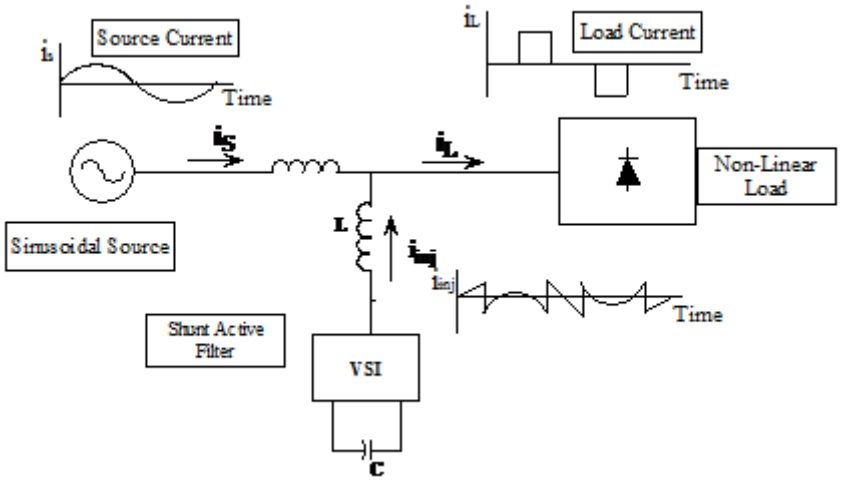

Figure 1-21: Basic Compensation Principle of Shunt Active Filter

$$i_L = I_{Lf}\sin(\omega t - \phi_{Lf}) + \sum_{h=3,5....}^{\infty} I_{Lh}\sin(h\omega t - \phi_{Lh})$$

$$= I_{Lf}\sin\omega t\cos\phi_{Lf} - I_{Lf}\cos\omega t\sin\phi_{Lf} + \sum_{h=3,5.....}^{\infty} I_{Lh}\sin(h\omega t - \phi_{Lh})$$

$$= i_{Lfp} + i_{Lfq} + i_{Lh} \qquad (1.19)$$

where, I_{Lf} is the peak value of the fundamental load current, I_{Lh} is the peak value of the harmonic load current, ϕ_{Lf} and ϕ_{Lh} are the phase angle of the fundamental and harmonic component of the load currents, respectively. In equation (1.19), the instantaneous current of non-linear load is divided into three terms. The first term i_{Lfp} is the load instantaneous fundamental phase current. The second term i_{Lfq} is load instantaneous fundamental quadrature current and the third term i_{Lh} is the load instantaneous harmonic current. From the Figure 1-21 it is clear that

$$i_s + i_{inj} = i_L = i_{Lfp} + i_{Lfq} + i_{Lh} \qquad (1.20)$$

Instantaneous supply current i_s, is having only fundamental component that is almost in phase with v_s , hence from equation (1.20)

$$i_{inj} = i_{Lfq} + i_{Lh} \qquad (1.21)$$

Equation (1.21) concurs that for obtaining clean sinusoidal and power factor corrected supply current, the shunt active filter has to inject the instantaneous fundamental quadrature current and instantaneous harmonic currents of non-linear load.

1.2.3.2 Classification of active filters

APFs are classified on the basis of the topology used as series active filter, shunt active filter, combination of active and passive filters named hybrid filters and combination of series and shunt active filters known as Unified Power Quality Compensator (UPQC).

Figure 1-21 shows the configuration of a shunt active power filter, which is one of the most fundamental system configurations. It is most widely used to eliminate current harmonics, reactive power compensation and balancing unbalanced currents. It has the capability of damping harmonic propagation in power system. It is recommended to install shunt active power filters at the customer end, because nonlinear loads inject current harmonics. It injects an equal compensating current, in phase opposition, to cancel harmonics and/or reactive component of the load current.

Figure 1-22 show the configuration of a series active filter. It is connected before the load in series with the mains, using a matching transformer. It is mainly used to eliminate voltage harmonics, to reduce the negative sequence voltage and regulate the voltage on the three-phase system. It is mainly installed by the utilities to compensate voltage harmonics and damping harmonic propagation.

Figure 1-23 shows three configurations of hybrid filters, which are the combination of an active series/shunt and a passive filter. The main purpose is to reduce the rating of the active filter and initial cost. The advantage of these configurations is that they can be used with the existing passive filters and are considered as prospective alternatives to the shunt or series active filter used alone.

The combinations of shunt active plus shunt passive filters as shown in Figure 1-23(a) are used for harmonic compensation or harmonic damping and are reactive power controllable. These filters are already put into commercial stage. A series

active/shunt passive hybrid filter shown in Figure 1-23(b), is used for harmonic isolation and harmonic damping. It is quite popular as the size of active filter is reduced to 5% of the load size. A series active filter connected in series with the shunt passive filter, shown in Figure 1-23(c) is used mainly for harmonic damping or harmonic compensation.

Recently a new topology, combination of active series and active shunt filter is proposed known as Unified Power Quality Conditioners (UPQC) or Active Power Line Conditioners (APLC), shown in Figure 1-24. It is considered to be an ideal solution for power quality improvement in near future, which not only compensate voltage and current harmonics but is also capable to balance and regulate the terminal voltage, eliminate voltage flickers and negative sequence current. However, the main drawbacks are its high cost and control complexity.

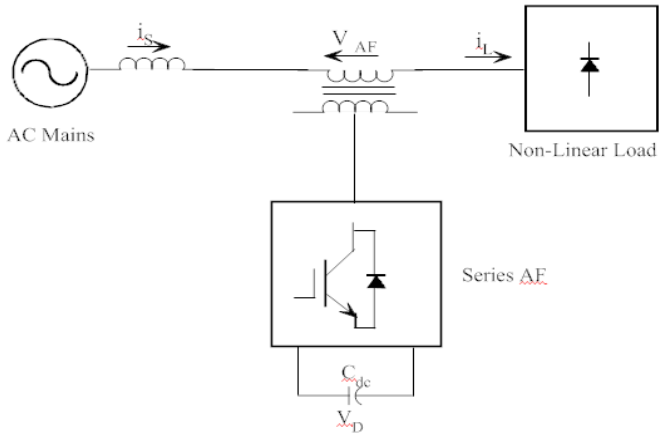

Figure 1-22: Series Active Power Filter

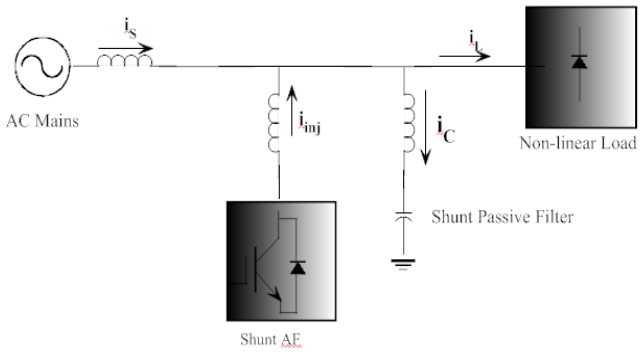

(a) Combination of Shunt Active and Shunt Passive Filter

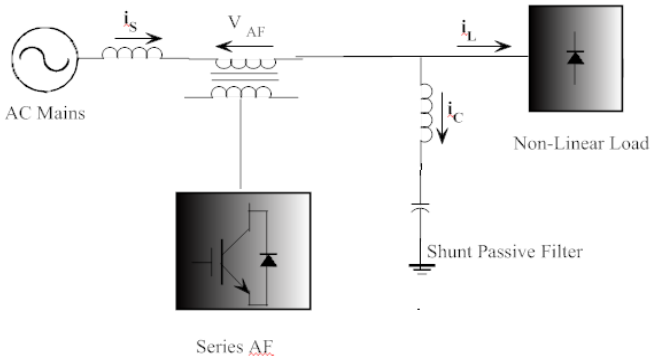

(b) Combination of Series Active and Shunt Passive Filter

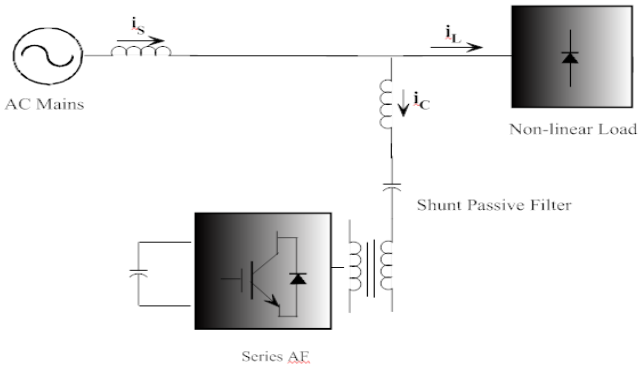

(c) Series Active Filter Connected in Series with Shunt Passive Filter

Figure 1-23: Hybrid filters

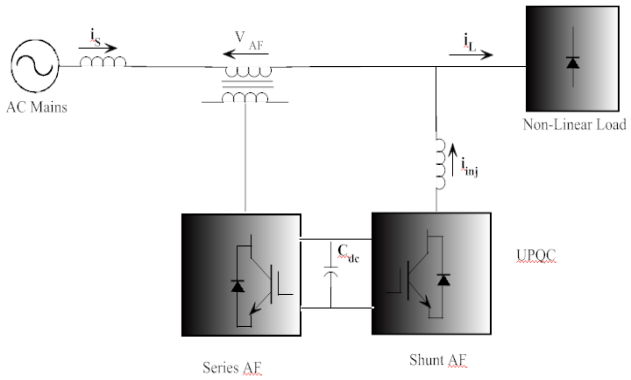

Figure 1-24: Schematic Diagram of Unified Power Quality Conditioner

1.3 INTEGRATION OF PV SYSTEM AND APF

The grid connected PV power generation converter is not utilized during low intensity sunlight and no sunlight conditions. In order to improve the efficiency of grid connected PV generation system and improve the quality of electrical power, a combined grid connected PV inverter and APF is used. Several systems incorporate both these features of PV active power injection and active filter reactive power injection in a common circuit. In such an integrated circuit, during day time PV source acts as active power source whereas during night hours the same converter performs active filtering. It is possible and can be convenient to integrate such a system by appropriately controlling the interfacing inverter. Here the main idea is the optimum utilization of inverter rating so that the hardware cost is also reduced while performing both these functions through a common inverter.

Here too, one can use all the advantage of multilevel inverters if we can replace the interfacing inverter with a multilevel inverter. An appropriate control strategy and the gating signals are required to incorporate a multilevel inverter which will perform a dual function of real and reactive power injection in a grid connected PV system. At the same time the circuit complexities and control algorithm should not raise implementation problems.

In this research work it is proposed to design, analyze and simulate a novel topology for a three level voltage source inverter (VSI) used to integrate PV system to the grid with additional feature of APF.

1.3.1 Existing methods of integration of PV and APF in single phase power systems.

The system being studied is shown in Figure 1-25. It consists of a current controlled voltage source inverter (CC-VSI) fed from a PV source. It feeds current into the grid and the local load through a series connected filter inductance L_c. The output DC voltage of PV cell is maintained constant by capacitor C_{dc} at the input of the inverter as the power output of the inverter oscillates at twice the line frequency. Also it is required to connect a smoothing reactor in series with the local load to suppress the load current spikes.

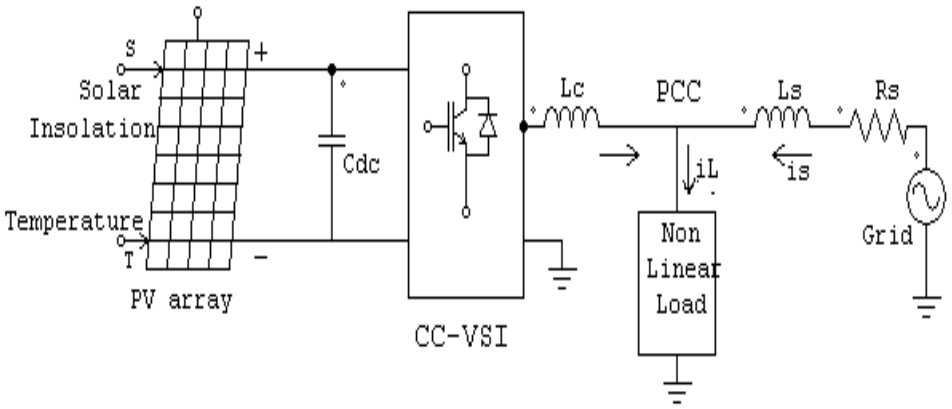

Figure 1-25 : Grid connected PV system

Figure 1-26 shows the model of a single-stage, single-phase grid interactive system. Here single-phase grid system is feeding a local non-linear load consisting of a diode rectifier bridge driving R-L load. At this load bus (PCC), a PV fed inverter is connected through filter inductor. This PV fed inverter consists of an IGBT driven H-bridge. The input DC voltage is the MPPT output voltage to this inverter.

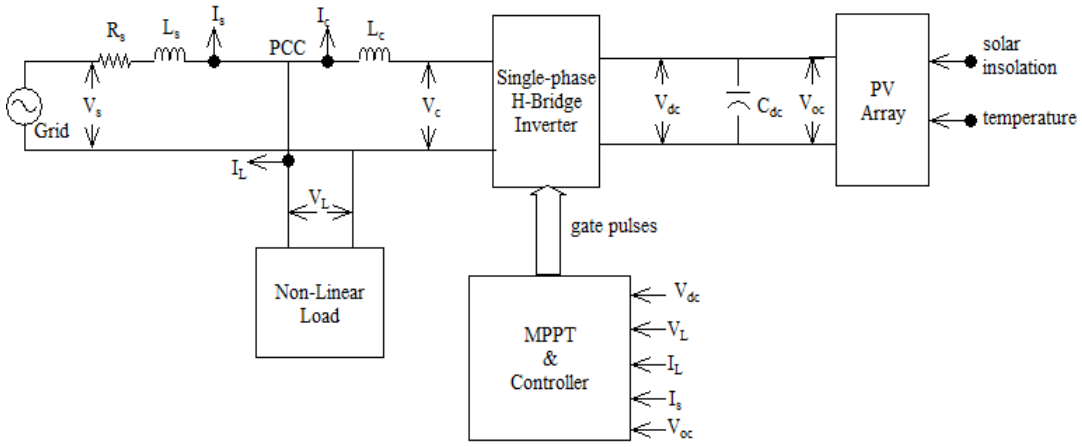

Figure 1-26: System model

PV array is modeled separately with different combination of solar insolation and temperature as explained in Appendix - I. The output voltage corresponding to the maximum power is calculated and made available by the MPPT block as described in sub section MPPT technique.

1.3.2 Existing methods of integration of PV and APF in three phase power systems

Figure 1-27 shows the schematic power circuit of the three phase grid-interactive PV system that comprises of a PV array, a DC-bus capacitor, filter inductors, smoothing inductors, a current controlled voltage source inverter (CC-VSI) and utility power grid. Among different components as shown in Figure 1-27, DC-bus capacitor, filter inductors and VSI form an APF. A transformer may also be connected towards AC-side of the VSI in the case grid voltage differs from output voltage of the VSI. To allow the exchange of active power between PV system and grid, a bi-directional interface is provided typically at point of common coupling (PCC). The diode D, as shown in Figure 1-27, prevents the flow of reverse current into the PV array.

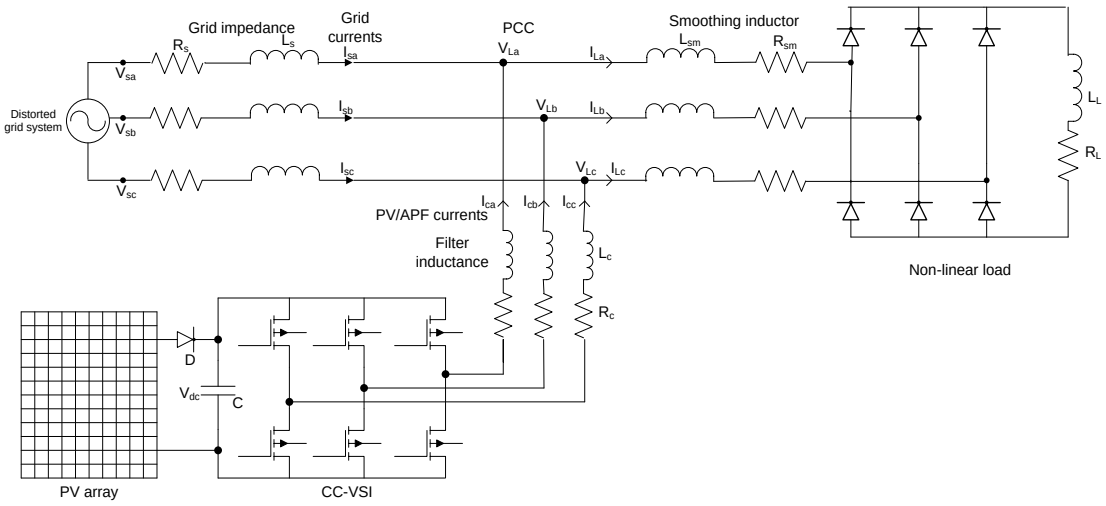

Figure 1-27 : Power circuit of three-phase Grid-interactive PV system.

1.4 OBJECTIVES OF THESIS

The use of renewable sources of energy is inevitable in the present global scenario. These renewable energy sources have to be interfaced to the grid through power electronics devices. The effectiveness and the efficiency of such a system need to be checked. Obvious choice to increase efficiency of such a system is a multilevel converter. This motivated many researchers to use this topic of multilevel interfacing of grid connected PV systems.

Secondly, energy conservation too has become vital to control the excessive energy demand. Many methods including custom made electrical loads, automated systems and DC systems in place of traditional AC system at consumer end are often used to conserve energy. But it has adverse effect on the grid as these types of loads can pollute the existing system. Hence it is required to clean the system using some form of filters. An active filter with multilevel feature is the first choice in such a situation.

An attempt has been made here to explore the possibility of combining the above referred subjects in a single system. The scope here is to combine the grid connected PV system with additional function of active power filtering. This led to motivate us to use multilevel inverter as interfacing device which would also serve as APF.

With this background the following objectives were set for the thesis.

1. To study and analyze the existing methods of integration of PV system and APF in a single phase and three phase systems.
2. To investigate the dual inverter topology of a three level inverter for a grid connected PV system.
3. To analyze different control strategies used in shunt APF. To carry out design, modeling and simulations of a novel three level inverter topology in APF.
4. To design, model and simulate an integrated system of PV and APF with dual inverter based three-level inverter topology.

1.5 THESIS ORGANISATION

The content of this thesis is divided into the following chapters.

Chapter 1 deals with the introduction to the topics covered in the thesis namely grid connected PV systems, APF and integrated PV system with APF. It also covers the PV system related topics used in this work like PV modeling and its characteristics and MPPT. The power quality issues, causes, effects and remedies are also discussed. The existing methods of integration of PV and APF in single-phase and three-phase systems is also covered in this chapter. Lastly the motivation behind this thesis topic and objectives of the work are specified. Also the thesis organization is covered at the end.

Chapter 2 exclusively covers the literature study on the topics such as grid connected PV system, grid connected PV system with multilevel inverters, APF, APF with multilevel inverters, SVPWM for multilevel inverters and integration of PV system and APF.

Chapter 3 deals with PV system interfaced to the grid with the help of a dual inverter type three level inverter. The controller for this system is developed and tested in MATLAB/Simulink environment. The system is tested for different environmental conditions and at different electrical loads.

Chapter 4 is dedicated for the study the various control strategies used in three-phase APF. Their performance is compared at various conditions. Then a three level APF with dual inverter topology is analyzed. Its performance is verified at different nonlinear load conditions.

Chapter 5 is a combined study of grid connected PV system with APF with a common three level inverter. Two PV identical PV systems with individual MPPT circuits through interfacing inverter perform the function of active and reactive power generator for the system. This system is modeled and simulated in MATLAB/Simulink at different solar insolation and cell temperature. It is also tested for any change in load conditions.

Chapter 6 covers the summary of the work carried out briefly outlining the main contribution based on the investigations carried out in the thesis. It also enlists the scope for future investigations in the area of grid connected PV system with APF functionality.

Chapter 2 : LITERATURE REVIEW

2.1 INTRODUCTION

Grid-connected or utility-interactive PV systems are designed to operate in parallel with and interconnected with the electric utility grid. The primary component in grid-connected PV systems is the inverter or power conditioning unit (PCU). The PCU converts the DC power produced by the PV array into AC power consistent with the voltage and power quality requirements of the utility grid. The research in the field of PV system is going on since 50-60 years and various topics are being studied by many researchers. Following is the brief description of research carried out in the past in the field of grid connected PV system.

2.2 GRID CONNECTED PV SYSTEM

In early days, PV systems were used as power supplies only for special applications like communication satellites. With the development of power electronics devices, the role of PV source has been widened in all domestic and few commercial fields. In order to overcome global energy crisis, the PV system is a ray of hope. A general mathematical description of I-V characteristics for a PV cell has been studied over the past five decades (Angrist, 1982; Wasynczuk, 1983; Phang *et al*., 1984; Hua and Shen, 1998; Wasynczuk, 1989). A more exact mathematical analysis of a solar cell which is termed as the double exponential model is given in (Gow and Manning, 1999). There exists a considerable volume of the technical literature that deals with economical and technical aspects of the grid connected PV system (Bzura, 1990; Bzura, 1992; Abouzahr and Ramakumar, 1993). The issue of grid connected PV modeling is addressed by many researchers like (Armstrong and Hurley, 2004; Theocharis *et al*., 2005; Villalva *et al*., 2009; Ropp and Gonzalez, 2009; Hamrouni and Chérif, 2007).

Unfortunately the conversion efficiency of PV cells/modules is very low. Hence it is required to optimize the design of all the elements of a PV cell. In other words, a monitoring circuit called maximum power point tracking(MPPT) is used to extract maximum power from the PV modules at all times. The main function of

MPPT circuit is to operate PV module at its maximum power point (MPP) depending upon the state of load, PV generation, PV cell temperature and solar radiation variations (Ahmed and Miyatake, 2008). There are different MPPT methods mentioned in the literature. Hill climbing or Perturb & Observe (P&O) method involves a perturbation in the duty ratio of a power converter interfacing the PV array and load. This method is very common and is described in (Buciarelli *et al*., 1980; Femia *et al*., 2005; Teulings *et al.*, 1993; Kim *et al.*, 1996; Koutroulis *et al*., 2001; Veerachary *et al*., 2001; Xiao *et al.*, 2004; Wasynczuk,1983; Hua and Lin, 1996). Another method called incremental conductance is based on the fact that the slope of PV array 'power – voltage' characteristics is zero at MPP. This method is used by (Boehringer, 1968; Costogue and Lindena, 1976; Harada and Zhao, 1989; Hussein and Mota, 1995; Brambilla, 1999). Beside these, there are two simple offline methods namely fractional open circuit voltage method and fractional short circuit current method. The PV array voltage at MPP is a specific fraction of its open circuit voltage (Schoeman and VanWyk, 1982; Buresch, 1983; Hart *et al*., 1984; Patterson, 1990; Masoum *et al*., 2002). Similarly the PV current at MPP is a specific fraction of its short circuit current (Bekker and Beukes, 2004; Noguchi *et al*., 2000; Mutoh *et al*., 2002; Yuvarajan and Xu, 2003). Microcontrollers and artificial intelligence are used together to develop MPPT techniques. In (Patcharaprakiti and S. Premrudeepreecharn, 2002; Wilamowski and Li, 2002; Veerachary *et al*., 2003; Khaehintung *et al*., 2004) use of fuzzy logic is shown in implementing MPPT. Similarly neural network technique is used in (Kyoungsoo and Rahman, 1998; Hussein *et al*., 2002; Sun *et al*., 2002; Zhang *et al*., 2002). Other MPPT methods include Ripple Correlation Control (RCC) (Midya et al., 1996) which uses ripple to perform MPPT, the current sweep (Bodur and Ermis, 1994) method which uses a sweep waveform for the PV array current such that the *I–V* characteristic of the PV array is obtained and updated at fixed time intervals. The voltage at MPP can then be computed from the characteristic curve at the same intervals. DC-link capacitor droop control (Matsui *et al*., 1999), (Kitano et al., 2001) is an MPPT technique which is specifically designed to work with a PV system that is connected in parallel with an AC system line. In few applications, the concept of load power maximization is used to achieve MPPT (Shmilovitz, 2005).

2.3 GRID CONNECTED PV SYSTEM WITH MULTILEVEL INVERTERS

Higher power usually demands higher voltages, in order to maintain currents at an acceptable level. Isolation voltage limit of PV panels constrains the number of series-connected panels in a PV array, thus limiting its maximum DC voltage level. Therefore, multilevel inverters appear to be a very good solution for solar applications, as PV arrays concatenation is straight forward to each level of the DC link. In this scenario, power control of multilevel inverters for photovoltaic applications is recently being considered. For high power, medium voltage applications, multilevel converters offer many advantages compared to 2-level converters. (Calais *et al*., 2000) have described the current control method and switching schemes of a cascaded five level inverter based grid connected single phase PV system. Here the redundant inverter states in the five level cascaded inverter allow for a cyclic switching scheme which achieves equal stress on all switches, minimum switching frequencies and minimum DC bus capacitor ripple. A zero average current error method is presented by (Calais *et al*., 1998) that can handle the voltage transition in a single-phase multi-level inverter. A hybrid cascaded multilevel inverter application for renewable energy resources including a reconfiguration technique is developed in (Khomfoi *et al*., 2010). Here the authors claim that the proposed topology can reduce the number of required power switches compared to traditional cascaded multilevel inverter. The system efficiency and also the reliability are improved in this topology. A cascaded H-bridge multilevel converter for grid connected PV generators with independent MPPT of each solar array is presented by (Alonso *et al*., 2003). Here the control makes each H-bridge module to supply at different power levels. Low ripple sinusoidal waveforms are generated with almost unity power factor in a single phase cascaded H-bridge multilevel inverter for a grid connected PV system. This is experimentally demonstrated by (Villanueva *et al*., 2009). Use of diode clamped three level inverter is presented in (Alepuz *et al*., 2006; Nabae and Akagi, 1981; Pou *et al*., 2005). Similarly, flying capacitor type and cascaded H-bridge type multilevel converters are presented by (Kang et al., 2005; Lin and Huang, 2006; Meynard and Foch, 1992) and (Kou *et al*., 2006; Marchesoni *et al*., 1998; Rodriguez *et al*., 2005) respectively.

2.4 ACTIVE POWER FILTERS

Use of solid state power devices such as thyristors, MOSFETs, IGBTs and many more is increasing rapidly to feed a variety of electrical loads like adjustable speed drives (ASD), uninterrupted power supplies (UPS) etc., for improving distribution system efficiency. These 'power electronic devices fed loads' behave as non-linear loads, inject harmonic currents and draw reactive power from AC mains. The flow of injected harmonic currents through the utilities results in distorted voltage drop across the source impedance and thereby voltage distortion at utilities' point of common coupling (PCC). As a consequence, of late, the issue of power quality has sdrawn significant attention. Both electric utilities and end users of electric power are becoming increasingly concerned about the quality of electric power. Research work in this area together with the availability of the fast switching and high power semiconductor devices, microelectronics devices, microcontrollers, digital signal processors (DSPs) have widened the scope of application of various compensators in practice**.**

The extensive analysis on the estimation, measurement of harmonics and uncompensated load generated power quality problems are reported to precipitate main causes and their impacts on the utility and other equipments (IEEE Working Group on Power System Harmonics, 1983; Barker *et al*., 1994; Phipps *et al*., 1994; Eichert *et al*., 1999; Rahmani *et al*., 1999; Subjak and Mcquilkin, 1990; Amoli and Florence, 1990; Packebush and Enjeti, 1994; Mansoor *et al*., 1994; IEEE Task force on the effects of harmonics on equipment, 1993; A report by load characteristics task force and effects of harmonics task force, 1998; Duffey and Stratford , 1989).

Classically shunt passive filters, consisting of tuned LC components, are used to suppress the harmonics. Power capacitors are employed to improve the power factor of the mains. (Steeper and Stratford, 1976) have discussed briefly the conventional methods for reactive power compensation like use of fixed capacitors, synchronous motors, synchronous condensers etc. (Gyugyi, 1978; Gyugyi 1979, Gyugyi 1988) have analyzed the important theoretical foundations to compensate large fluctuating unbalanced industrial loads by using variable reactance, realized by thyristor switched capacitors banks, combination of fixed capacitors and thyristor

controlled reactor, current source type VAR generators and voltage source type VAR generators. (Ortmeyer and Zeher, 1991; Baghzouz, 1991) have discussed the reduction of harmonics level in distribution systems. (Chu *et al*., 1994) have investigated the optimization of capacitors and tuned filters based on costs, harmonic constraints and fundamental frequency consideration in distribution networks.

In three-phase systems, several papers on balancing (Baghzouz and Cox, 1991; Ledwich *et al*., 1992; Best and De La Parra, 1996), reactive power compensation based on optimized LC combination (Richards *et al*., 1989), fixed capacitor and thyristor controlled reactor in distribution network (Ortmeyer *et al*., 1988; Hiyama *et al*., 1989; Ortmeyer and Hiyama, 1996) are reported.

The various drawbacks with passive shunt filters such as size of filter, resonance problem, fixed compensation etc are reported in (Chu *et al*., 1994; Baghzouz and Cox, 1991; Ledwich *et al*., 1992; Best and De La Parra, 1996; Richards *et al*., 1989; Ortmeyer *et al*., 1988; Hiyama *et al*., 1989).

Dynamic and adjustable devices to overcome power quality problems, generally known as active filters (AFs), also known as active power line conditioners (APLCs), have been considered as a standard solution for the harmonic elimination and reactive power compensation in the last two decades (Singh *et al*., 1992; Akagi, 1994; Akagi, 1996; *Active Filters: Technical Document*, 1989; Kikuchi, 1992). The principle of active shunt filter is to inject a compensating current of same amplitude and opposite phase of the load harmonic current into the line, thus eliminating the harmonic current flowing into the source. Several topologies of AFs such as active shunt (Singh *et al*., 1992; Akagi, 1994; Akagi, 1996; *Active Filters: Technical Document*, 1989; Kikuchi, 1992; Chandra *et al*., 2000; Singh *et al*., 1998; Singh *et al*., 1999; Singh *et al*., 2005), active series (Akagi, 1996; Bhattacharya and Divan, 1995), hybrid of active series with passive shunt (Bhattacharya and Divan, 1995; Bhattacharya *et al*., 1995; Cheng *et al*., 1996) and unified power quality conditioner (UPQC) (Tey *et al*., 2004) have been reported either in current source inverter (CSI) configuration with inductive energy storage or voltage source inverter (VSI) configuration with capacitive energy storage.

The control strategy of active filter has a great impact not only on the compensation objectives and required KVA of active filters, but also on the filtering

characteristics in transient as well as in steady state. There are numerous techniques based on time, as well as frequency domain, to calculate the appropriate compensating reference current signals. Both, time-domain and frequency-domain techniques are used for the voltage source type and current source type PWM converters. (Akagi, 1994) proposed a concept based on the theory of instantaneous reactive power in the *α-β* reference frame; this theory stimulates the realization of three phase, three-wire APFs. The active power filter control algorithm, based on synchronous reference frame (SRF) method (Nabae and Tanaka, 1996), relies on Clarke's and Park's transformations. Based on the instantaneous reactive power theory (IRPT) and discrete Fourier transform (DFT) theories, (Li *et al*., 2005) developed a novel current detection algorithm of shunt APFs, based on current decomposition for harmonic elimination, power factor correction and balancing of nonlinear loads. (Jinn-Chang *et al.,* 2011) introduced an improved instantaneous *p-q* theory based control algorithm for APF of three-phase three-wire systems under distorted supply voltage conditions. The method needs only one multiplier, and less number of sensors, as compared to the *p-q* methods. Using current-controlled pulse width-modulated converters, (Mattavelli , 2001) employed a closed-loop synchronous frame based APF controller for selective harmonic compensation. The approach is based on the measurement of line currents, and performs the compensation of selected harmonics. Full compensation of the desired harmonics is achieved even in the presence of a significant delay in the current control.

(Chandra *et al*., 2000) developed a new control scheme to eliminate harmonics, to compensate for reactive power and neutral current and to balance the supply current. In this approach, two closed loop PI controllers were employed. The DC- bus voltage of the APF and three-phase source voltages are used as feedback signals for the PI controllers.

(Chang, 2006) developed a new steady-state approach to determine the optimal reference compensation current for shunt APF, by minimizing the source current THD and maximizing the compensated load power factor, under ideal or non-ideal supply voltages. The APF reference current is generated in *a-b-c* reference frame, and thus, this scheme does not need reference frame transformation. (Chang and Chen, 2006) extended the same concept for the series active power filter control.

(George and Agarwal, 2007) realized a DSP based optimal algorithm for shunt APF, which is suitable under distorted source voltage and unbalanced load conditions. They minimized the total apparent input volt amperes considering the constraints on active power balance between load and source and THD of source current.

(Bhuvaneswari and Nair, 2008) presented a simple current compensation algorithm for three-phase shunt APF to provide harmonic compensation only. Later, they extended the work and developed an analog circuit based $I\cos\varphi$ control algorithm for three-phase shunt APF. This algorithm provided both reactive power and harmonic compensation in which the source is suppose to supply only the active component of the load current.

(Jain *et al*., 2004) suggested a control algorithm for shunt APF that maintains similar distortion in the compensated current as is present in the source/utility voltage. This attributes the responsibilities of the customer and utility at the point of common coupling. In this approach, the nonlinear loads behave as a linear load after compensation, and the resultant source current has the same waveform as that of the source voltage.

(Kim and Enjeti, 2002) developed a new topology of hybrid power filter to achieve harmonic current compensation. In this configuration, a combination of IGBT and MOSFET based inverters operating at different switching frequencies are used.

(Singh and Verma, 2006) proposed an indirect control algorithm for parallel hybrid power filter (PHPF) to compensate harmonics and reactive power. PHPF consists of a set of tuned shunt passive filters connected in series with a shunt APF through a coupling transformer at PCC, to eliminate harmonics produced by the nonlinear loads. In order to find the reference source current at the fundamental frequency, the fundamental component is extracted from the source current using SRF theory.

(Jou *et al*., 2005) proposed an APF that can be regarded as a new family of hybrid power filter, and combines a parallel active filter and an ac power capacitor. This configuration has the advantages of lower voltage rating for dc-bus capacitor and power switching devices, smaller filter inductor with better filter performance.

(Dixon *et al*., 1997) proposed a control strategy for the series active filter (SAF), working as a sinusoidal current source in phase with the mains voltage. In this

scheme, the SAF acts as a harmonic isolator instead of a harmonic generator, such that the line current is made sinusoidal using a combination of shunt passive and active filters. (George and Agarwal, 2007) extended the control algorithm presented by (Wang *et al*., 2001) to series active filter, which is suitable for compensating loads producing voltage type harmonics.

(Jou *et al*., 2008) proposed a three-phase four-wire APF, comprising of a three phase, three-wire APF and a zig-zag transformer. In this APF topology, development of three-phase four-wire APF configuration is not required.

Soft computing has experienced an exponential growth in the last decade, partially due to uncertainties and vagueness in processing signal and occurrence of random events, and partially due to nonlinearity and complexity of the processes. Many intelligent algorithms for designing the control of APF are also proposed (Singh *et al*., 2007; Jain *et al*., 2006). (Jain *et al*., 2006) used a fuzzy logic technique for the control of an active filter.

(Singh *et al*., 2007) developed an adaline based current decomposer for estimating reference currents. Here a neural network based control scheme is used to decompose the load current into four parts; positive sequence active power current, positive sequence reactive power current, harmonic current and negative sequence current.

2.5 GENERATION OF GATING SIGNALS TO THE CONTROL SWITCHES

Another important stage in APF design is selection of gating pulse generation for the power electronic devices of the converter circuit. These switching signals are obtained by comparing the reference compensating signals with the actual current in a controller. Various control techniques for generation of gating signals are reported such as linear PWM, predictive, hysteresis, SVM, etc. by (Jou *et al*., 2008; Massoud *et al*., 2007; Jou *et al*., 2006; Zeng *et al*., 2004; Kale and Ozdemir 2005; Routimo *et al*., 2003; Buso *et al*., 1998; Huang and Wu, 1999). The performance of an APF is significantly affected by the selection of appropriate control techniques (Buso *et al*., 1998).

The control techniques for harmonic current tracking are either analog or digital based and are generally categorized into two control schemes, linear and

nonlinear controls (Jou *et al*., 2006; Huang and Wu, 1999). In linear current control technique, voltage or current PWM, ramp comparison control, sinusoidal internal model control, etc. are used for obtaining the PWM signals (Zeng *et al*., 2004). Nonlinear current control technique includes hysteresis control and space vector modulation (SVM). The hysteresis control is robust, but leads to a widely varying switching frequency, and is difficult to implement (Jou *et al*., 2006; Zeng *et al*., 2004).

2.6 MULTILEVEL ACTIVE POWER FILTERS

Recently there has been increasing interest in using multilevel inverters for high power drives, reactive power and harmonic compensation. Multilevel PWM inverters are used as APF in high power applications solving the limitations on semiconductor devices. In (Saad and Zellouma, 2009) the three-level inverter is used as a shunt active power filter, making use of the multilevel inverter advantages of low harmonic distortion and reduced switching losses. In this paper, fuzzy logic control algorithm is proposed for harmonic current and inverter DC voltage control to improve the performances of the three levels APF's. A synchronous reference frame controller based cascaded shunt active power filter for the harmonics and reactive power mitigation of the non-linear loads is presented in (Ajami, 2011; Karuppanan and Mahapatra, 2010). A simplified three-level SVPWM with neutral point potential adaptive control applied to control multi-level active filter is presented in (Guojun *et al*., 2010)**.** A cascaded H-bridge multilevel inverter based direct connected active power filter for medium high voltage application without using the bulky transformer or passive filter is described in (Zhou *et al*., 2004). In (Amini *et al*., 2011) multilevel inverter advantages in active filtering task in a shunt APF based on flying capacitor multilevel inverter is shown. A predictive current control algorithm of an active filter built with Multilevel Diode Clamped Inverter is developed by (Verne and Valla, 2009). A three-phase three-wire hybrid power filter configured by a three-phase passive power filter and a three-phase diode-clamped multilevel power converter with a small power capacity of zero-sequence current loop connected in series to compensate for the harmonic currents of nonlinear load is shown in (Jinn-Chang *et al*., 2011).

2.7 SPACE VECTOR PULSE WIDTH MODULATION FOR MULTILEVEL INVERTERS

Pulse width modulation (PWM) is widely used for voltage source inverters (VSI). Space vector PWM (SVPWM) is widely used for two level inverters in over modulation region (Gupta and Khambadkone, 2007). SVPWM is also favorable in multilevel inverters as it directly uses the control variable obtained from the controller and identifies each switching vector as a point in complex space of (α, β). The harmonic elimination is better and the fundamental voltage ratios are higher in SVPWM schemes compared to Sine PWM schemes. In addition to this, the maximum peak value of the output voltage is 15% greater than triangular carrier-based modulation techniques (Massoud *et al*., 2003). The SVPWM method uses a number of level-shifted carrier waves to compare with the reference phase voltage signals when applied to multilevel inverters. (Gupta and Khambadkone, 2007) proposes a simple space vector PWM scheme to reduce common mode voltage for cascaded multilevel inverter. This scheme is explained for 5-level inverter. In (Hu *et al*., 2007) a hardware design and implementation of the three-level SVPWM for the NPC three-level converter is presented. A simplified algorithm of the three-level SVWPM is introduced to reduce the hardware requirements. A simple SVPWM algorithm for a multilevel inverter based on a standard two-level inverter has been proposed in (Gupta and Khambadkone, 2007). The computations do not increase with level. The proposed method can be easily implemented using a commercially available motion control DSP or microcontroller, which normally supports only two-level modulation. A pulse width modulation (PWM) scheme for multilevel inverters is proposed by (Kanchan *et al*., 2005) generates the inverter leg switching times, from the sampled reference phase voltage amplitudes and centre's the switching times for the middle vectors, in a sampling interval, as in the case of conventional space vector PWM (SVPWM). The SVPWM scheme, presented for multilevel inverters, can also work in the over modulation range, using only the sampled amplitudes of reference phase voltages. This PWM technique does not involve any sector identification and considerably reduces the computation time when compared to the conventional space vector PWM technique. (Kanchan *et al*., 2007) extended this work to generate synchronised carrier-

based SVPWM signal generation scheme for the entire modulation range extending up to six-step mode using the sampled amplitudes of reference phase voltages. (Purkait and Sriramakavacham, 2006) showed the generalized space vector modulation algorithm for neutral-point-clamped multilevel converters. The various studies have been realized to reduce complicated calculations of vectors and simplify the required SVM algorithms in order to control multilevel inverters that generate five-level and above output voltage like in (Gupta and Khambadkone, 2006(a); Hu *et al*., 2007; Gupta and Khambadkone, 2006(b); Kanchan *et al*., 2005).

2.8 INTEGRATION OF PV SYSTEM AND APF

In standalone mode, PV power systems supply power to fixed loads. Hence PV power generated is not used optimally. The current trend is to connect PV systems to the utility lines. Due to more electronics products being used which use switching systems the power system gets polluted. Hence many researchers have devoted their efforts in developing PV interfacing inverter so that it injects real power and also performs APF function. A prototype current-controlled power conditioning system has been developed and tested by (Borle *et al*., 1997) on a weak rural feeder line. This system sources 20 kW of power from a photovoltaic array with a maximum power point tracking control. In addition, it provides voltage support for the grid, varying its reactive power in response to the measured voltage at the point of connection. It has been shown that a grid connected inverter, acting as an active filter, can correct the power factor of a group of nonlinear loads (Pottker and Barbi, 2000). (Patidar *et al*., 2010; Neves *et al*., 2009) have presented a behavioral model and control of a single-phase single-stage Grid-interactive PV system with active filter functioning suitable for changing atmospheric conditions and varying load demand. The overall system has been co-simulated in TMS320F2812 digital signal processor through processor in loop. After compensation, the grid current is sinusoidal and in-phase with grid voltage. The grid current THD is shown to be well within the IEEE 519-1992 recommended limits. In (Mastromauro *et al*., 2009), it is shown that the PV inverter not only supplies the power produced by the PV panels but also improves the voltage profile. The presented topology adopts a repetitive controller that is able to compensate the selected harmonics. The incremental conductance method of MPPT

algorithm has been modified in order to take into account power oscillations on the PV side, and it controls the phase of the PV inverter voltage. A case of unbalanced non linear load in 3-phase, 4-wire system is presented in (Patel and Agarwal, 2006). The various PV and APF configurations and their control schemes in terms of their ability to compensate reactive power, harmonics and phase-imbalances caused by unbalanced linear and nonlinear loads in a three-phase, four-wire distribution system is studied in (Patel and Agarwal, 2010). Furthermore, use of multilevel inverters in this application is explored by many researchers. In (Pouresmaeil *et al*., 2011) the authors have shown the multilevel converters control strategy for renewable energy resources integration in distribution grids. The control scheme ensures the injection of the generated power in the distribution grid with fast dynamic response, while providing an additional active power filtering capability supplying the required harmonic and reactive currents to the considered non-linear loads. The control scheme is validated by means of simulations with a three-level diode-clamped converter. A grid connected photovoltaic (PV) system is carried out via a three phase three level neutral point clamped (NPC) inverter in (Tsengenes and Adamidis, 2011). To control the inverter, a modified version of voltage oriented control (VOC) method and the space vector pulse width modulation (SVPWM) technique have been applied. With these modifications the PV system operates as a shunt active power filter (SAPF), a reactive power compensator and a load current balancer simultaneously.

2.9 OUTCOME OF LITERATURE REVIEW

From the extensive study of the literature in the field of Photovoltaic system it has been observed that the performance of a grid connected system is improved considerably with the use of multilevel inverters. However the implementation and operating complexities increase as number of levels is increased. Hence three or five level inverters are mostly used in such systems. Also it has been observed through this literature study that there is a scope to explore possibility of using new multilevel topologies.

The active power filtering (APF) concept exists for last several years and lot of research is carried out in this field. The APF are generally having low VA ratings and as such there is no need for any multilevel inverter to realize it. The current which flows through the inverter switches acting as APF is only the non sinusoidal component of load current which is small compared to sinusoidal component. However its magnitude depends upon the nonlinear load and the operating voltages. The MLIs can be used to realize APF as well as interconnecting converter for a renewable source like PV**.** Besides the applications where high VA rating is required, the MLIs offer other advantages like improved output voltage waveforms, smaller filter size, lower EMI compared to square wave inverter. However these factors do not contribute in any sense in APF application.

Multilevel PWM inverters are used as APF for high power applications. MLIs are able to generate better output quality while operating at lower switching frequency. With the use of MLI topology in the APF, the switching losses are reduced. Compared to conventional two level inverters working as APF, MLIs have received more attention due to their capability of high voltage operation, high efficiency and low EMI. It also reduces the dv/dt stress across each of the inverter switches.

Integration of PV and APF is comparatively new concept and not much research has gone through. Here more research is carried out in the control logic used as it decides the functionalities of APF along with PV power injection. The features of active filtering can be combined with the PV source connected to the grid so that active and reactive power transfer takes place at the point of common coupling.

2.10 PROBLEM STATEMENT

Based on the literature study and its outcome the research problem statement is given as: “The features of active filtering can be combined with the PV source connected to the grid so that active and reactive power transfer takes place at the point of common coupling (PCC). A PV source can be connected to the grid through a dual inverter which also acts as active power filter. A dual inverter topology can be a simple three level inverter topology compared to existing multi level topologies. A grid connected

photovoltaic system can be integrated with active power filtering functionality to address both issues of real power injection and harmonic filtering. The performance of such system could be enhanced by using multilevel inverters."

2.11 RESEARCH OBJECTIVES

The research objectives are stated as

1. To study and analyze the existing methods of integration of PV system and APF in a single phase and three phase systems.
2. To investigate the dual inverter topology of a three level inverter for a grid connected PV system.
3. To analyze different control strategies used in shunt APF. To carry out design, modeling and simulations of a novel three level inverter topology in APF.
4. To design, model and simulate an integrated system of PV and APF with dual inverter based three-level inverter topology.

Chapter 3 : GRID INTERCONNECTED PHOTOVOLTAIC SYSTEM WITH DUAL INVERTER TOPOLOGY

3.1 INTRODUCTION

PV system technology is explored extensively over the last few years by many researchers and environmentalists as it has emerged as prime source of renewable energy. There are many advantages posed by PV source such as clean and green energy, easy and abundant availability and availability at load centers. To make use of PV source, it is necessary to know its operating characteristics as well as design limitations. PV source can be used to drive small standalone loads and also can be connected to the power system grid. When connected to the electric grid, it is interfaced using DC-AC converter whose prime function is to match PV system characteristics with the grid in terms of voltage and frequency. Also, it is essential for such a PV system to inject pure/sinusoidal current into the grid. Use of multilevel inverter as interfacing converter largely helps in achieving this goal.

In this chapter, a grid connected PV system with three-level dual inverter topology is explored. Already a brief study on PV characteristics and modeling and MPPT method to extract the maximum power generated by PV source is covered in chapter1. Here the PV system is simulated to study the use of three-level inverter in grid connected PV system at different atmospheric and load conditions.

3.1.1 Grid integration through Multilevel Inverters

3.1.1.1 Introduction to Multilevel Inverters

The current that PV system injects to the grid should obey the regulations, such as the EN61000-3-2 and the IEEE1547, which state the amount of injected harmonics and other parameters. The grid injected current contains lesser amount of harmonic contents if the AC output voltage from the interconnecting inverter has more levels. Multilevel inverters offer improved output waveforms, smaller filter size, lower EMI, and lower total harmonic distortion (THD). Multilevel inverter is an array of power semiconductor switching devices and capacitor voltage sources. The output

voltage of multilevel inverter is a stepped waveform resulting in reduced harmonics compared to a square wave inverter. The main function of the multilevel inverter is to generate the desired output voltage with many levels of DC sources. By increasing the number of output levels, the quality of the output voltage and load current is increased. Due to the production of less harmonic components, the PV power is transferred to the load or to the grid in a high-quality form by multilevel inverter structures. However the complexity of control circuit increases as the number of levels increases. Different three level inverter topologies used in PV grid connection are mentioned in the literature. The three important topologies are

1) Diode clamped (neutral point clamped) (DC-MLI)

2) Capacitor clamped (flying capacitors) (FC-MLI) and

3) Cascaded H-bridge inverter (CHB-MLI).

Figure 3-1 shows one leg of a three-phase, three level inverter of above mentioned topologies. One phase of a three level diode clamped inverter configuration as shown in Figure 3-1(a) consists of four switches associated with freewheeling diodes and two additional clamping diodes.

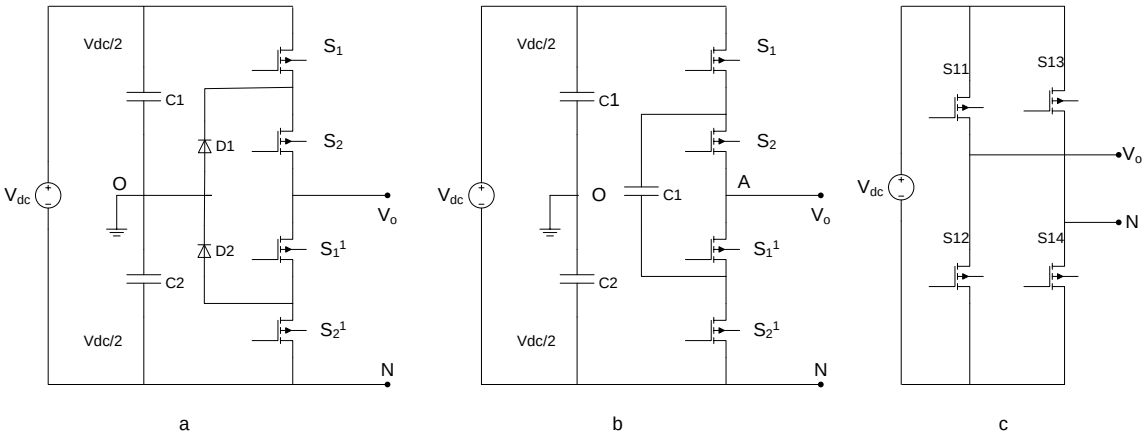

Figure 3-1: Multilevel inverter topologies: (a) three-level DC-MLI, (b) three-level FC-MLI, (c) three-level CHB-MLI.

The minimum number of components for multilevel diode clamped topology is given in Table 3-1 .

Table 3-1: Components required for q-level diode clamped inverter

Number of Levels	**Switching Devices**	**Clamping Diodes**	**DC-bus Capacitors**
3	12	6	2
4	18	9	3
-	-	-	-
-	-	-	-
q	6(q-1)	3(q-1)	(q-1)

The switches S_1 and S_1^1 are complementary. Similarly S_2 and S_2^1 are complementary. When the upper pair (S_1, S_2) is turned ON, the output is connected to the positive rail of the DC-bus. When the lower pair (S_1^1, S_2^1) is turned ON the output is connected to the negative rail of the DC-bus. When the two inner switches (S_2, S_1^1) are turned ON, the output is clamped to 0 through one of the inner switches and its associated clamping diode. These switch combinations are given in Table 3-2.

Table 3-2: Switching states and definitions of diode clamped inverter.

Switching symbol	Switching state						Phase voltage
	S_1	S_2	S_1^1	S_2^1	D_1	D_2	
1	ON	ON	OFF	OFF	OFF	OFF	$V_{dc}/2$
0	OFF	ON	ON	OFF	Depending on polarity of load voltage		0
-1	OFF	OFF	ON	ON	OFF	OFF	$-V_{dc}/2$

The circuit shown in Figure 3-1(b) is called the flying capacitor inverter as independent capacitors clamp the device voltage to one capacitor voltage level.

As given in table 3.3, , a q-level inverter requires a total of 3(q-1)(q-2)/2 clamping capacitors in addition to (q-1) main DC-bus capacitors.

Table 3-3: Capacitors required for q level capacitor clamped inverter

Number of Levels	Clamping Capacitors
3	3
4	9
-	-
-	-
Q	3(q-1)(q-2)/2

The number of switching devices is same as that of diode clamped inverter. The inverter provides a three level output across A and O as shown in Table 3-4. When S_1 and S_2 are ON the voltage level is $V_{dc}/2$, when S_1^1 and S_2^1 are ON the voltage level is $-V_{dc}/2$ and when either S_1 and S_1^1 or S_2 and S_2^1 are ON the voltage level is 0. The clamping capacitor C_1 is charged when S_1 and S_1^1 are ON and is discharged when S_2 and S_2^1 are ON. The charge of C_1 can be balanced by proper selection of 0-level switch combination. The main advantages of this topology are: (1) with independent capacitor, the device voltage can be clamped to one capacitor voltage level (2) by proper selection of capacitor combinations, it is possible to balance the capacitor charge (3) voltage synthesis is more flexible than diode clamped inverter. The disadvantages of this topology are: (1) the capacitor clamping requires a large number of bulk capacitors to clamp the voltage (2) q- level inverter requires 3(q-1)(q-2)/2 bulk capacitor to clamp the voltage in addition to q-1 main DC-bus capacitors.

Table 3-4: Switching status of capacitor-clamped three level inverter

Switches	Switching States		
S_1	ON	OFF	OFF
S_2	ON	ON	OFF
S_1^1	OFF	ON	ON
S_2^1	OFF	OFF	ON
O/P voltage	$V_{dc}/2$	0	$-V_{dc}/2$

The cascaded H-Bridge three-level inverter (one-phase) shown in Figure 3-1(c) has certain benefits such as high reliability and requires least number of devices to realize

q-levels over other topologies. H-bridge cells with different voltages can be used in cascade to improve THD of output voltage and two cells can also operate at two different frequencies (one at higher frequency using IGBT and other at lower frequency using GTO). However, as each cell requires separate DC source a multiple winding transformer is required at the input stage. The number of switching devices required to realize a q-level inverter is given in Table 3-5 .

Table 3-5: Components required for q-level cascaded H-bridge inverter

Number of Levels	Switching Devices
3	12
5	24
-	-
-	-
Q	6(q-1)

The cascaded H-bridge inverter uses series connection of single phase bridge inverter called H-bridge cell to construct multilevel inverter with separate DC source. Each single phase full bridge inverter generates three voltage levels at the output $+V_{dc}$, 0 and $-V_{dc}$ as shown in Table 3-6.

Table 3-6: Switching states of cascaded H-bridge three level inverter for phase A

Switches	Switching States	Voltage level
S_{11} S_{14}	ON	+Vdc
$S_{13}S_{12}$	ON	-Vdc
$S_{11}S_{13}$ or $S_{12}S_{14}$	ON	0

3.1.1.2 Space Vector Pulse Width Modulation for multilevel inverters

An alternative popular control method for multilevel inverters is defined as Space Vector PWM (SVPWM) that directly uses the control variable given by the control system and identifies each switching vector as a point in complex space of (d, q). The harmonic elimination and fundamental voltage ratios in SVPWM schemes are obtained in better values compared to Sine PWM schemes. In addition to this, the maximum peak value of the output voltage is 15% greater than triangular carrier-based modulation techniques. The SVM method uses a number of level-shifted carrier

waves to compare with the reference phase voltage signals when applied to multilevel inverters.

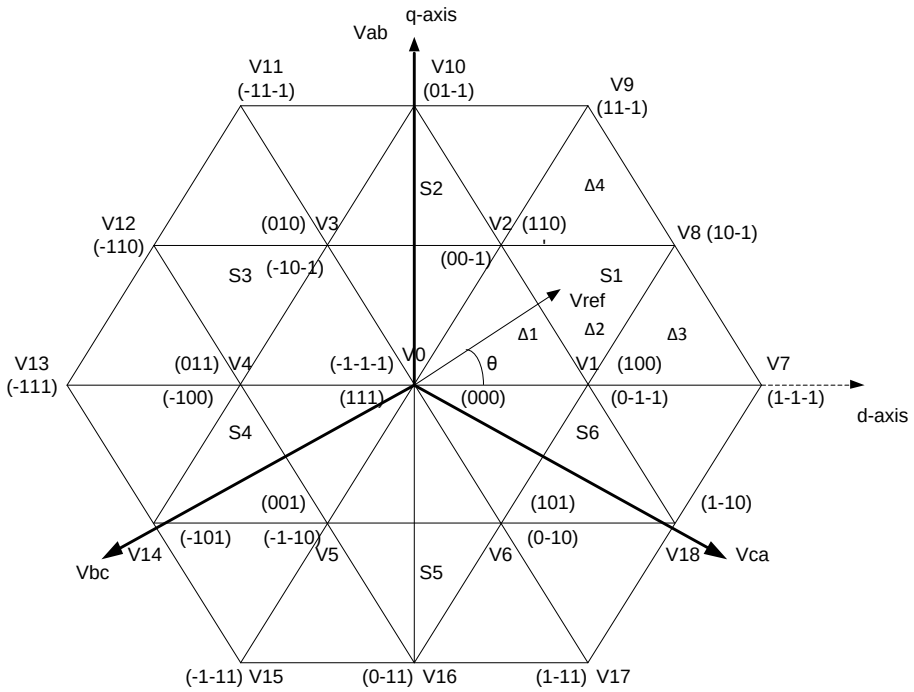

Figure 3-2: Space vector diagram for a three level inverter

Figure 3-1(a) shows a three-level neutral point clamped inverter. It contains 12 switching devices. Each phase leg consists of 4 series-connected switching devices (IGBT's) and two clamping diodes. Their job is to clamp the six middle switches potential to the DC-link point at zero. Specific combinations of the twelve switches give the three level output voltage. The four switches in one phase leg can only be turned on two at a time and so be connected to the DC-link points $+V_{dc}/2,0,-V_{dc}/2$. These are represented with the switching states +1, O and -1. This means that three voltage levels can be created using O as the reference. Figure 3-2 shows the space vector diagram of a three-phase three-level DC-MLI. All 27 switching states and 19 voltage vectors and the generated output voltage is shown in table 3.7.

Table 3-7: Switching states and the voltage vector in three level inverter

Switching States			Vector
a	b	c	
1	1	1	V0
0	0	0	
-1	-1	-1	
1	0	0	V1
0	-1	-1	
1	1	0	V2
0	0	-1	
0	1	0	V3
-1	0	-1	
0	1	1	V4
-1	0	0	
0	0	1	V5
-1	-1	0	
1	0	1	V6
0	-1	0	
1	-1	-1	V7
1	0	-1	V8
1	1	-1	V9
0	1	-1	V10
-1	1	-1	V11
-1	1	0	V12
-1	1	1	V13
-1	0	1	V14
-1	-1	1	V15
0	-1	1	V16
1	-1	1	V17
1	-1	0	V18

The zero voltage vectors has three switching states as (0 0 0, 1 1 1,-1 -1-1). The vectors given in Figure 3-2 are classified into three groups that are named as small vectors (V1 -V6), middle vectors (V8, V10, V12, V14, V16, V18), and the large vectors (V7, V9, V11, V13, V15, V17). By assuming the reference voltage vector V_{ref} located in the 2nd region (Δ2) of S1 sector, it can be constituted by voltage vectors of V1, V2, and V8 during the sampling period (Ts). The reference voltage also depends on the dwelling times of voltage vector. Hence, the equation for ON time of the voltage vectors that constitutes the reference voltage can be given as in equation (3.1).

$$V_{ref}.T_s = V_1.t_a + V_2.t_b + V_3.t_c \qquad (3.1)$$

ON times of voltage vectors can be determined using equation (3.1) as given in equation (3.2);

$$\begin{aligned} t_a &= T_s - 2n\sin\theta \\ t_b &= 2n\sin(\pi/3+\theta) - T_s \\ t_c &= T_s - 2n\sin(\pi/3+\theta) \end{aligned} \qquad (3.2)$$

where $n = (4\sqrt{3}/3)(V_{ref}/V_{dc})T_s$

The various studies have been realized to reduce complicated calculations of vectors, and simplify the required SVM algorithms in order to control multilevel inverters that generate five-level and above output voltage.

3.2 PRINCIPLE OF OPERATION

The system being studied is shown in Figure 3-3. It consists of a dual inverter feeding open end primary of a three phase transformer. The star connected secondary of this transformer is connected to PCC. Two PV sources are connected at the two inputs of the VSI's. They feed current into the grid and the local load through transformer inductance L which acts as filter inductance. The output DC voltage of PV cell is maintained constant by capacitor C_{dc} at the input of the inverter. The configuration like this can provide three level output voltage from the PV source into the grid. Also due to the presence of interconnecting transformer the PV source of lower voltage level can be used by selecting proper transformer voltage ratio. This topology of a three level inverter is simple compared to other three level topologies. Hence all the benefits of a three level inverter are obtained in a simpler way.

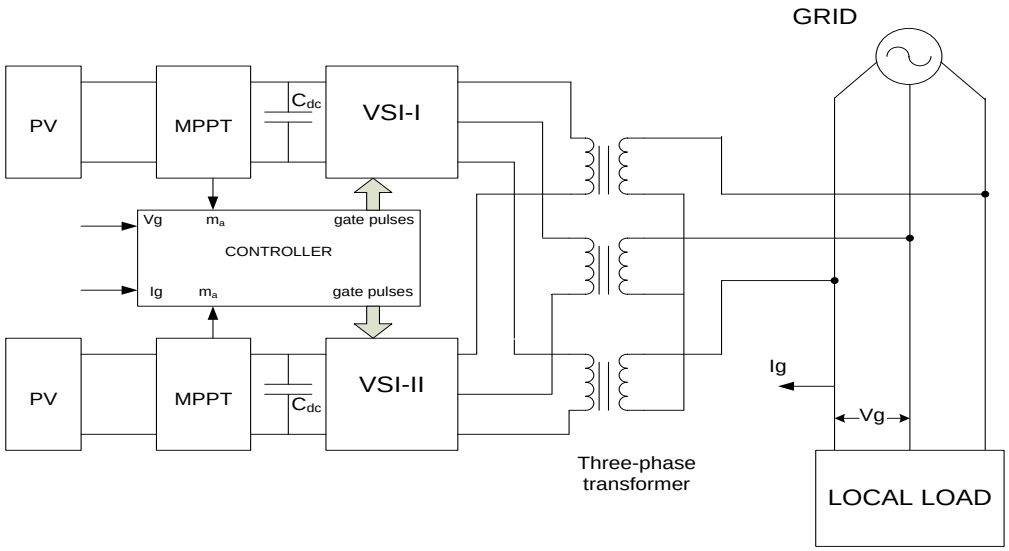

Figure 3-3: Grid connected PV system

3.3 CONTROL METHOD

The proposed inverter is used in a grid connected PV system. Therefore a PI controller is used to keep the output current sinusoidal and to have high dynamic performance under rapidly changing atmospheric condition. The amount of electric power generation by solar module is always changing with weather condition. To extract the maximum power at any given atmospheric conditions, MPPT is used. MPPT algorithm will ensure that maximum power is delivered from solar module. Here perturb & observation (P&O) algorithm is used.

The feedback controller used in this application utilized the PI algorithm (Selvaraj Rahim, 2009). As shown in Figure 3-4, the current injected into the grid I_g is sensed and fed back to a comparator which compares it with the reference current I_{ref}. I_{ref} is obtained by measuring the grid voltage and multiplying it with variable m_a. Therefore,

$$I_{ref} = m_a V_g \qquad (3.3)$$

Here m_a is a modulation index obtained from MPPT to generate I_{ref}.

Variable m_a is dependent on the solar irradiation. Therefore,

m_a α Solar irradiation

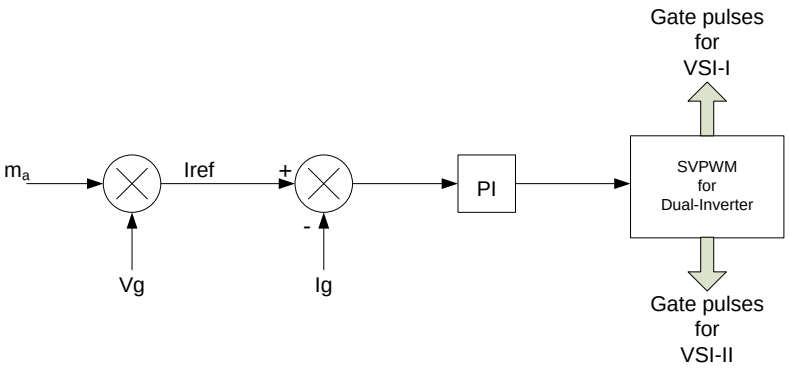

Figure 3-4: Controller used to generate firing pulses for two inverters

The PI algorithm shown in Figure 3-4, can be expressed in the continuous time

domain as, $u(t) = K_p e(t) + K_i \int_{\tau=0}^{t} e(\tau) d\tau$ (3.4)

where, error *e(t)*= set point-plant output

K_p = Proportional gain

K_i = Integral gain

The reference signal is generated in this way is fed to the dual converter SVPWM algorithm which is already explained above.

3.4 DUAL INVERTER TOPOLOGY FOR A THREE LEVEL INVERTER

Recently, open - end winding structure multilevel inverter topology for Induction Motor drive is being used (Stemmler and Geggenbach, 1993; Shivakumar *et al*., 2002; Baiju *et al*., 2004; Mohapatra *et al*., 2003; Somasekhar *et al*., 2004; Somasekhar *et al*., 2007) because of the various advantages compared to the conventional topologies like DC-MLI, FC-MLI and H-Bridge MLI. The open end winding scheme consists of two 2-level inverters as shown in Figure 3-5. Hence this topology is also known as dual inverter topology. The open-end winding scheme is free from capacitor voltage unbalance issues of three-level NPC inverter, doesn't require any clamping diodes and additional capacitor banks are not needed as in flying capacitor multilevel inverter topology.

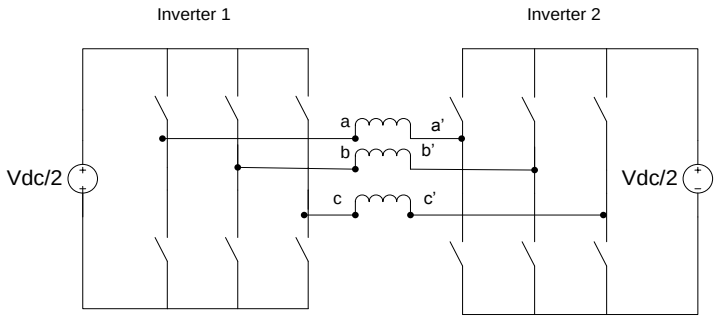

Figure 3-5: Schematic of a Dual-inverter topology

In the scheme, that shown in Figure 3-5, each two level inverter is capable of producing two voltage levels at the inverter pole namely, '$V_{dc}/2$' and '0' which are represented as switching symbols '+' and '-' respectively. With this topology, it is possible to switch two two-level inverters independently; thereby each inverter will have 8 switching states as shown in Figure 3-6. Therefore, a total 64 (8 X 8) switching combinations are possible for a conventional open-end winding three-level inverter topology, which are spread over 19 locations, as shown in Figure 3-7.

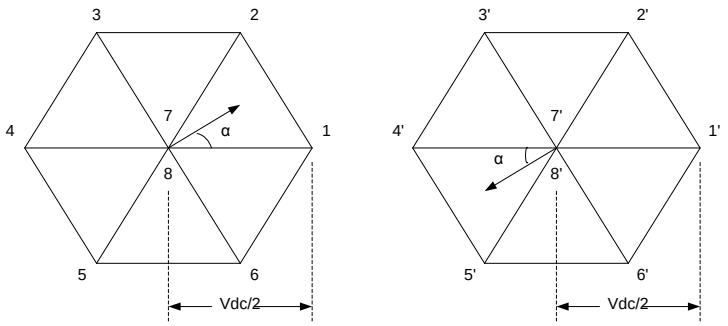

Figure 3-6: Voltage vector locations for inverter –I and II

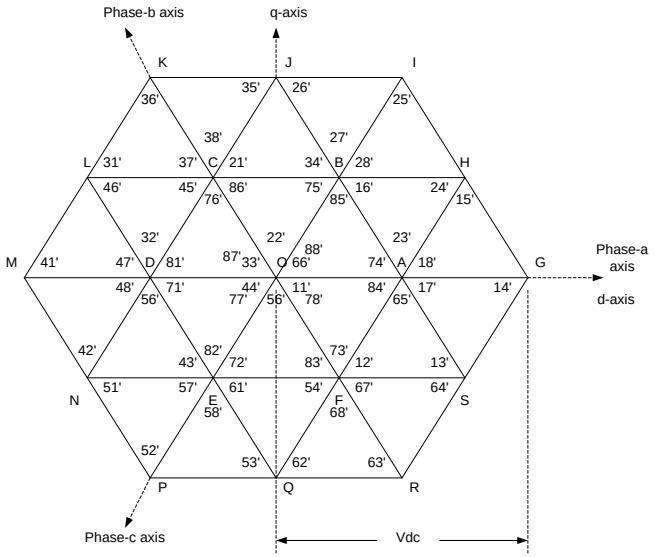

Figure 3-7: Switching states and space vector locations of open-end winding three level inverter

In the Figure 3-5, open end primary winding of a three phase transformer is fed from two 2-level inverters at the two ends. The DC power supply at the two inverter inputs is isolated to suppress the zero sequence components in the transformer phase windings. In case of a single DC power supply, zero sequence voltages (common-mode voltages) are generated across the phase windings which may lead to flow of zero-sequence current in the transformer windings. When isolated DC power supplies are used for individual inverters, the zero sequence current cannot flow as it is denied a path.

3.4.1Nearest sub-hexagon centre PWM Algorithm

The space vector algorithm for a dual inverter can be obtained by using this simple nearest sub-hexagon centre (NSHC) PWM algorithm (Somasekhar *et al*., 2008). It can be also observed from the Figure 3-7 that the core hexagon ABCDEF with centered O can be plotted by single inverter to obtain the other hexagons with centers A, B, C, D, E, F respectively. The hexagons namely OBHGSF, OCJIHA, ODLKJB, OENMLC, OFQPND and OASRQE are called as sub-hexagons. The centers A, B, C, D, E, F are called as sub-hexagons centers (SHCs). The resultant space vector combination locations shown in Figure 3-7 are obtained by superposing the space vector locations resulting from the inverter-2 at each space vector location caused by the inverter-1. All the seven locations of a given sub hexagonal center (i.e six vertices and the

corresponding sub hexagonal center) show redundancy of space vector combinations. For the sub hexagon OFSGHB, the space vector combinations for these seven locations may alternatively be obtained by clamping inverter-2 to state -4 (- + +) while the other inverter switches in all eight states. The NSHC scheme is based on the observation that the space vector combinations at the vertices and the center of a given sub hexagon are obtained by clamping one inverter with an active state, while the other inverter switches in all eight states. The center of the nearest sub hexagon is obtained from the instantaneous reference voltage quantities. In the Figure 3-8, vector OT represents the reference vector with its tip located in sector 8 (in the triangle AHB). It is resolved into two components OA and AT. The vector OA may be output of inverter-1which is clamped to state 1 (+ - -) through the sampling interval and the vector AT may be the output of other inverter-2, which is switched in all eight states.

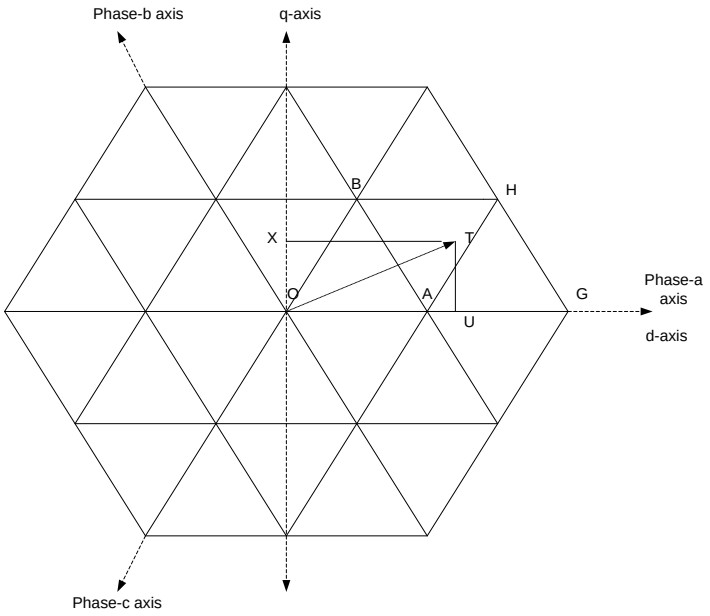

Figure 3-8: Switching vector components along d and q axis

In other words, inverter-2 is switched with center A (the nearest sub hexagon center of OFSGHB). Otherwise the first vector OA is the output of the inverter -2 which is clamped to the state 1(+ - -) and the vector AT is generated by switching the inverter -1. At each step of the interval the NSHC is identified by resolving the OT vector into two components and the first component is the output of the one inverter by clamped to an active state and other inverter is switched in all eight centers. In this scheme for

the odd numbered centers inverter -1 is clamped i.e for A, C, E sub hexagon centers and the inverter -2 is switched, and for the other centers i.e B, D, F center sub hexagons inverter -2 is clamped and inverter -1 is switched. The roles of the individual inverters at each center are summarized in Table 3-8.

The instantaneous phase reference voltage denoted by V_{as}, V_{bs}, V_{cs} corresponding to the reference voltage space vector OT are obtained by projecting the tip of OT onto the respective phase axes and multiplying them by a factor (2/3). The symbols V_{ds} and V_{qs} denote the components of OT on the d and q axes, respectively. The reference voltages corresponding to the actual switching vector AT, denoted by V_a, V_b and V_c, are obtained by the following procedure:

Table 3-8: Roles of each inverter in NSH centers

	A	B	C	D	E	F
Inverter – 1	Clamped to state-1(+--)	Switching mode	Clamped to state-3(-+-)	Switching mode	Clamped to state-5(--+)	Switching mode
Inverter – 2	Switching mode	Clamped to state-2(++-)	Switching mode	Clamped to state-4(-++)	Switching mode	Clamped to state-6(+-+)

1. By using classical 3 phase to 2 phase transformation method we can obtain the equivalent two-phase system references V_{ds} and V_{qs} of the reference vector OT from the instantaneous phase reference voltages V_{as}, V_{bs} and V_{cs}.

$$\begin{bmatrix} Vds \\ Vqs \end{bmatrix} = \begin{bmatrix} \frac{3}{2} & 0 & 0 \\ 0 & \frac{\sqrt{3}}{2} & -\frac{\sqrt{3}}{2} \end{bmatrix} \begin{bmatrix} Vas \\ Vbs \\ Vcs \end{bmatrix} \qquad (3.5)$$

2. The Sub Hexagonal Center situated nearest to the tip of the reference vector OT is then determined.

3. The coordinates of the NSHC in the $V_d - V_q$ plane (the point 'A' in this example, Figure 3-9), denoted by V_{dnshc} and V_{qnshc} are identified for all the six Sub Hexagonal Centers. For example, the coordinates of the point 'A' in the $V_d - V_q$ plane are given by ($V_{dc}/2$, 0), similarly the coordinates of the point 'D' in the $V_d - V_q$ plane are given by ($-V_{dc}/2$, 0).

4. Since the vector OA is output by the clamping inverter, the coordinates of the switching vector (AT in the present case) denoted by V_{dsw} and V_{qsw} are given by

$$V_{dsw} = V_{ds} - V_{dnshc} \qquad (3.6)$$

$$V_{qsw} = V_{qs} - V_{qnshc} \qquad (3.7)$$

5. By using the classical two-phase to three-phase transformation, the modified reference phase voltages V_{asw}, V_{bsw} and V_{csw} for the switching inverter are then obtained by transforming V_{dsw}, V_{qsw} into the corresponding three-phase variables.

$$\begin{bmatrix} Vasw \\ Vbsw \\ Vcsw \end{bmatrix} = \begin{bmatrix} \frac{2}{3} & 0 \\ -\frac{1}{3} & \frac{1}{\sqrt{3}} \\ -\frac{1}{3} & -\frac{1}{\sqrt{3}} \end{bmatrix} \begin{bmatrix} Vdsw \\ Vqsw \end{bmatrix} \qquad (3.8)$$

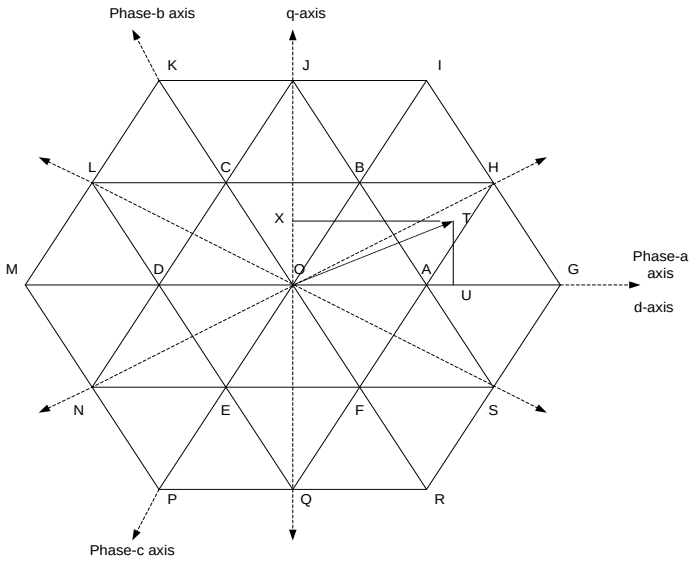

Figure 3-9: Principle of NSH switching scheme

6. If inverter-2 is employed as the clamping inverter, the modified references are used directly to generate the switching vector AT with inverter-1. On the other hand, if inverter-1 is used as the clamping inverter, it is obvious that the modified references must be negated to generate the switching vector AT with inverter-2.

7. It is important to note that the most important part of this algorithm is to find the nearest sub hexagonal center to the tip of the reference vector OT. The instantaneous reference voltages V_{as}, V_{bs} and V_{cs} normalized with respect to V_{sr} and their respective negations are shown in Figure 3-10.

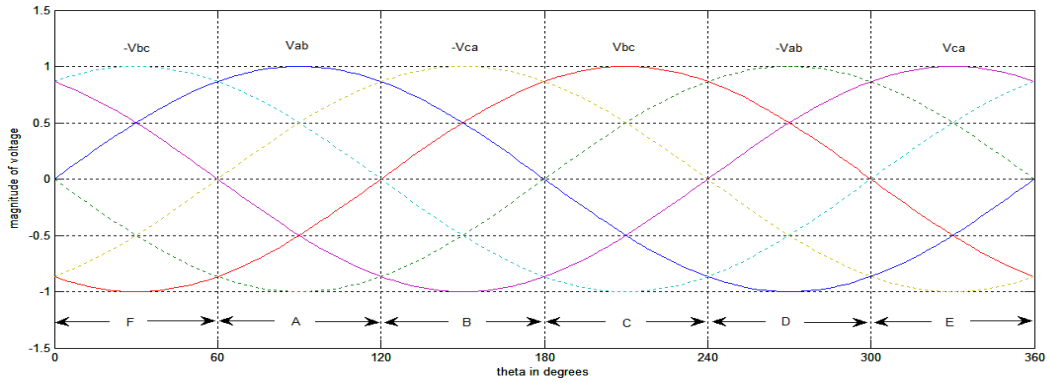

Figure 3-10: Recognition of the nearest sub hexagonal centers with instantaneous reference quantities

From the Figure 3-10, it may be noted that V_{as} is more positive quantity amongst these six quantities when $60^o \leq \theta \leq 120^o$ and A is the nearest sub hexagonal center as recognized by Figure 3-9. Similarly $-V_{as}$ is the most positive amongst these six quantities when $240^o \leq \theta \leq 300^o$ and D is the nearest sub hexagonal center. Thus it is clear that by finding the maximum value amongst these six quantities, one can determine the nearest sub hexagonal center.

The overall SVPWM algorithm of a dual inverter is shown in Figure 3-11. The reference signal generated by the control method used is initially transformed into its 2-phase equivalent. The magnitude and angle of this reference signal is obtained using rectangular to polar transformation block available in the simulation tool of MATLAB/Simulink. The angle of the reference signal provides the information about the sector in which the reference signal lies at any sampling instant. Also the angle

information is used to find the NSHC using the step 7 of the above mentioned procedure. The coordinates of each of the NSHC's are known in advance and hence this data is used to generate switching signals for a clamping inverter. Depending upon the location of reference signal vector, the d and q axis coordinates of the sub hexagon centre are subtracted from the coordinates of the reference vector. This data is then converted into three phase equivalent and samples for switching inverter are generated using normal 2-level SVPWM algorithm. In this way the gating signals for the two inverters (clamping and switching) are generated at every sampling instants. The function of each inverter i.e. inverter-I and inverter-II is again decided by the location of reference vector or sector.

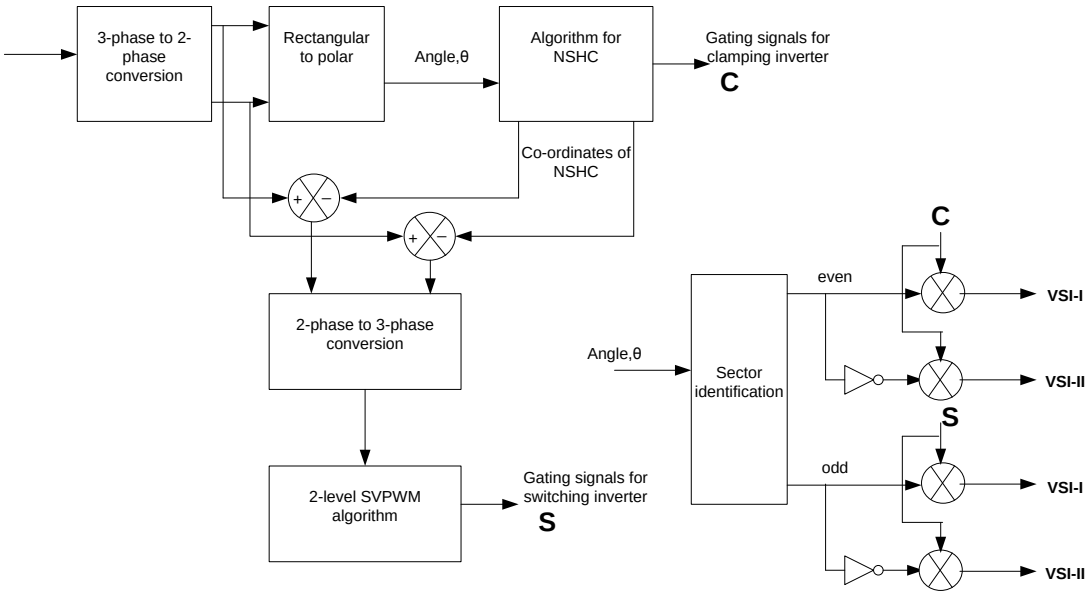

Figure 3-11: The dual inverter SVPWM functional diagram

3.5 RESULTS AND DISCUSSION

The grid connected system as shown in Figure 3-3 is modeled and then simulated in MATLAB/Simulink. The various parameters used for simulation are given in Table 3-9. A grid of 230V, 50 Hz is considered and a three phase R-L load is connected across it. A PV system of 12 kW peak is connected to this system. The overall system

is simulated for different PV operating conditions. Also the local load connected to the system is varied to test the dynamics of the model.

Table 3-9: Simulation parameters (three-level PV system)

Location	Parameter	Value
PV	Total no of modules Maximum power generated by PV array	$N_s x N_p = 15x4 = 60$ 200x60 = 12000 W
Interconnecting Transformer	Open primary, star connected secondary	10kVA, 500V/500V
Grid	Grid voltage at 50 Hz	230 V
Load	(i)Three phase R-L load (ii)Three phase R-L load	5 kVA 5kVA+1.7kVA

For simplicity let us consider the entire operation of the system in different modes. These modes are represented in terms of simulation time. Figure 3-12, Figure 3-13 and Figure 3-14 show the operation of this system in different modes.

Mode I: Here the system operates without PV power injection. From Figure 3-12, it is clear that the source current is equal to the load current. The PV injects no current into the grid system. This can be observed from t=0 to t=0.1 sec. Figure 3-13 shows that the active power demand of the load is supplied by the grid. Figure 3-14 shows the dual inverter phase voltage during this interval.

Mode II: Now at t=0.1 sec PV power generated is added to the grid. The PV power generated depends upon the operating conditions of the PV system namely the solar insolation and the cell temperature. This operation is carried out during the simulation interval of t=0.1sec to 0.2 sec. three-level VSI is connected to the system with 320W of PV power generation. The corresponding grid, PV and load currents are shown in Figure 3-12. Now the grid/source current is reduced. The active power demand of the load is shared by grid and PV as shown in Figure 3-13. The grid and PV active power together has to compensate for the load active power demand as well as the inverter switching losses and transformer losses.

Mode III: In this mode the system is tested for change in PV power generated such that now the PV power generated is more than the local load demand. At t=0.2 sec of simulation time, the PV system operating conditions are changed such that now it generates power of 1500W per phase which is more than the load active power (1100W per phase) demand. As seen from Figure 3-13, the grid active power is now negative which means that PV feeds extra power generated into the grid. The grid current direction is reversed as seen from Figure 3-12 for this time interval. Also the PV current magnitude is increased. The system takes time of around 1-2 cycles to stabilize to new values of operation.

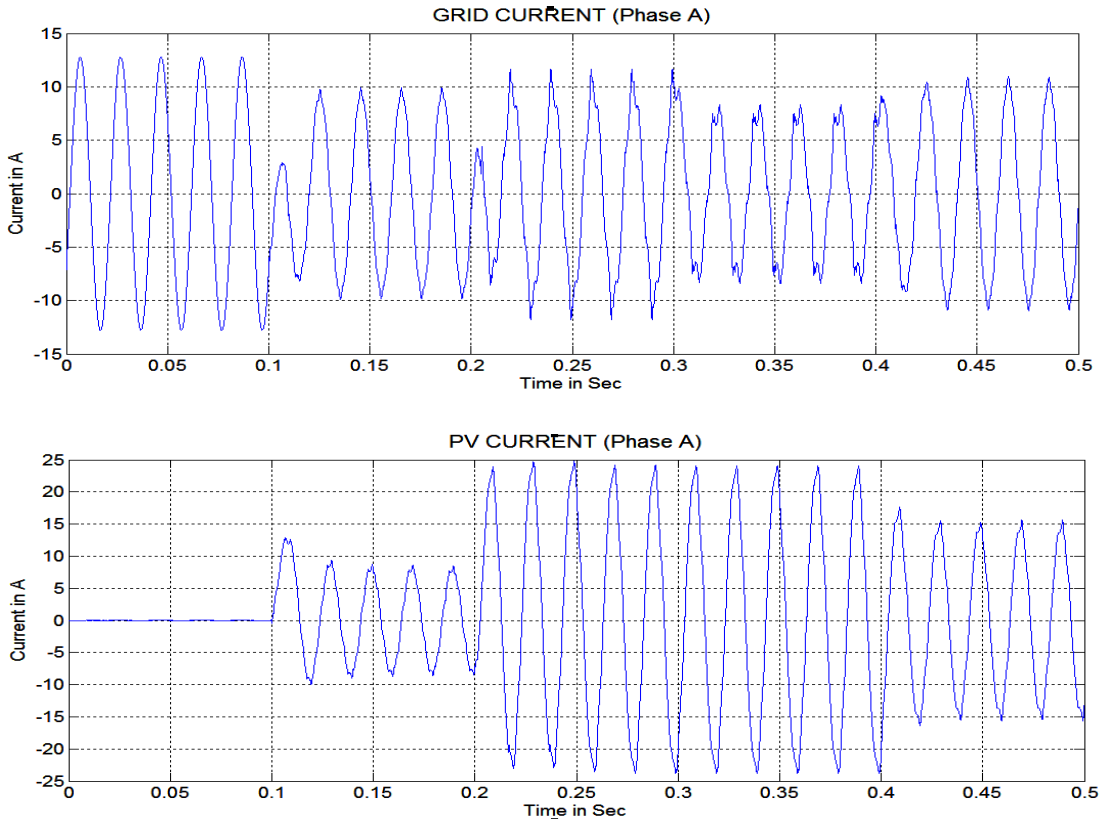

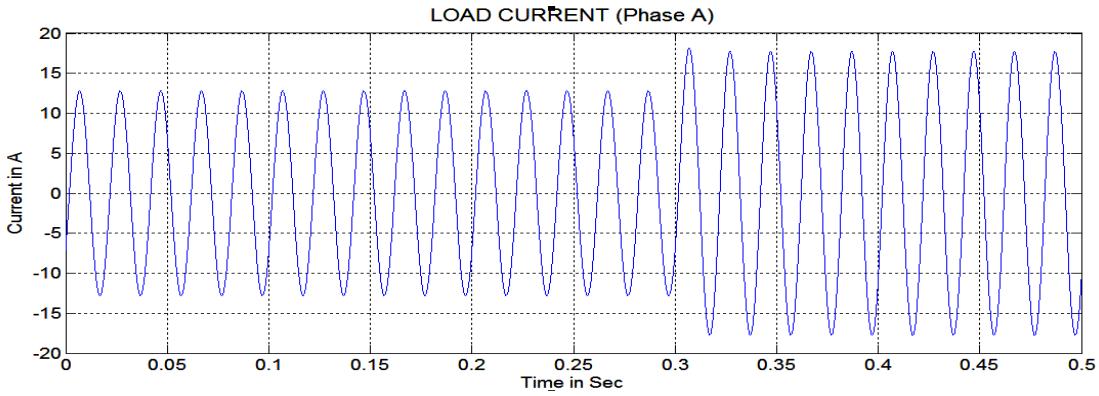

Figure 3-12: Currents at different points

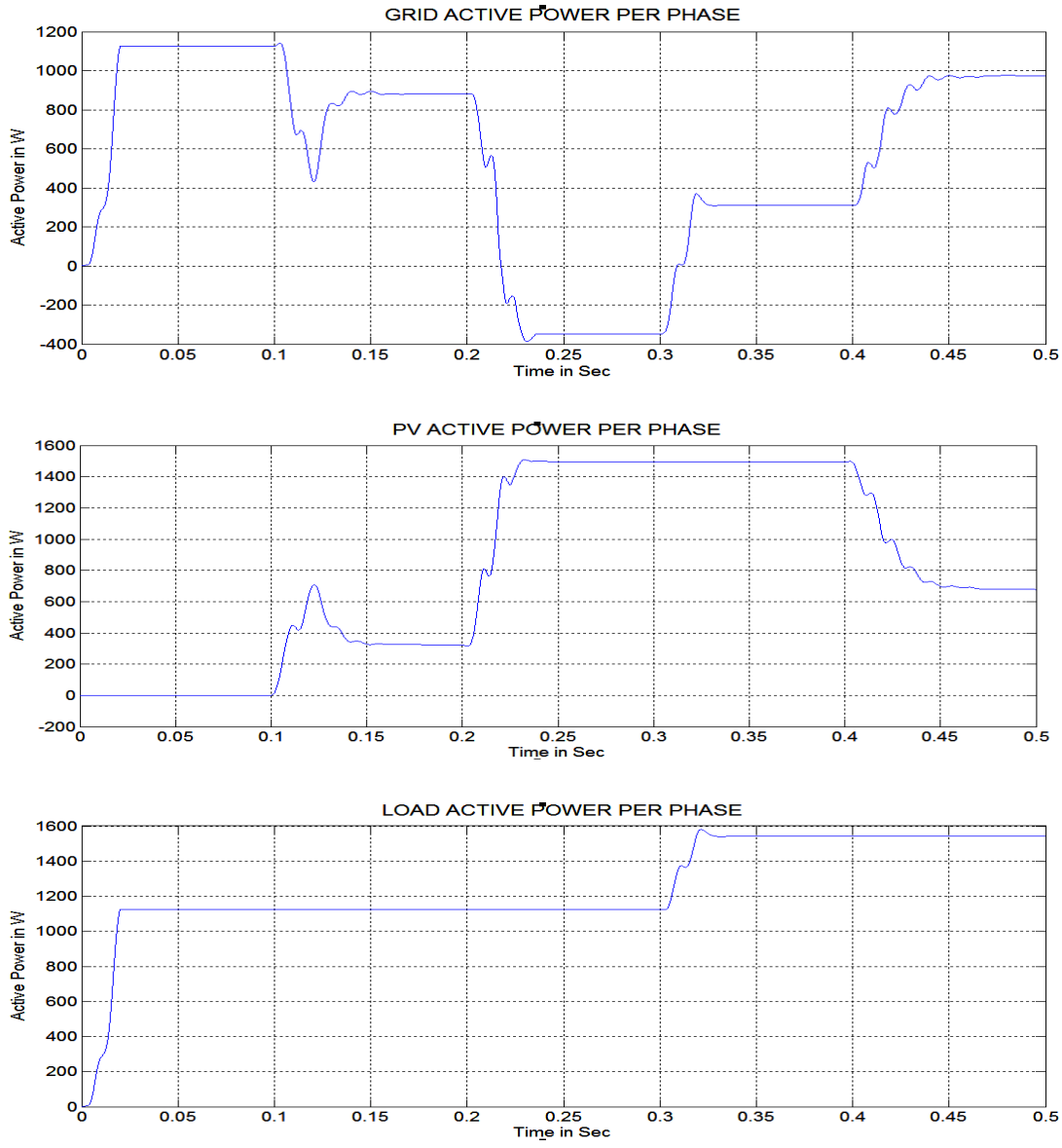

Figure 3-13: Active power distribution

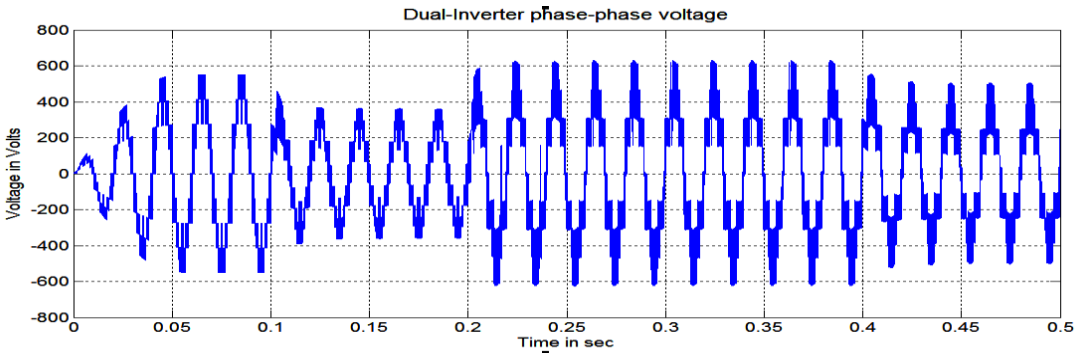

Figure 3-14: Dual-Inverter output phase-phase voltage

Mode IV: Now with PV system operating conditions remaining same the local load of the system is increased to see its effect on the overall performance of the system. So at t=0.3 sec of simulation time, the local load on the system is increased by another 400 W per phase keeping PV generated power same. Now the total load active power demand is more than the PV generated power. Hence the extra load power demand is partly shared by the PV and the grid. Out of total load power of 1550 W, PV shares 1500W of power whereas remaining load power and the loss power is shared by the grid.

Mode V: Now with the new load conditions of increased load, at t=0.4 sec of simulation time the PV generated power is decreased to 700W per phase. Accordingly there is change in grid current and active power as seen in Figure 3-12 and Figure 3-13. Now the PV current and power is reduced while gird current and power is increased.

The inverter phase voltage in all these modes of operation is shown in Figure 3-14.

3.6 CONCLUSION

This chapter presented the modeling and simulation of a grid connected PV system. Firstly, a brief study on PV characteristics and modeling is carried out. A suitable MPPT method to extract the maximum power generated by PV source is included. Then various three level topologies used are covered in the study. The PV current is injected into the grid through a three-level dual inverter. The active power supplied by

the PV system depending on environmental condition is injected into the grid. The local load active power is compensated by the PV system depending upon the PV power generated at the given instant. All the benefits of a multilevel inverter can be used in such a system. Also the control algorithm is very simple and easy to implement. An attempt has been made here to use the dual inverter topology in a grid connected PV system. The system is simulated to study the use of dual three-level inverter in grid connected PV system at different atmospheric and load conditions.

Chapter 4 : A NOVEL SHUNT ACTIVE POWER FILTER TOPOLOGY

4.1 INTRODUCTION

In past, majority of the loads in power distribution systems were constant in nature with respect to power, impedance, current or any of their combinations e.g. incandescent lamp, heaters, AC motors etc. However in recent years with the developments in the field of semiconductor devices the requirement for more efficient and automated loads has significantly changed the nature of loads. The modern power distribution system has to feed more and more nonlinear loads intermittently to save power. This nonlinearity results in non-sinusoidal periodic waves and in turn harmonics. Besides harmonics the power distribution systems also suffer from other issues like high reactive current or low power factor, unbalanced active and reactive power demand, voltage unbalance etc. non-sinusoidal and unbalanced voltage and/or current have several adverse effects on utilities and load connected to it. Hence an effective elimination of harmonics, unbalance and improvement of power factor is essential for the utilities and the end users. As a consequence, the issue of power quality is being paid significant attention in academic and industrial research. In this chapter a three level voltage source converter is studied as an active power filter. A novel dual inverter shunt active power filter is introduced in this chapter.

4.1.1 Active filter control strategies

The control strategy of active filter has a great impact not only on the compensation objectives and required KVA of active filters, but also on the filtering characteristics in transient state as well as in steady-state. Control strategy is the heart of the AF and is implemented in three stages. In the first stage, the essential voltage and current signals are sensed using power transformers (PTs), CTs, Hall-effect sensors, and isolation amplifiers to gather accurate system information. In the second stage, compensating commands in terms of current or voltage levels are derived based on control methods and AF configurations. In the third stage of control, the gating signals for the solid-state devices of the AF are generated using PWM, hysteresis, sliding-mode, or fuzzy-logic-based control techniques. The control of the AF's is

realized using discrete analog and digital devices or advanced microelectronic devices, such as single-chip microcomputers, DSPs etc.

There are numerous techniques based on time as well as frequency-domain, to calculate the appropriate compensating reference current signals. Both, time-domain and frequency-domain techniques are used for the voltage source type and current source type PWM converters.

The two most commonly used control techniques are:

a. Instantaneous Reactive Power Theory

(Akagi *et al.* 1984) proposed a concept based on the theory of instantaneous reactive power in the *α-β* reference frame; this theory stimulates the realization of three phase, three-wire APFs. According to the instantaneous reactive power theory (IRPT), unless used for harmonic cancellation, there is no need to use an energy-storage device in the APF implementation for reactive power compensation. The instantaneous value of voltage and current in a three-phase system can be represented by instantaneous space vectors. In *a-b-c* coordinates, *a*, *b* and *c*-axis are on the same plane, but separated by 120°, as shown in Figure 4-1. The supply voltage and the load current (v_{sa}, i_{La}) in phase-*a* are set on the *a*-axis, similarly (v_{sb}, i_{Lb}) are set on the *b*-axis, and (v_{sc}, i_{Lc}) are set on the *c*-axis. Their amplitude and direction vary with the passage of time.

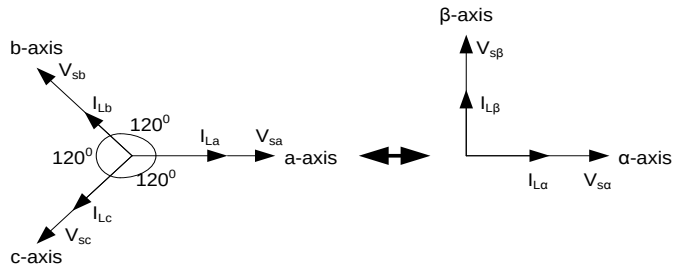

Figure 4-1: Three-phase to two-phase conversion.

In this theory, the instantaneous source voltage and current signals in *a-b-c* coordinates are transformed into two-phases *i.e. α-β* orthogonal coordinates as follows.

$$\begin{bmatrix} V_{s\alpha} \\ V_{s\beta} \end{bmatrix} = \sqrt{\frac{2}{3}} \begin{bmatrix} 1 & -\frac{1}{2} & -\frac{1}{2} \\ 0 & \frac{\sqrt{3}}{2} & -\frac{\sqrt{3}}{2} \end{bmatrix} \begin{bmatrix} V_{sa} \\ V_{sb} \\ V_{sc} \end{bmatrix} \qquad (4.1)$$

$$\begin{bmatrix} i_{L\alpha} \\ i_{L\beta} \end{bmatrix} = \sqrt{\frac{2}{3}} \begin{bmatrix} 1 & -\frac{1}{2} & -\frac{1}{2} \\ 0 & \frac{\sqrt{3}}{2} & -\frac{\sqrt{3}}{2} \end{bmatrix} \begin{bmatrix} i_{La} \\ i_{Lb} \\ i_{Lc} \end{bmatrix} \qquad (4.2)$$

For simplicity, the zero-phase sequence component voltage and current signals are eliminated in (4.1) and (4.2). The instantaneous active power (p) and the instantaneous imaginary power (q) in a three-phase circuit are defined in (4.3).

$$\begin{bmatrix} p \\ q \end{bmatrix} = \begin{bmatrix} V_{s\alpha} & V_{s\beta} \\ -V_{s\beta} & V_{s\alpha} \end{bmatrix} \begin{bmatrix} i_{L\alpha} \\ i_{L\beta} \end{bmatrix} \qquad (4.3)$$

Using (4.3) load current in α-β frame can be calculated as:

$$\begin{bmatrix} i_{L\alpha} \\ i_{L\beta} \end{bmatrix} = \frac{1}{V_{s\alpha}^2 + V_{s\beta}^2} \begin{bmatrix} V_{s\alpha} & V_{s\beta} \\ -V_{s\beta} & V_{s\alpha} \end{bmatrix} \begin{bmatrix} p \\ q \end{bmatrix} \qquad (4.4)$$

The block diagram of this method is as shown in Figure 4-2.

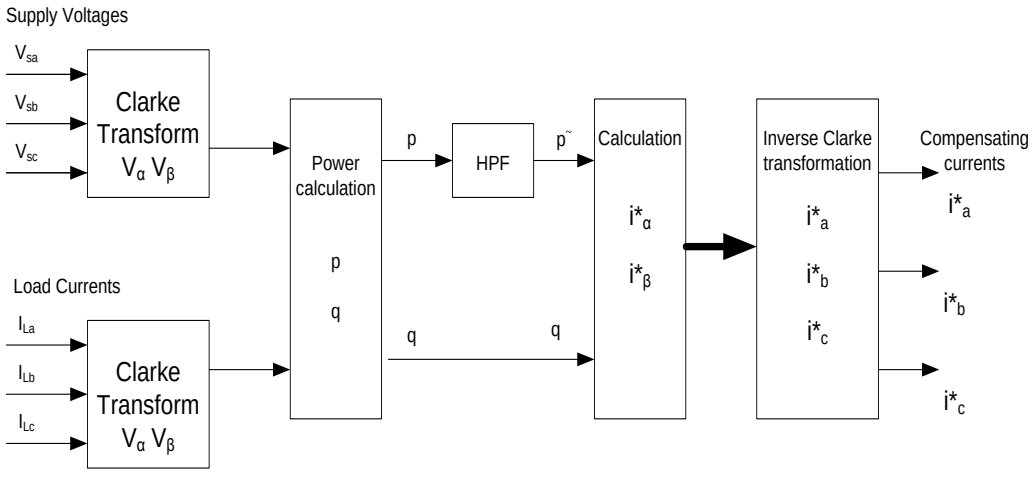

Figure 4-2: Block diagram of the instantaneous reactive power theory.

The reference compensating current can be calculated in such a way that it supplies the instantaneous reactive power (q) and the harmonic component of the instantaneous active power (p~). The reference compensating current (i_c^*) can be obtained as:

$$\begin{bmatrix} i^*_{c\alpha} \\ i^*_{c\beta} \end{bmatrix} = \frac{1}{V_{s\alpha}^2 + V_{s\beta}^2} \begin{bmatrix} V_{s\alpha} & V_{s\beta} \\ -V_{s\beta} & V_{s\alpha} \end{bmatrix} \begin{bmatrix} p \\ q \end{bmatrix} \qquad (4.5)$$

The compensating current signals in *α-β* frame can be transferred to *a-b-c* frame using inverse Clark's transformation as:

$$\begin{bmatrix} i^*_{ca} \\ i^*_{cb} \\ i^*_{cc} \end{bmatrix} = \sqrt{\frac{2}{3}} \begin{bmatrix} 1 & 0 \\ -\frac{1}{2} & \frac{\sqrt{3}}{2} \\ -\frac{1}{2} & -\frac{\sqrt{3}}{2} \end{bmatrix} \begin{bmatrix} i^*_{c\alpha} \\ i^*_{c\beta} \end{bmatrix} \qquad (4.6)$$

This method does not take into account the zero sequence components, and hence, the effect of unbalanced voltages and currents. The instantaneous reactive power (*p-q*) theory is widely used for three-phase balanced non-linear loads, such as rectifiers.

b. Synchronous Reference Frame

The active power filter control algorithm, based on synchronous reference frame (SRF) method (Nabae and Tanaka, 1996), relies on Clarke's and Park's transformations, as shown in Figure 4-3. In this method, the load current signals are first transformed into synchronous reference (*dq0*) frame. The fundamental component of the load current after transformation is a DC value and the harmonics appear like a ripple over this DC offset. A low power filter is used to separate harmonic components from the load current. The active power loss component is subtracted from this current to get the reference d and q component of filter currents. Then reference current in abc frame is obtained using inverse transformation. The reference current is compared with actual filter current and the error current is used by the hysteresis controller to generate the pulses. In general the rotating frame dq0 is obtained from abc quantities by the following transformation.

$$\begin{bmatrix} x_0 \\ x_d \\ x_q \end{bmatrix} = \sqrt{\frac{2}{3}} \begin{bmatrix} \frac{1}{\sqrt{2}} & \frac{1}{\sqrt{2}} & \frac{1}{\sqrt{2}} \\ \cos\theta & \cos(\theta - \frac{2\pi}{3}) & \cos(\theta + \frac{2\pi}{3}) \\ \sin\theta & \sin(\theta - \frac{2\pi}{3}) & \sin(\theta + \frac{2\pi}{3}) \end{bmatrix} \begin{bmatrix} x_a \\ x_b \\ x_c \end{bmatrix} \quad (4.7)$$

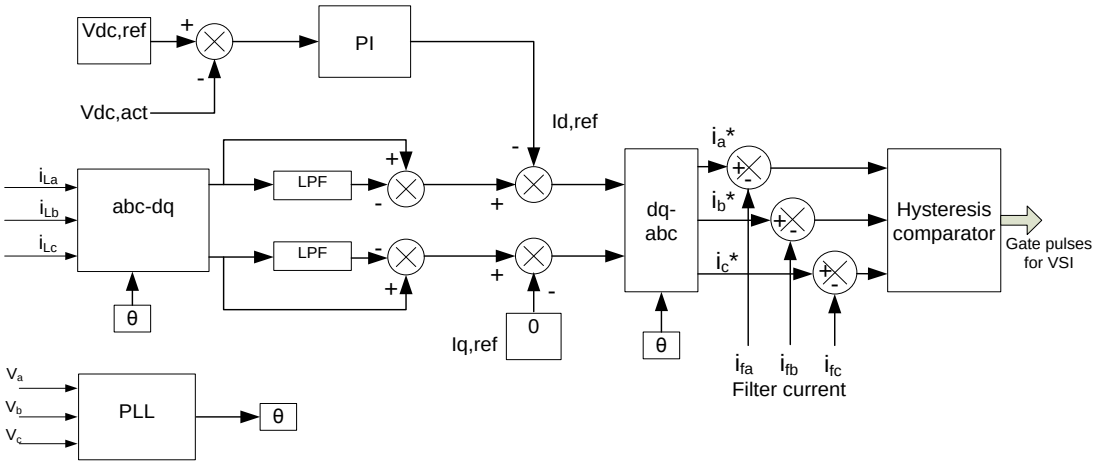

Figure 4-3: Block diagram of SRF method.

For synchronization, a PLL is used which derives phase angle θ from the AC supply voltage.

c. Indirect power control method

The instantaneous source voltage of any one phase, say v_{sa}, actual DC-bus capacitor voltage V_{dc} and the actual instantaneous source currents (i_{sa}, i_{sb}, i_{sc}) are the main inputs to the algorithm. To maintain a constant DC-bus capacitor voltage in the CC-VSI, the error $V_e(k)$ between the square values of reference DC-bus capacitor voltage and actual DC-bus capacitor voltage at the kth sampling instant is computed as:

$$V_e(k) = V^2_{dcref} - V^2_{dc}(k) \quad (4.8)$$

where, $V_{dc,ref}$ is the reference dc-bus capacitor voltage and $V_{dc}(k)$ is the actual DC-bus capacitor voltage at k^{th} sampling instant. This DC-bus capacitor voltage error is processed through a PI controller. The output of the controller is considered as peak value I_{sm} of source currents at every sample which has two components. One of them

is the fundamental active component of load current and the other is loss component of the inverter circuit.

The output of the controller at k^{th} sampling instant in discrete system is given as:

$$I_{sm}(k) = K_{ep}V_e(k) + I_{sm}(k - 1) \qquad (4.9)$$

where, K_{ep} is the gain of the controller and $I_{sm}(k)$ and $I_{sm}(k-1)$ are the output of the controller at k^{th} and $(k-1)^{th}$ sampling instant, respectively. In the discrete system equation (4.9) can be written by taking its z transform as:

$$I_{sm}(z) = K_{ep}V_e(z) + z^{-1}I_{sm}(z) \qquad (4.10)$$

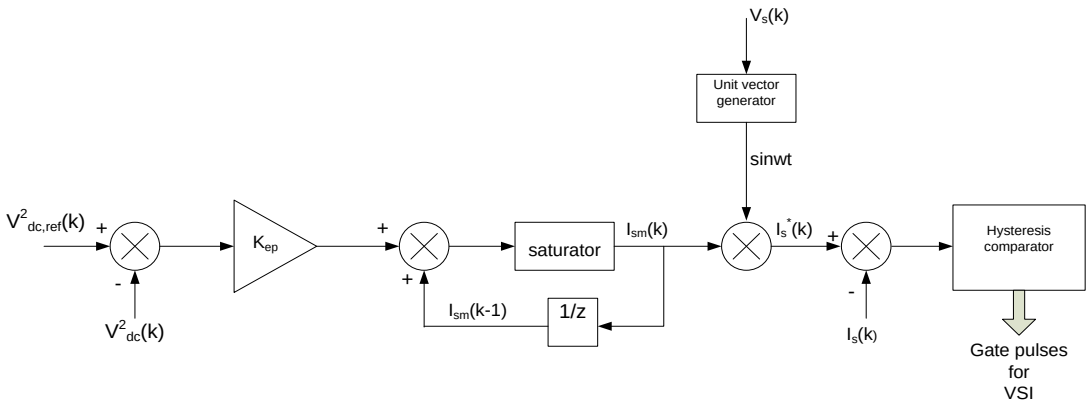

Figure 4-4: Control circuit

The various other control strategies used are already covered in the literature survey section of chapter 2.

To get to know the actual comparison between these various methods, simulations are carried on a common system using the three different control strategies mentioned above. Detailed analysis and comparison is covered in the next session.

4.1.2 Control strategies validation

All the three above mentioned control techniques are implemented for a common system that is represented in Figure 4-5. Here a three phase supply is used to feed a

non- linear load consisting of a diode bridge rectifier feeding RL load at its DC side. At PCC, a current controlled voltage source inverter (CC-VSI) is acting as SAPF. The DC side capacitor and AC side inductance of this VSI acts as filter components. The gate pulses to the inverter are generated by a hysteresis type pulse generator. The heart of APF is the reference current generator block. This unit takes voltage and/or current from the supply and/or load to generate the reference current depending upon the type of control strategy used.

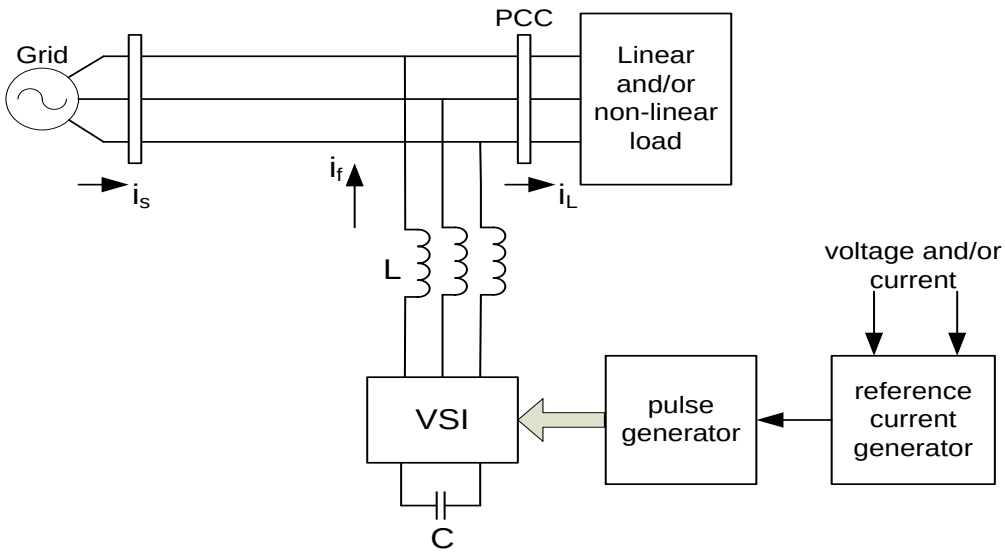

Figure 4-5: System description

4.1.3 Comparative Analysis

The system is simulated under two different conditions viz balanced and unbalanced system voltages. In both the cases load current, source current and the filter current are measured before and after the addition of APF. At t=0.4sec filter is added and the simulation is run for 4 sec. The source current THD before and after the addition of filter are also observed. The three different control strategies offer different performance and is summarized in the table 4.1 given below.

Table 4-1: Performance of three different control strategies

System/supply voltage	Parameter	pq control	dq control	Indirect power control
Balanced voltage	Load current THD	20.53	20.49	20.54
	Source current THD (after filtering)	1.74	3.29	1.95
	Displacement power factor	Near unity	poor	Near unity
Unbalanced voltage	Load current THD	21.29	21.22	22.69
	Source current THD (after filtering)	25.13	5.14	1.8
	Displacement power factor	Poor	poor	Near unity

The other important parameters to be considered while selecting the control strategy for APF are given in Table 4-2.

Table 4-2: Parameter comparison in three different control strategies

Parameter	pq control	dq control	Indirect power control
Number of conversions	Three	two	nil
Number of input signals(sensors) required	Two	three	three
PLL requirement	No	yes	yes
Complexity in digital implementation	More	more	less

Case (A): Balanced Supply Voltage Case:

(i) pq method: Figure 4-6 shows the currents at different nodes when the system voltage is balanced. The source power factor is illustrated in Figure 4-7.The load current and source current THD is shown in Figure 4-8 (a) and (b) respectively.

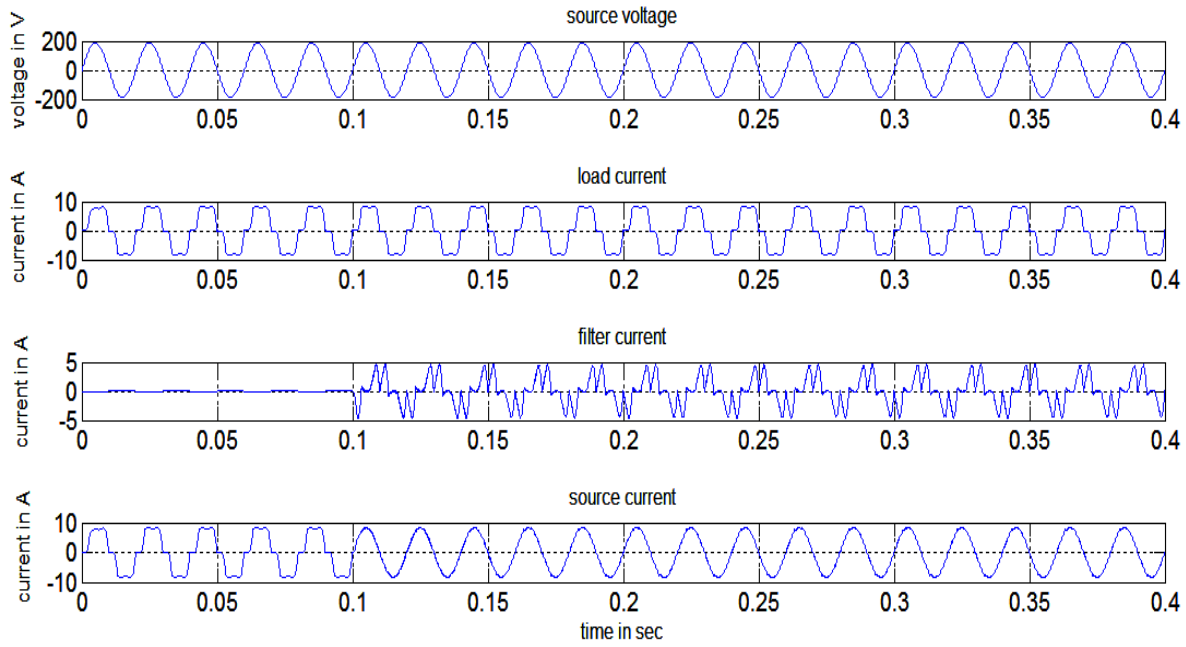

Figure 4-6: Pq method (balanced supply): Currents at different nodes

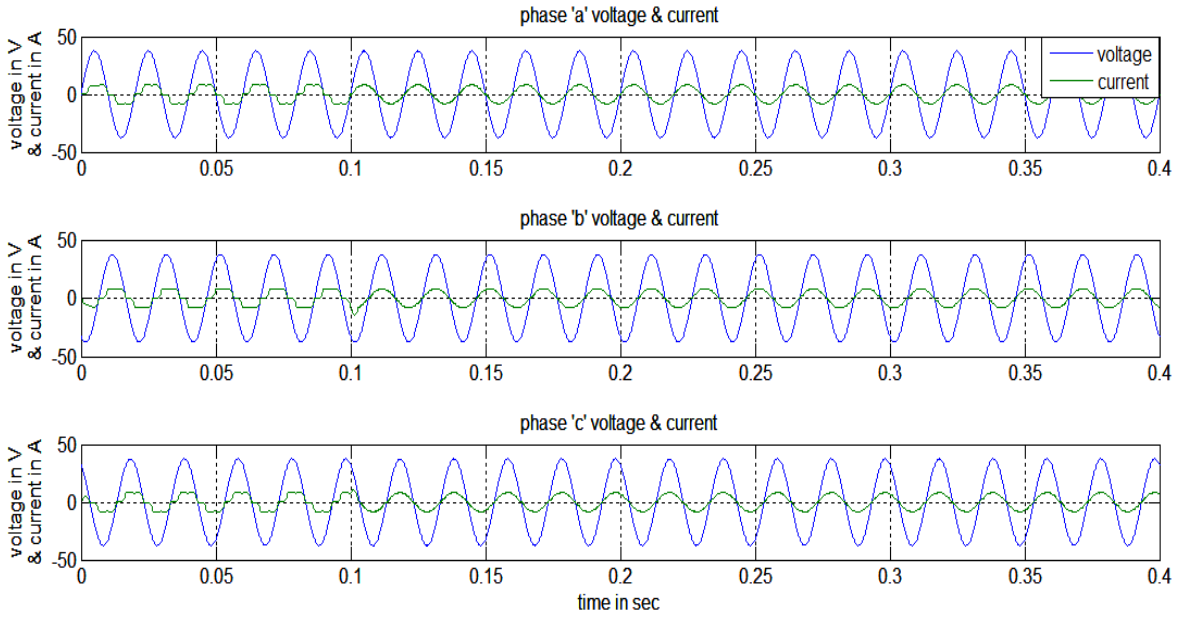

Figure 4-7: Pq method (balanced supply): Source voltage and current in three phases.

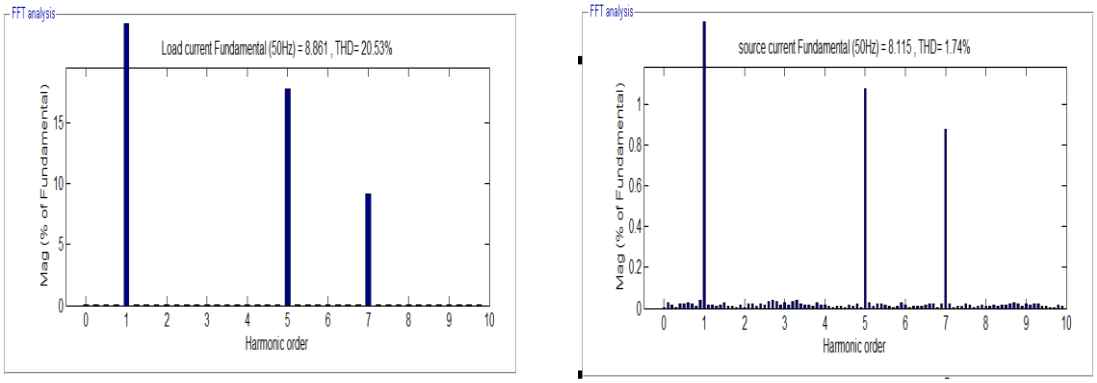

(a) (b)

Figure 4-8: Pq method (balanced supply):Load current and source current THD

(ii) dq method: Figure 4-9 shows the currents at different nodes when the system voltage is balanced. The source power factor is illustrated in Figure 4-10.The load current and source current THD is shown in Figure 4-11 (a) and (b) respectively.

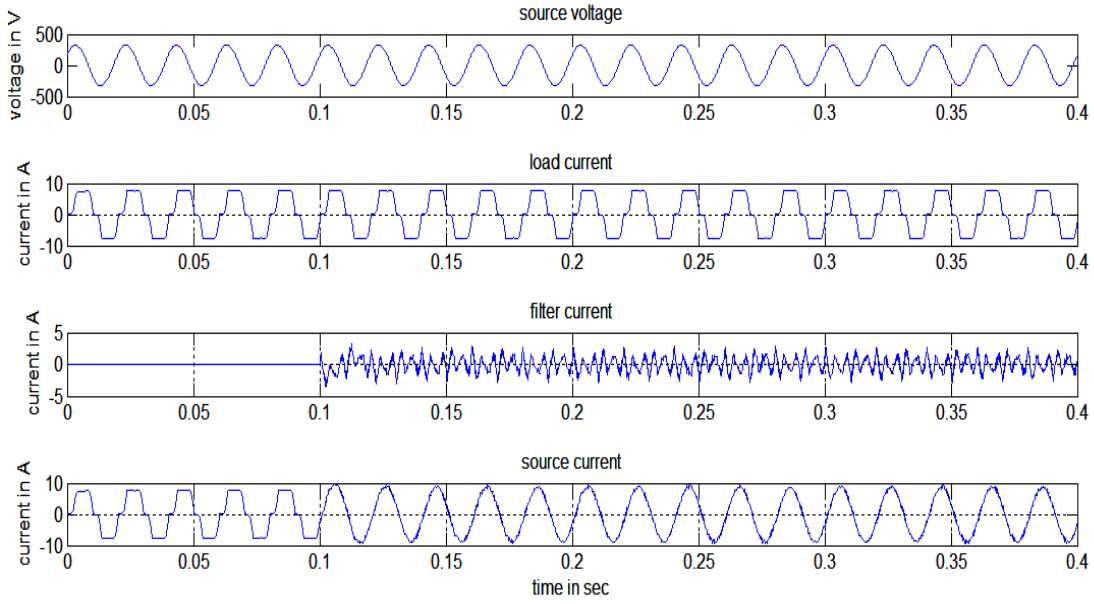

Figure 4-9: Dq method (balanced supply): Currents at different nodes

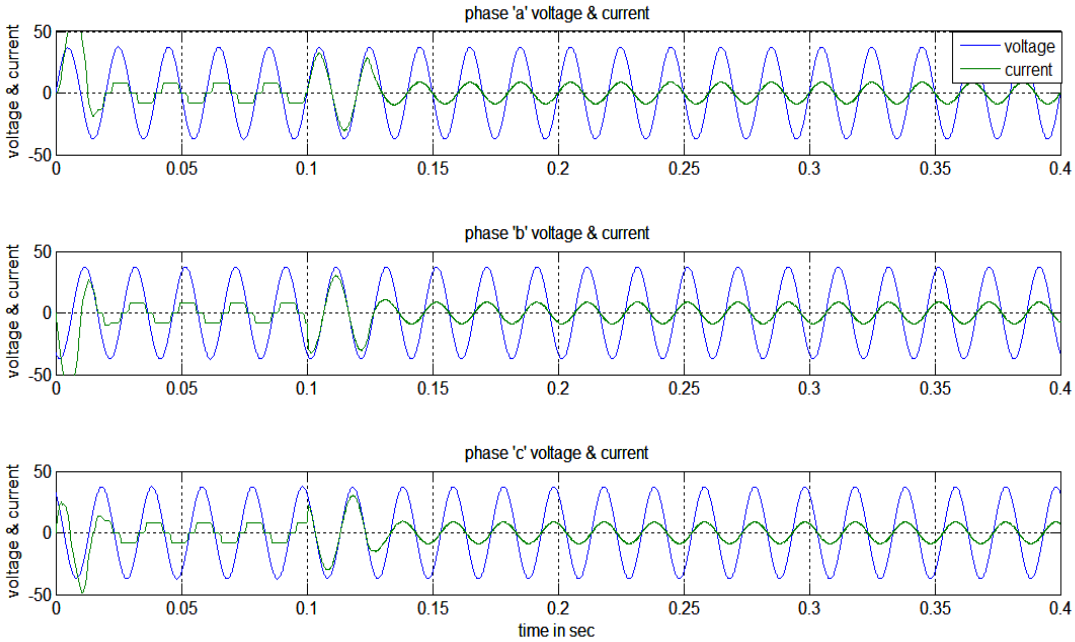

Figure 4-10: Dq method (balanced supply): Source voltage and current in three phases

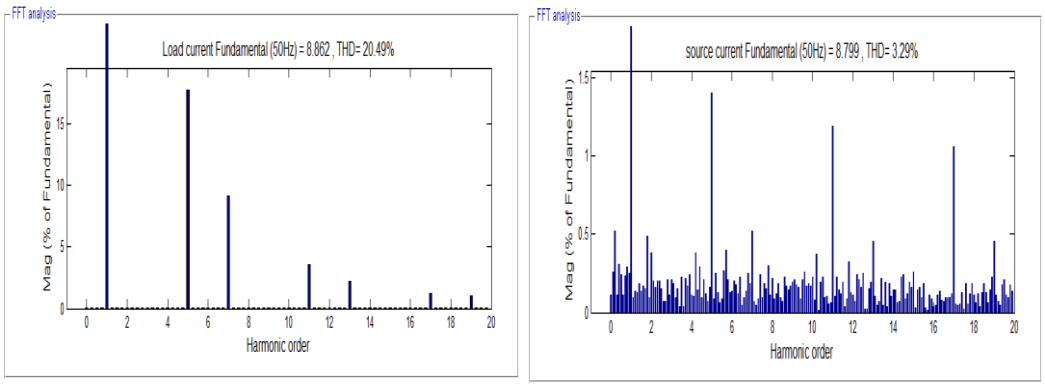

(a) (b)

Figure 4-11: Dq method (balanced supply): Load current and source current THD

(iii) Indirect Power: Figure 4-12 shows the currents at different nodes when the system voltage is balanced. The source power factor is illustrated in

(iv) Figure **4-13**.The load current and source current THD is shown in Figure 4-14 (a) and (b) respectively.

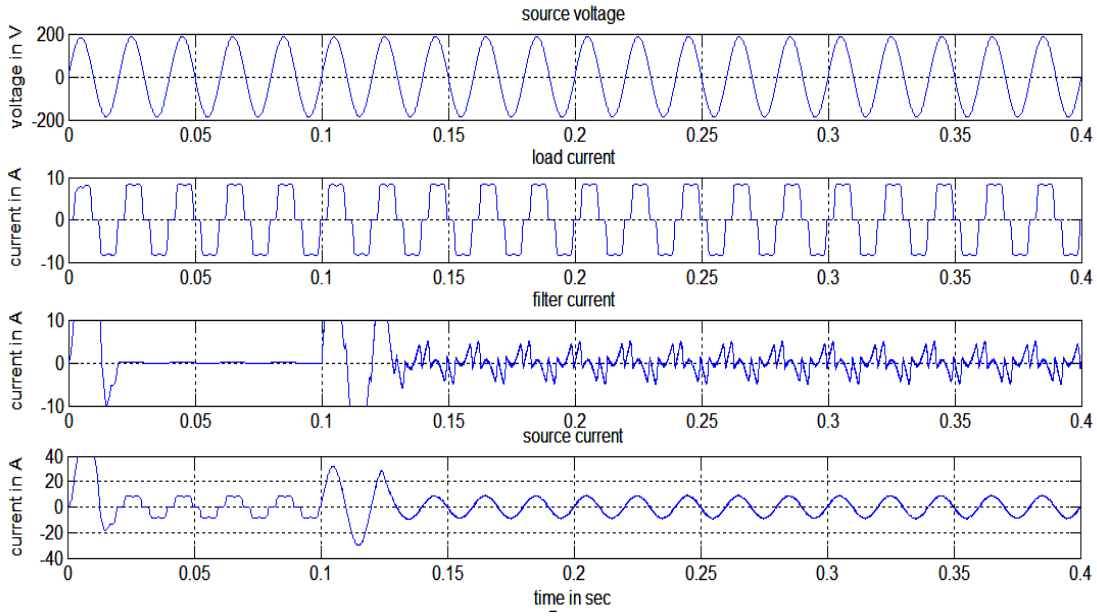

Figure 4-12**:** Indirect power method (balanced supply): Currents at different nodes

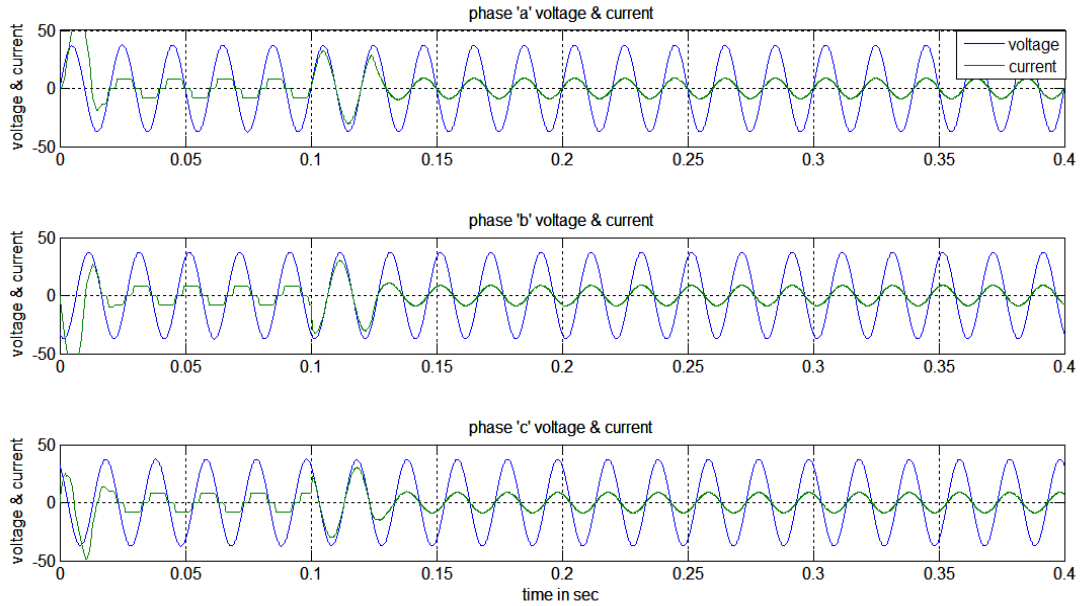

Figure 4-13: Indirect power method (balanced supply): Source voltage and current in three phases

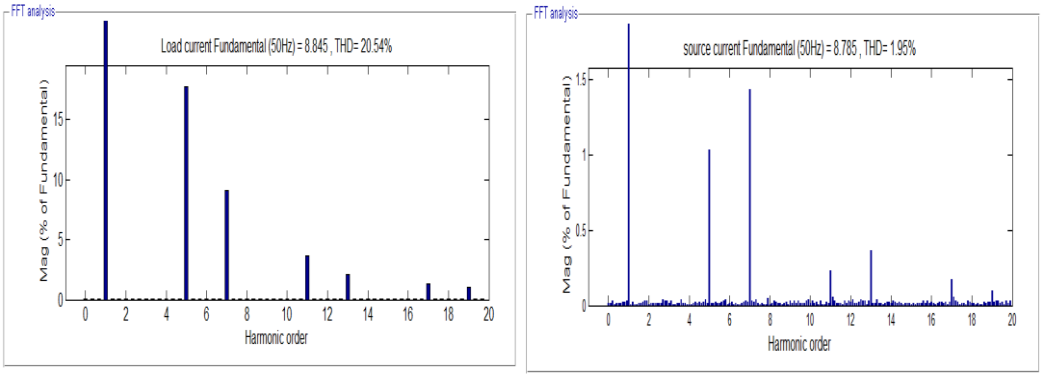

(a) (b)

Figure 4-14: Indirect power method (balanced supply): Load current and source current THD

Case B: Unbalanced Supply Voltage Case:

Now the supply voltage is made polluted with the introduction of 5^{th} and 7^{th} harmonic components.

(i) pq method: Figure 4-15 shows the currents at different nodes when the system voltage is balanced. The source power factor is illustrated in Figure 4-16.The supply voltage, load current and source current THD is shown in Figure 4-17 (a), (b) and (c) respectively.

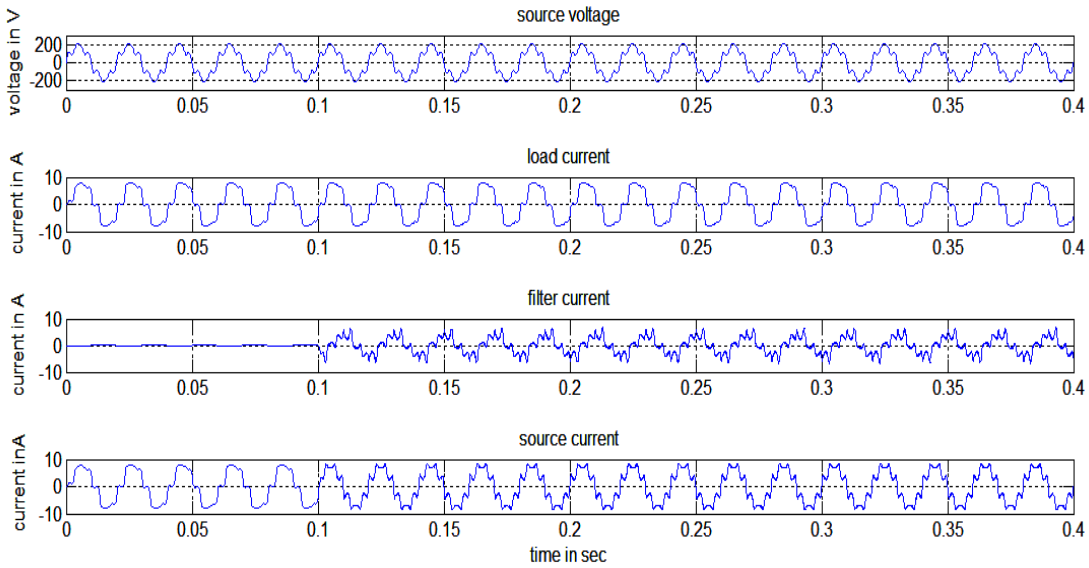

Figure 4-15: Pq method (unbalanced supply): Currents at different nodes

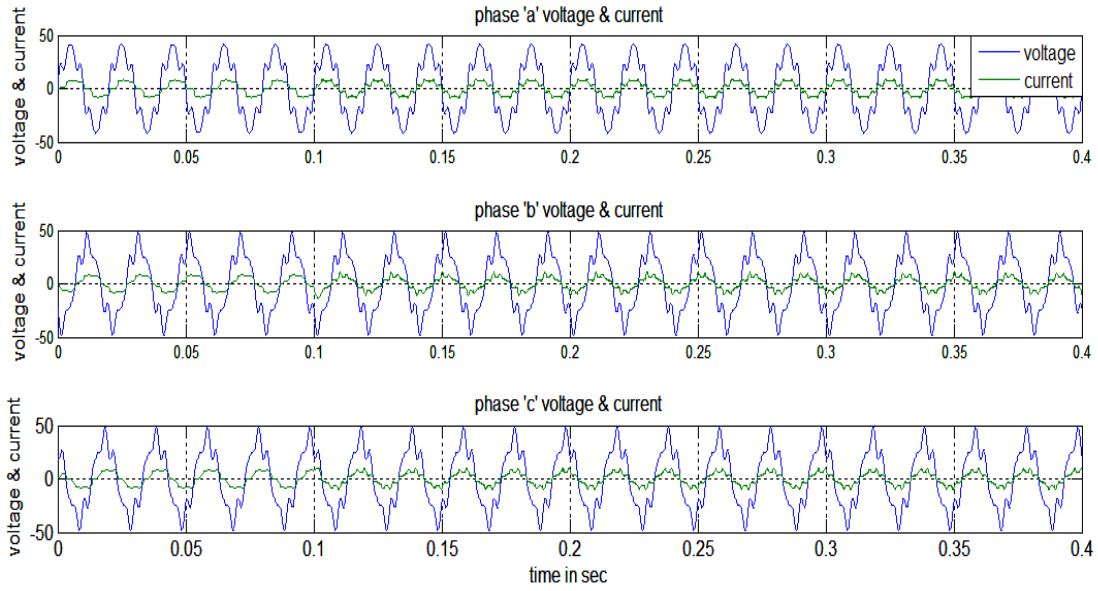

Figure 4-16: Pq method (unbalanced supply): Source voltage and current in three phases

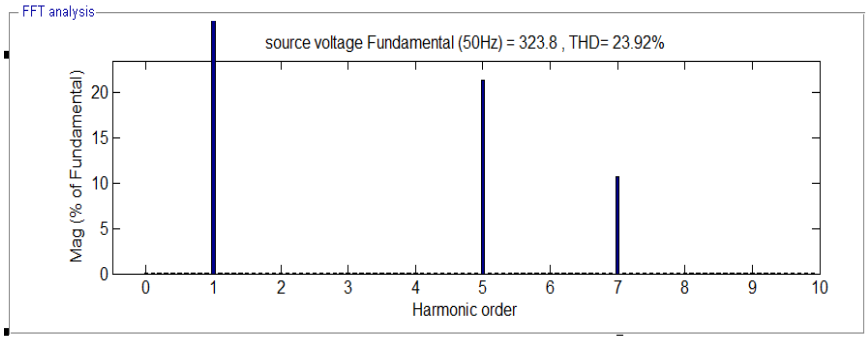

(a)

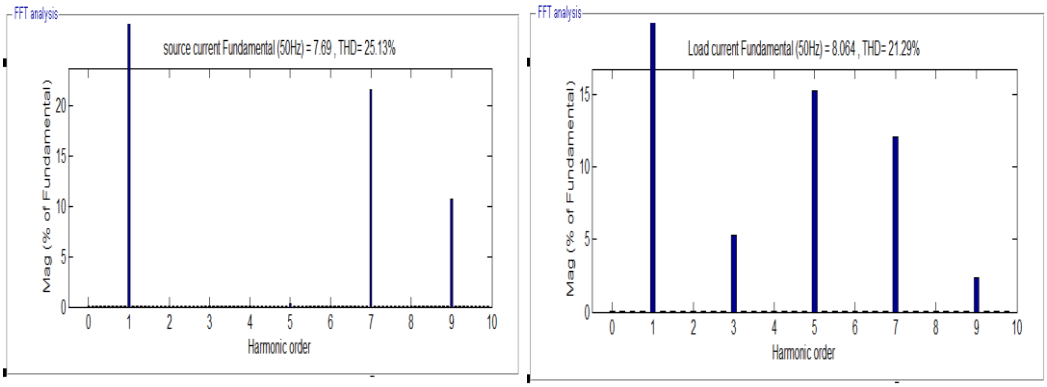

(b) (c)

Figure 4-17: Pq method (unbalanced supply): Source voltage, load current and source current THD

(ii) dq method: Figure 4-18 shows the currents at different nodes when the system voltage is balanced. The source power factor is illustrated in Figure 4-19. The supply voltage, load current and source current THD is shown in Figure 4-20 (a), (b) and (c) respectively.

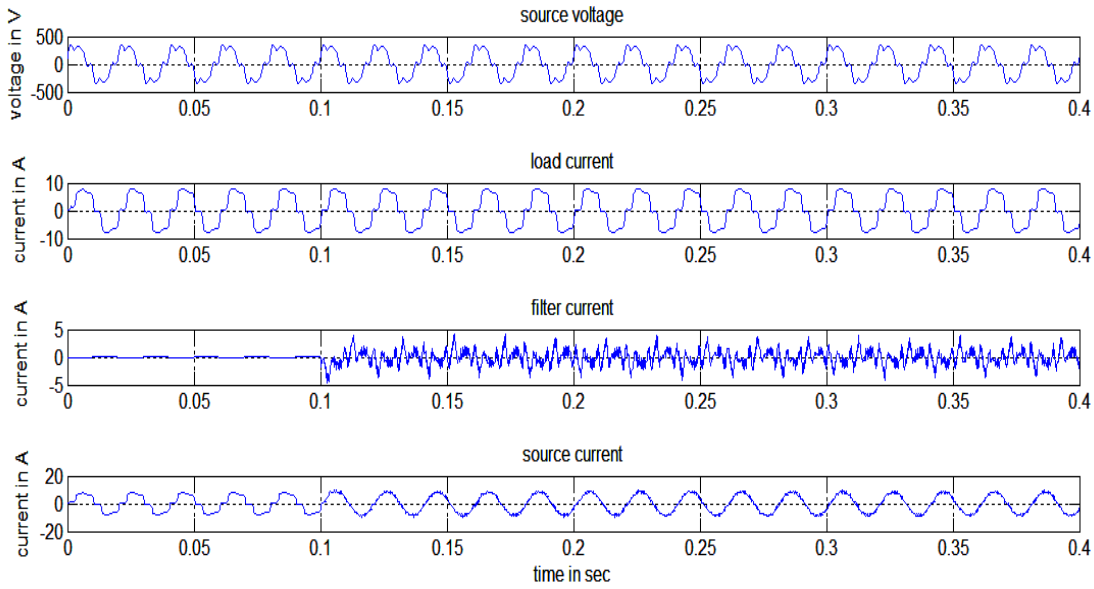

Figure 4-18: Dq method (unbalanced supply): Currents at different nodes

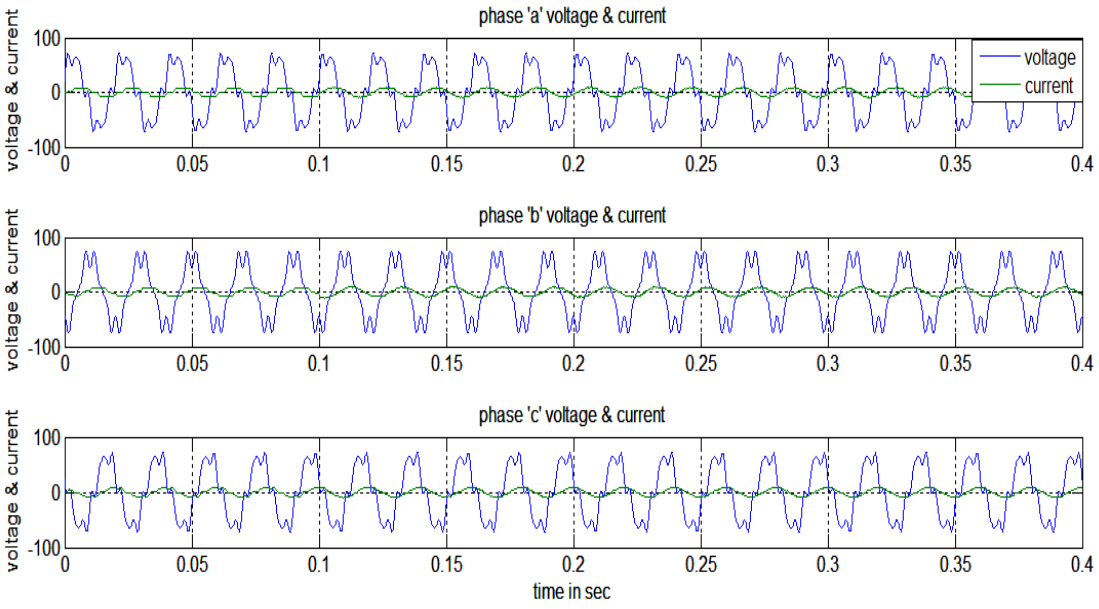

Figure 4-19: Dq method (unbalanced supply): Source voltage and current in three phases

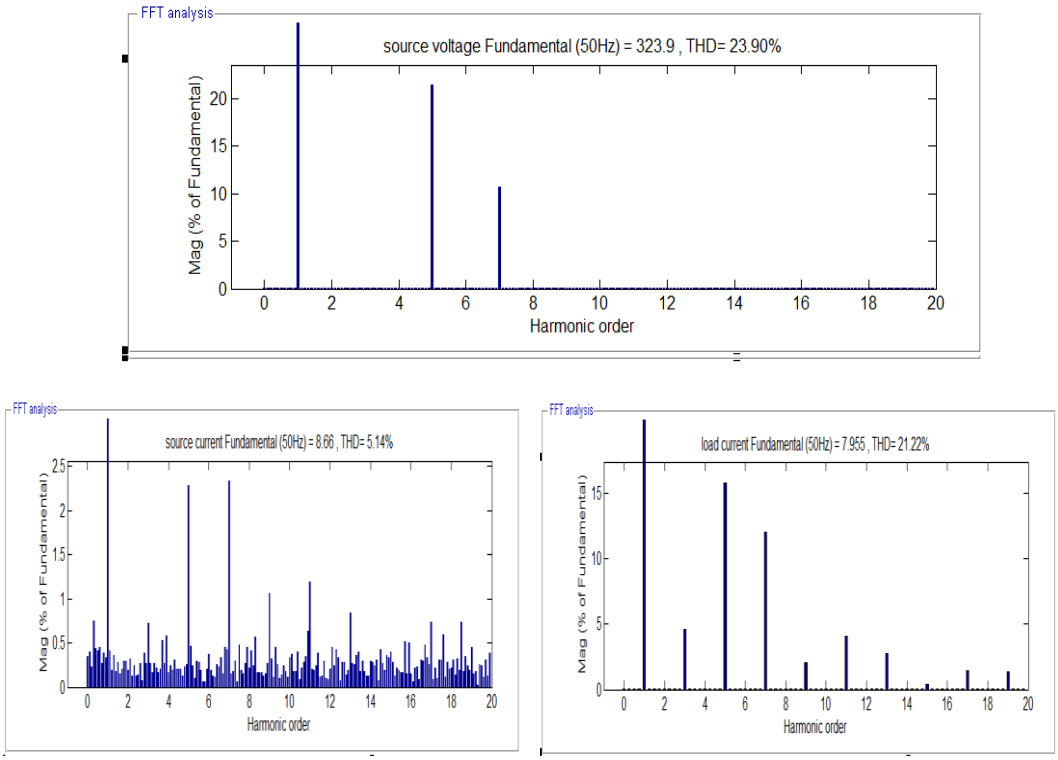

Figure 4-20: Dq method (unbalanced supply): Source voltage, load current and source current THD

(iii) Indirect Power: Figure 4-21 shows the currents at different nodes when the system voltage is balanced. The source power factor is illustrated in Figure 4-22.The supply voltage, load current and source current THD is shown in Figure 4-23 (a), (b) and (c) respectively.

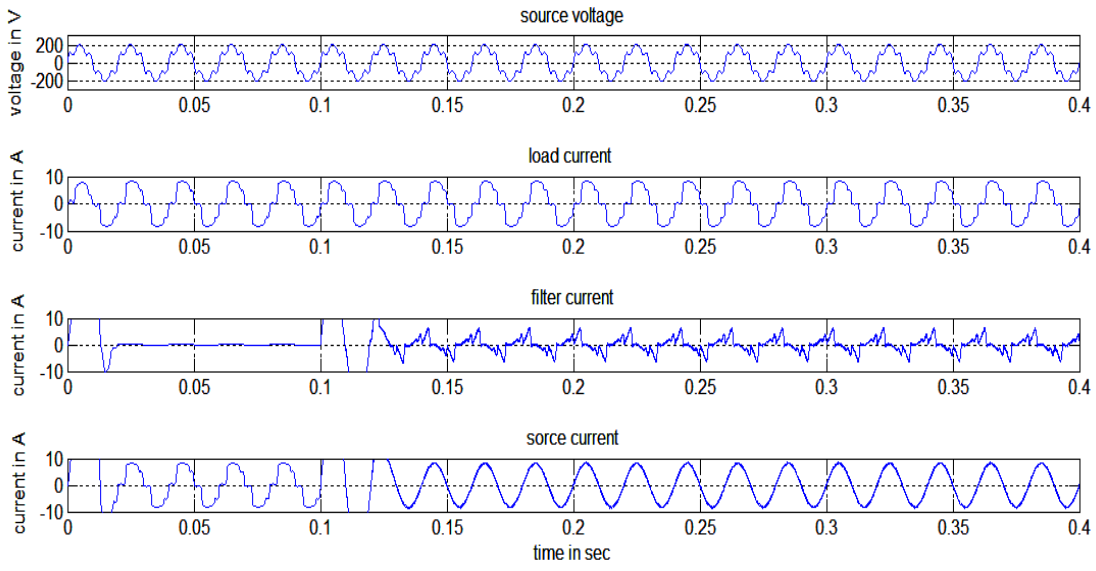

Figure 4-21: Indirect power method (unbalanced supply): Currents at different nodes

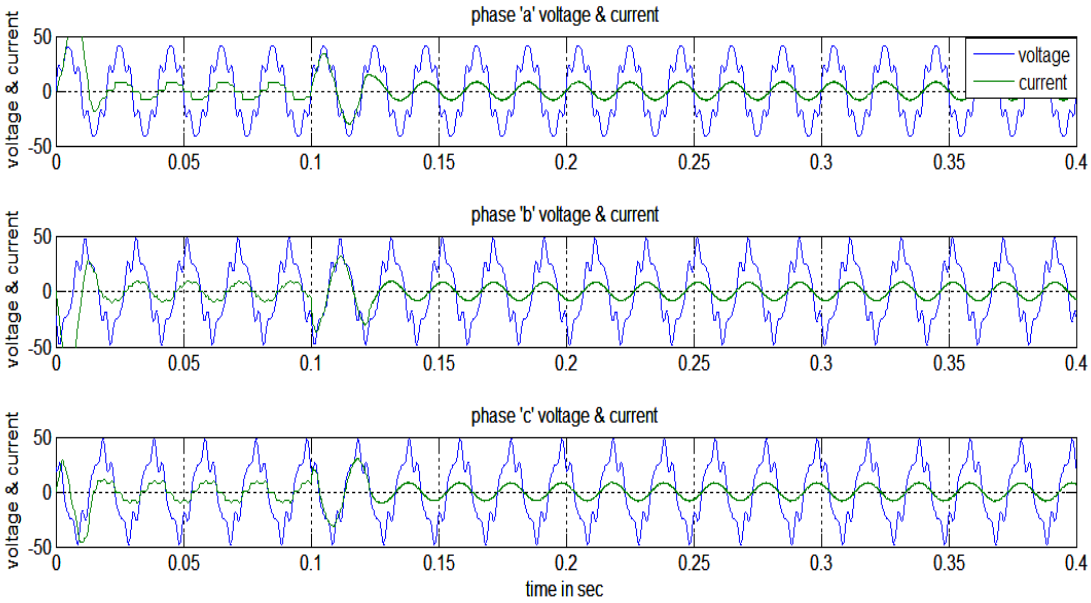

Figure 4-22: Indirect power method (unbalanced supply): Source voltage and current in three phases

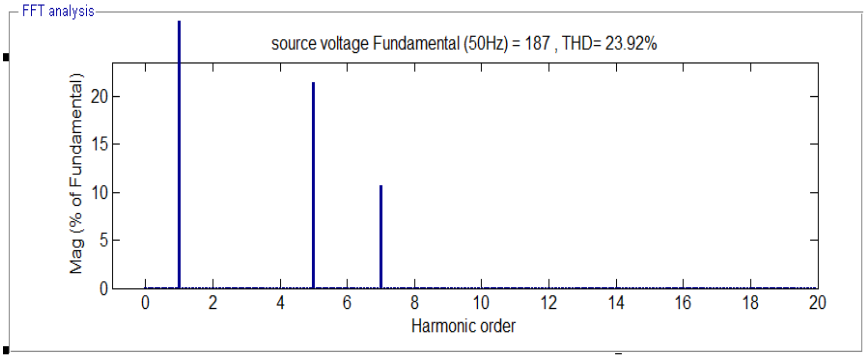

(a)

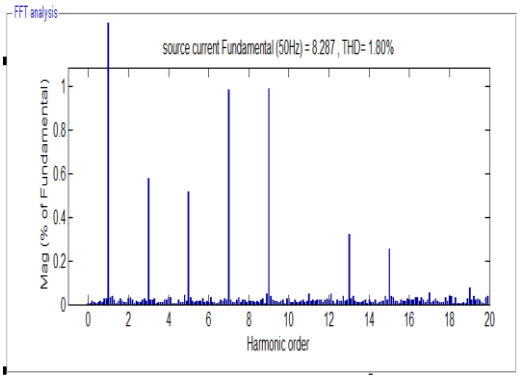

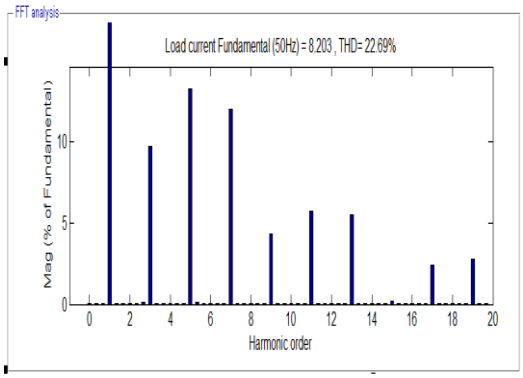

(b) (c)

Figure 4-23: Indirect power (unbalanced supply): Source voltage, load current and source current THD

4.1.4 Multilevel Active Power Filters

A Multilevel inverter is a power electronic device built to synthesize a desired A.C voltage from several levels of DC voltages. Multilevel inverters have gained more attention in high power applications because it has got many advantages. It can realize high voltage and high power output by using semiconductor switches without the use of transformer and dynamic voltage balance circuits. Active power filter (APF) has been widely used for harmonics and reactive power compensation and it has now become a mature technology for improving the power quality. They are most effective for harmonic compensation. Different types, such as shunt and series active power filters are used effectively. It acts as a harmonic current source which injects an anti-phase but equal magnitude to the harmonic and reactive load current to eliminate the harmonic and reactive components of the supply current. These active filters have limitations in medium and high voltage application due to semiconductor rating constraint, Use of transformer for high voltage applications, with active power filters requires high VA rating of transformer, high magnitude of current on low voltage side and also causes more losses and high cost of system. Multilevel inverters are effective in high voltage applications as it provides high output voltages with same voltage rating of individual device and also eliminate the need of transformer. Recently, semiconductor constraints and the voltage stress on the semiconductor switches have drawn the attention of the researchers. In order to achieve higher voltage level of the filtering operation, inverter configuration such as multilevel inverter is proposed. A cascaded shunt active power filter for the harmonics and reactive power mitigation of the non-linear loads is used as multilevel shunt active power filter. It has been applied for power quality applications due to increase in the number of voltage levels, low switching losses, low electromagnetic compatibility for hybrid filters and higher order of harmonic elimination. APFs based on three-level inverters are generally more expensive but can be compensated by using smaller filter inductors, assuming the same switching frequency. However, the control of a three-level inverter is more complicated than a two-level inverter because of the large number of inverter switching states. Therefore, there is greater difficulty in synthesizing the voltage reference vector.

In this chapter, a three-phase, dual inverter based three level VSI is proposed as SAPF to compensate for load harmonics and reactive power requirement so that the source current becomes sinusoidal and is in phase with the supply voltage. In the literature this type of multilevel topology is being used to drive induction motor namely open-end winding induction motor drive (Baiju *et al*., 2004; Shivakumar *et al*., 2002; Somasekhar *et al*., 2004). Based on similar lines a dual fed three phase transformer is used here in place of an induction motor.

4.2 PRINCIPLE OF OPERATION

After estimation of reference current signals, the next stage of APF control is the generation of switching signals for the power electronic devices of the converter circuit. These switching signals are obtained by comparing the reference compensating signals with the actual current in a controller. Various control techniques for generation of gating signals are reported such as linear PWM, predictive, hysteresis, SVM, etc. The performance of an APF is affected significantly by the selection of control techniques.

The system being studied is shown in Figure 4-24. It consists of a dual inverter feeding open end primary of a three phase transformer. The star connected secondary of this transformer is connected to PCC. Two DC capacitors are connected at the two inputs of the VSI's. Out of six free terminals of primary winding of this transformer, three ends are fed from VSI-I and other three free ends are fed from VSI-II. The control strategy of these two inverters is selected such that three level output voltage is generated across each phase of the transformer primary. The star connected secondary of this transformer is connected to the PCC so that the transformer acts as filter inductance of APF.

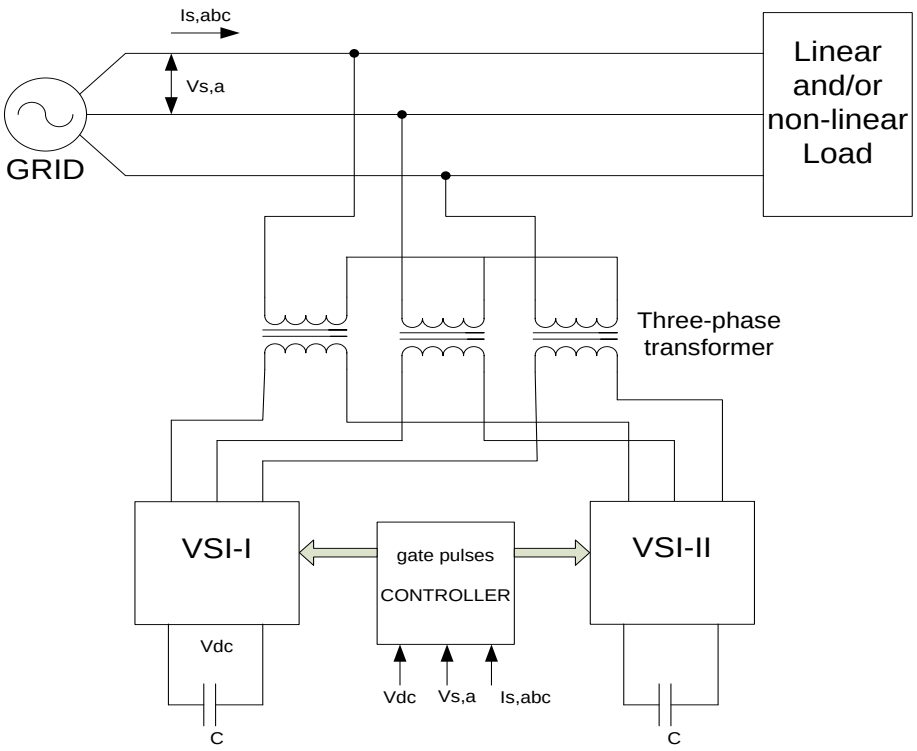

Figure 4-24: Three–phase system with dual inverter fed SAPF

As in this chapter we use a dual inverter topology for a three level SAPF, the gating signals for the control switches are generated by dual inverter SVPWM technique which is already explained in section 3.4.1. The generation of gating signals exactly remains the same. The control strategy to generate the reference signal is decided by the control strategy used. In the next section the novel method of three level SAPF operation is discussed. The system considered is modeled and simulated in MATLAB/Simulink.

4.3 SYSTEM DESCRIPTION

The basic compensation principle of the shunt APF for reactive and harmonic compensation is explained with the help of its single-phase equivalent circuit as shown in Figure 4-25. The instantaneous current of the non-linear load can be represented by

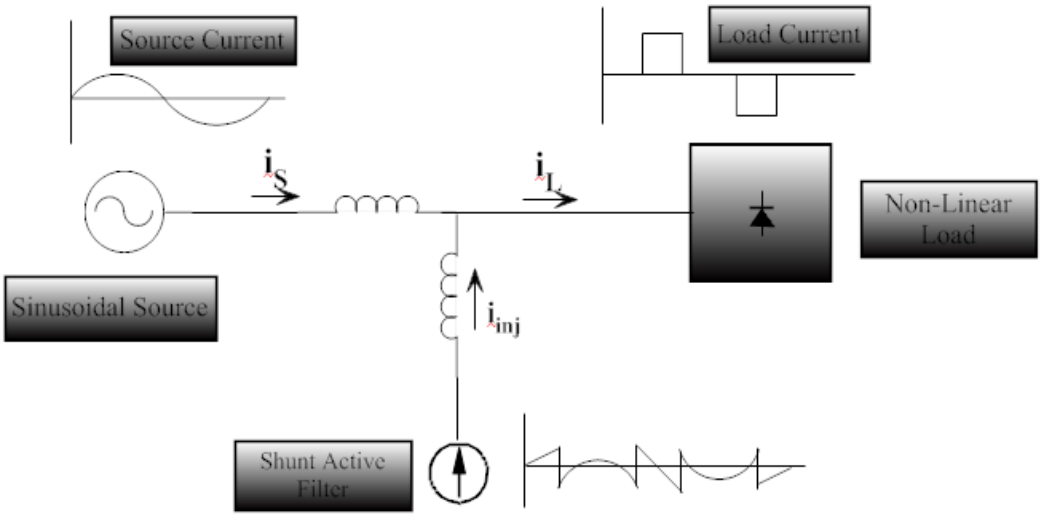

Figure 4-25: Basic shunt compensation principle.

$$
\begin{aligned}
i_L &= I_{Lf}\sin(\omega t-\phi_{Lf})+\sum_{h=3,5....}^{\infty} I_{Lh}\sin(h\omega t-\phi_{Lh}) \\
&= I_{Lf}\sin\omega t\cos\phi_{Lf}-I_{Lf}\cos\omega t\sin\phi_{Lf}+\sum_{h=3,5.....}^{\infty} I_{Lh}\sin(h\omega t-\phi_{Lh}) \\
&= i_{Lfp}+i_{Lfq}+i_{Lh} \qquad (4.11)
\end{aligned}
$$

where, I_{Lf} is the peak value of the fundamental load current, I_{Lh} is the peak value of the harmonic load current, ϕ_{Lf} and ϕ_{Lh} are the phase angle of the fundamental and harmonic component of the load currents, respectively. In equation (4.11), the instantaneous current of non-linear load is divided into three terms. The first term i_{Lfp} is the load instantaneous fundamental phase current. The second term i_{Lfq} is load instantaneous fundamental quadrature current and the third term i_{Lh} is the load instantaneous harmonic current. From the Figure 4-25, it is clear that

$$i_s + i_{inj} = i_L = i_{Lfp} + i_{Lfq} + i_{Lh} \qquad (4.12)$$

Instantaneous supply current i_s, is having only fundamental component that is almost in phase with v_s, hence, from equation (4.12)

$$i_{inj} = i_{Lfq} + i_{Lh} \qquad (4.13)$$

Equation (4.13) concurs that for obtaining clean sinusoidal and power factor corrected supply current, the shunt active filter has to inject the instantaneous fundamental quadrature current and instantaneous harmonic currents of non-linear load.

4.4 CONTROL METHOD

The instantaneous source voltage of any one phase (phase-*a* in this work) v_{sa}, actual DC-bus capacitor voltage V_{dc} and the actual instantaneous source currents (i_{sa}, i_{sb}, i_{sc}) are the main inputs to the algorithm. To maintain a constant dc-bus capacitor voltage in the CC-VSI, the error $V_e(k)$ between the square values of reference DC-bus capacitor voltage and actual DC-bus capacitor voltage at the kth sampling instant is computed as:

$$V_e(k) = V^2_{dcref} - V^2_{dc}(k) \qquad (4.14)$$

where, V_{dcref} is the reference dc-bus capacitor voltage and $V_{dc}(k)$ is the actual DC-bus capacitor voltage at k^{th} sampling instant. This DC-bus capacitor voltage error is processed through the proposed controller. The output of the controller is considered as peak value I_{sm} of source currents at every sample which has two components. One of them is the fundamental active component of load current and the other is loss component of the inverter circuit.

The output of the controller at k^{th} sampling instant in discrete system is given as:

$$I_{sm}(k) = K_{ep}V_e(k) + I_{sm}(k-1) \qquad (4.15)$$

where, K_{ep} is the gain of the controller and $I_{sm}(k)$ and $I_{sm}(k\text{-}1)$ are the output of the controller at k^{th} and $(k\text{-}1)^{\text{th}}$ sampling instant, respectively. In the discrete system equation (4.15) can be written by taking its z transform as:

$$I_{sm}(z) = K_{ep}V_e(z) + z^{-1}I_{sm}(z) \qquad (4.16)$$

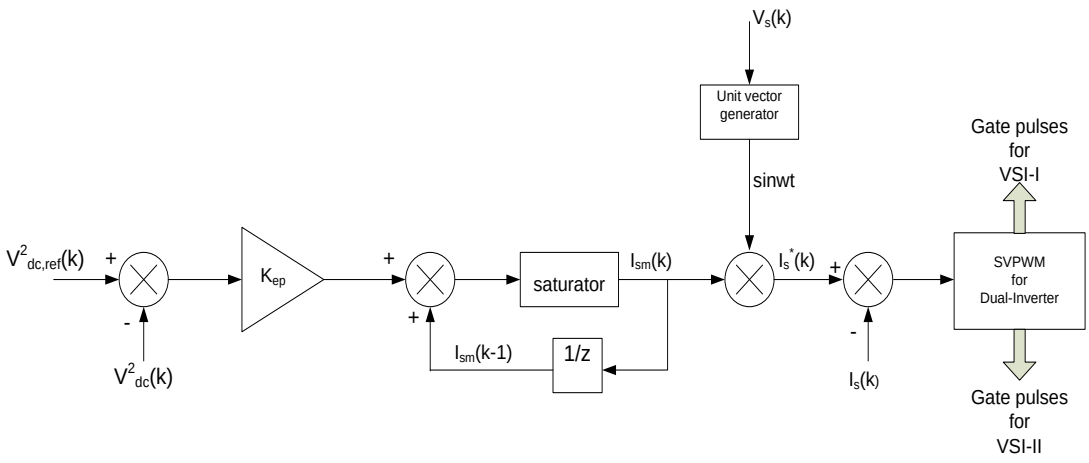

Figure 4-26: Control circuit

4.5 RESULTS AND DISCUSSION

The various parameters used for simulation are given in

Table 4-3

Table 4-3: Simulation parameters (three-level APF)

Location	Parameter	Value
Supply	Supply voltage	(i) 400 V, 3 phase, 50 Hz (ii) 400V+5th and 7th harmonic components
Active Power Filter	1) open end 3-phase transformer 2) DC-bus capacitance	10kVA, 800V/800V, 0.002 pu resistance and 0.045 pu reactance 1000 μF
Load	Three-phase diode bridge with R-L load on its dc side.	(i) P=5kW and Q=1kVAR (ii) P=3kW and Q=0.5kVAR

Case (a): Sinusoidal supply and non-linear load. (Figure 4-27 (a) to (d))

Here supply voltage is assumed to be balanced sinusoidal voltage. Initially the system runs without SAPF. The source current is equal to the load current. At t=0.1 sec, SAPF is added to the circuit. Now the source current becomes sinusoidal as shown in Figure 4-27(b) and the source current lies in phase with the source voltage as shown in Figure 4-27(c). Figure 4-27(d) shows the dual inverter phase voltage.

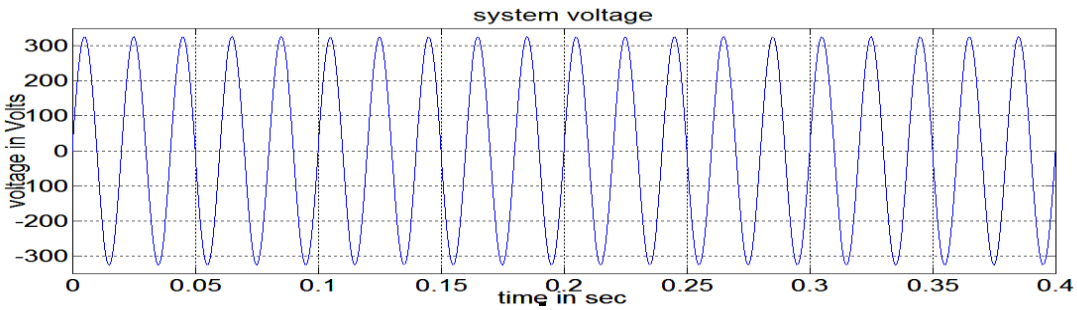

(a): Source phase voltage

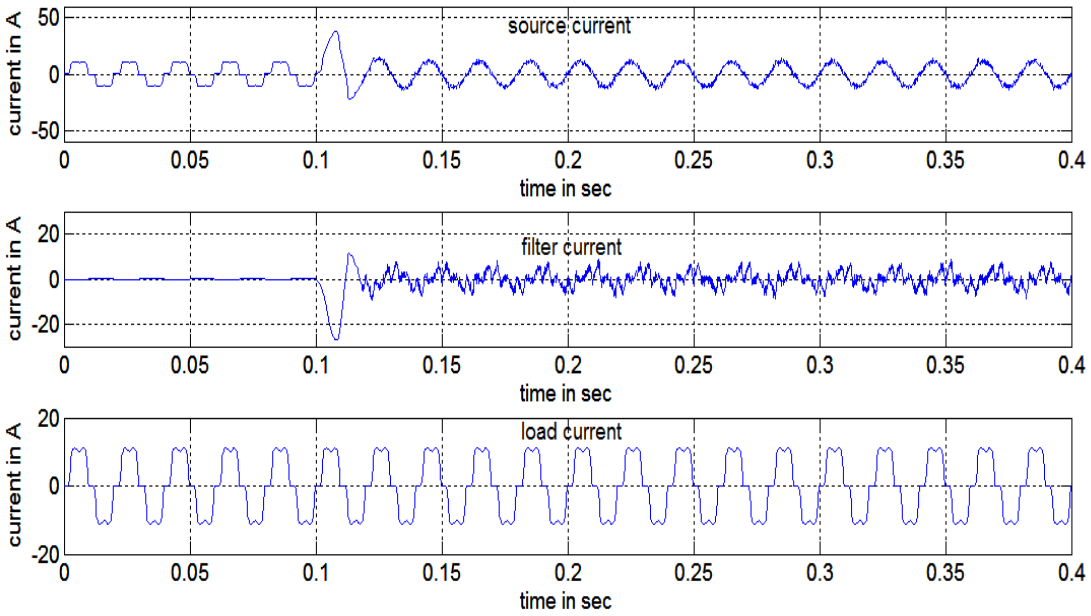

(b): Source, filter and load current

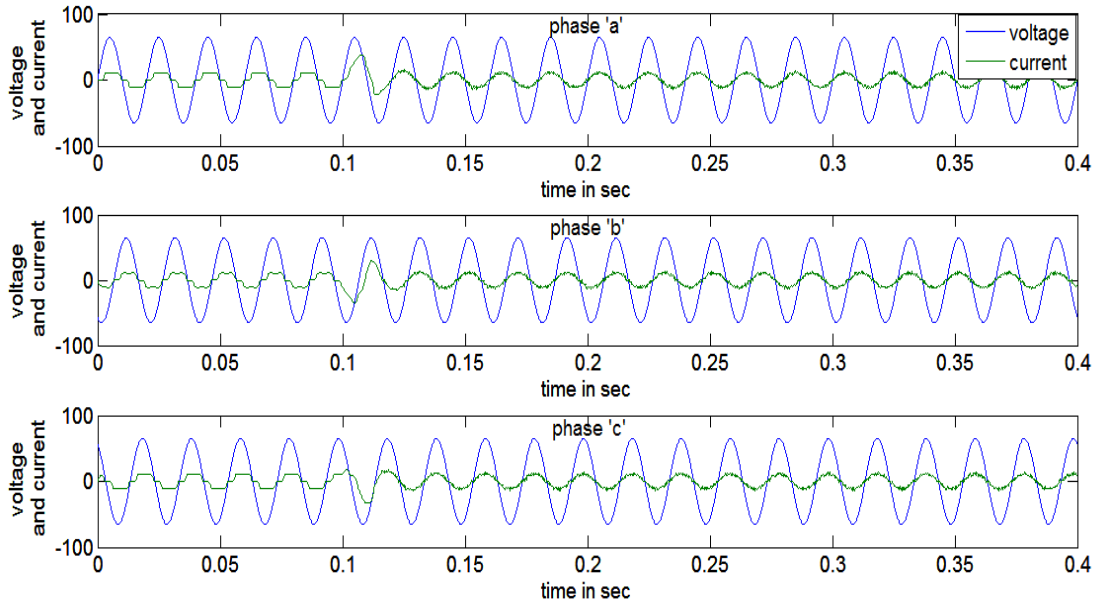

(c): Power factor

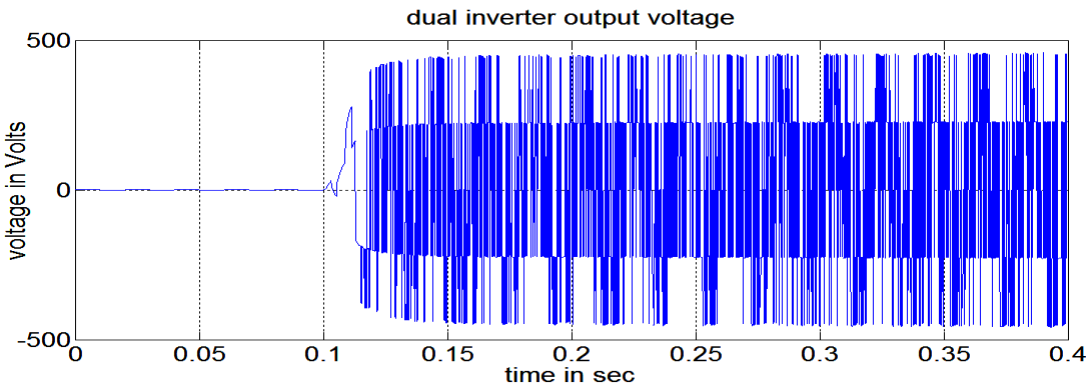

(d): dual inverter phase voltage

Figure 4-27: Sinusoidal supply and non-linear load

Case (b): sinusoidal voltage and different nonlinear load. (Figure 4-28 (a) to (d))

Here too supply voltage is assumed to be balanced sinusoidal voltage. Initially the system runs without SAPF. The source current is equal to the load current. At t=0.1 sec, SAPF is added to the circuit. Now the source current becomes sinusoidal as shown in Figure 4-28 (b) and the source current lies in phase with the source voltage as shown in Figure 4-28 (c). At t=0.4 sec additional load is connected and the effect is seen in Figure 4-28 (b) and (c). Still the system maintains unity pf. Figure 4-28 (d) shows the dual inverter phase voltage.

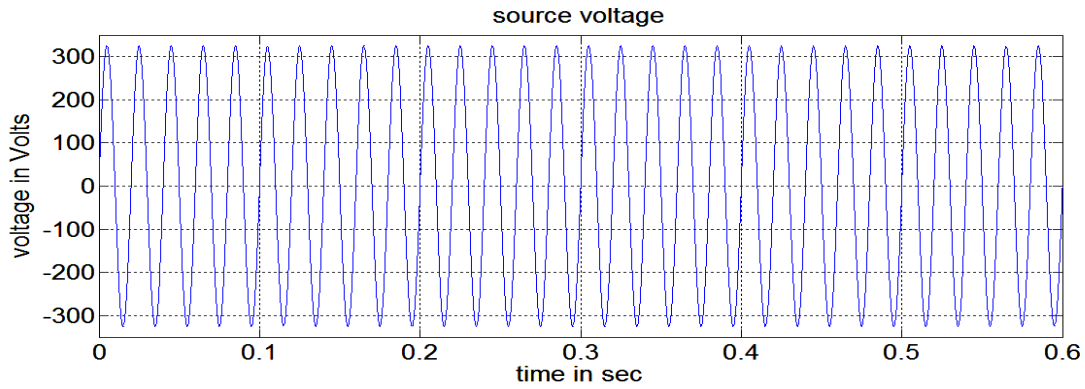

(a): Source phase voltage

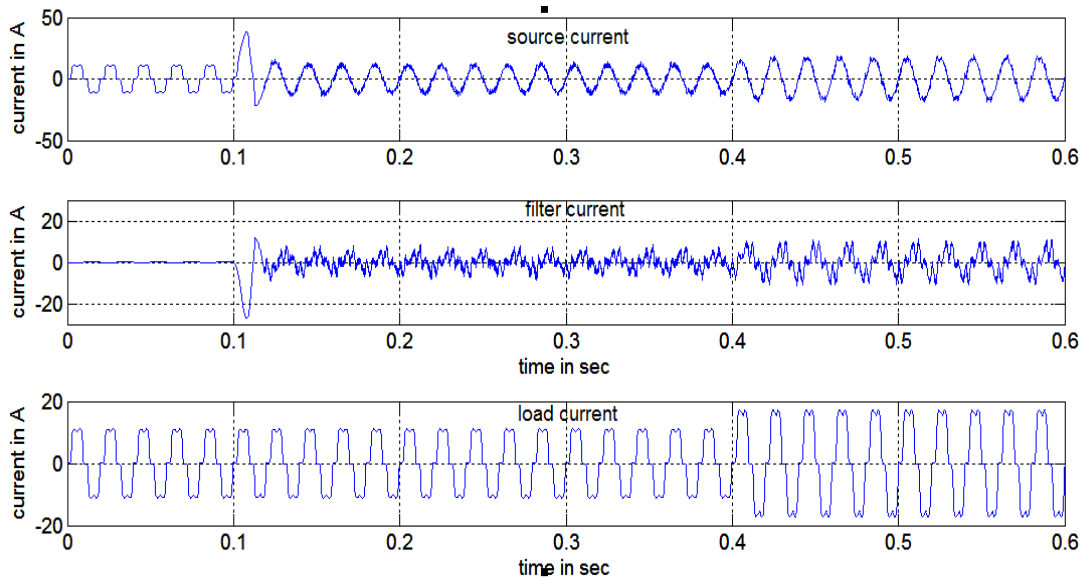

(b): Source, filter and load current

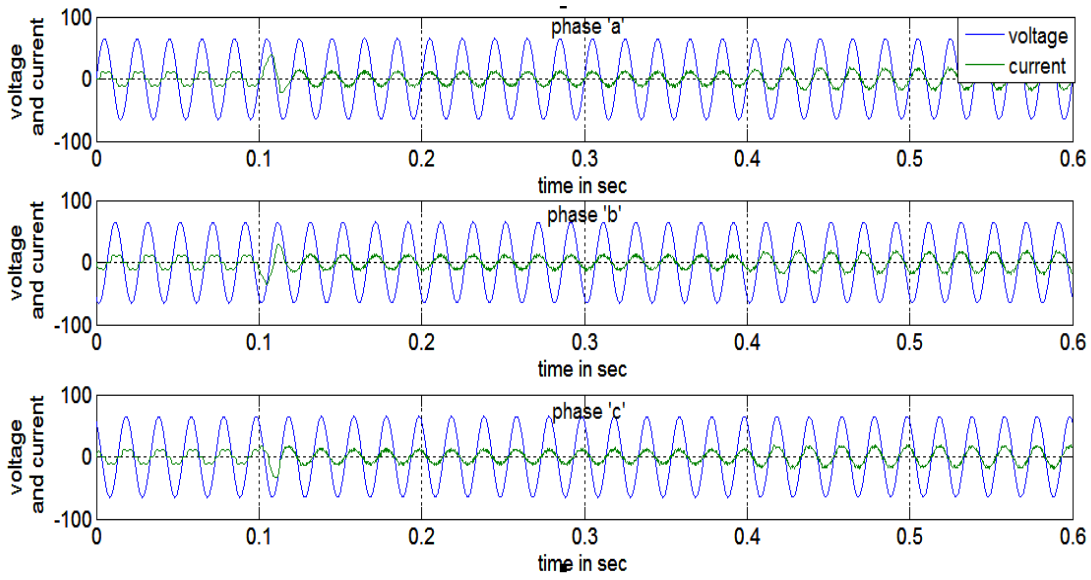

(c): Power factor

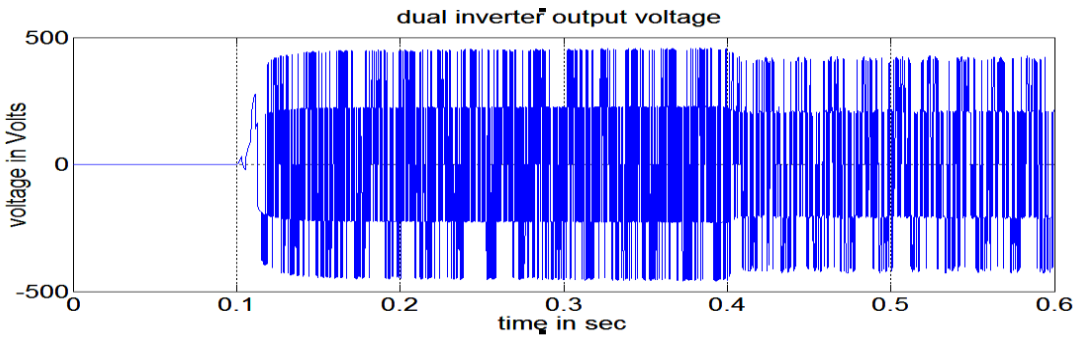

(d): Dual inverter phase voltage

Figure 4-28: Sinusoidal voltage and different nonlinear load

Case (c): non-sinusoidal supply and non-linear load. (Figure 4-29 (a) to (d))

Here supply voltage is distorted with 5^{th} and 7^{th} harmonic components of voltages added to the fundamental. Initially the system runs without SAPF. The source current is equal to the load current. At t=0.1 sec, SAPF is added to the circuit. Now the source current becomes sinusoidal as shown in Figure 4-29(b) and the source current lies in phase with the source voltage as shown in Figure 4-29 (c). Figure 4-29 (d) shows the dual inverter phase voltage.

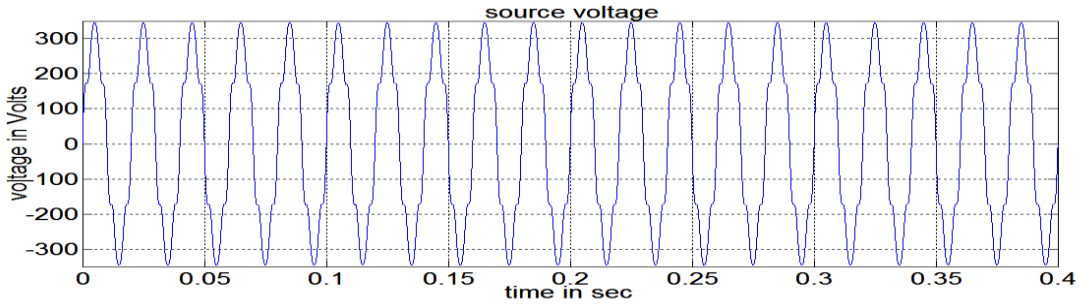

(a): Source phase voltage

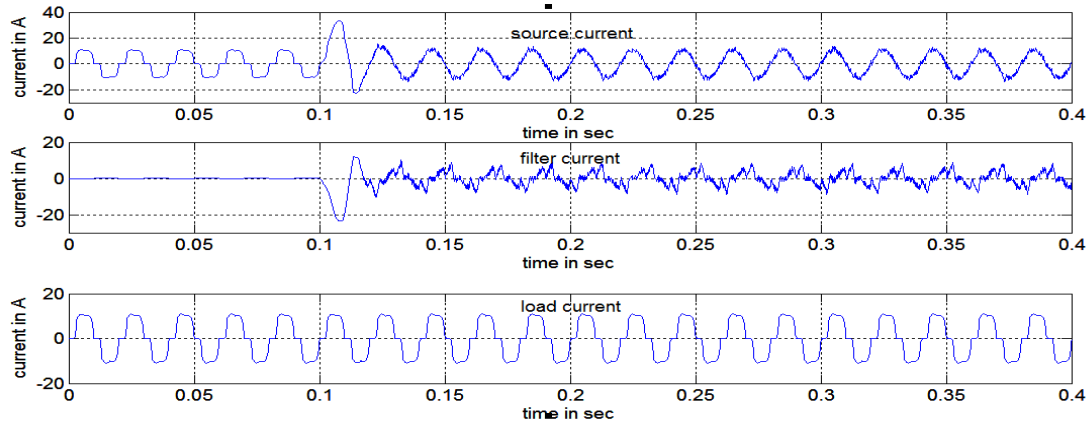

(b): Source, filter and load current

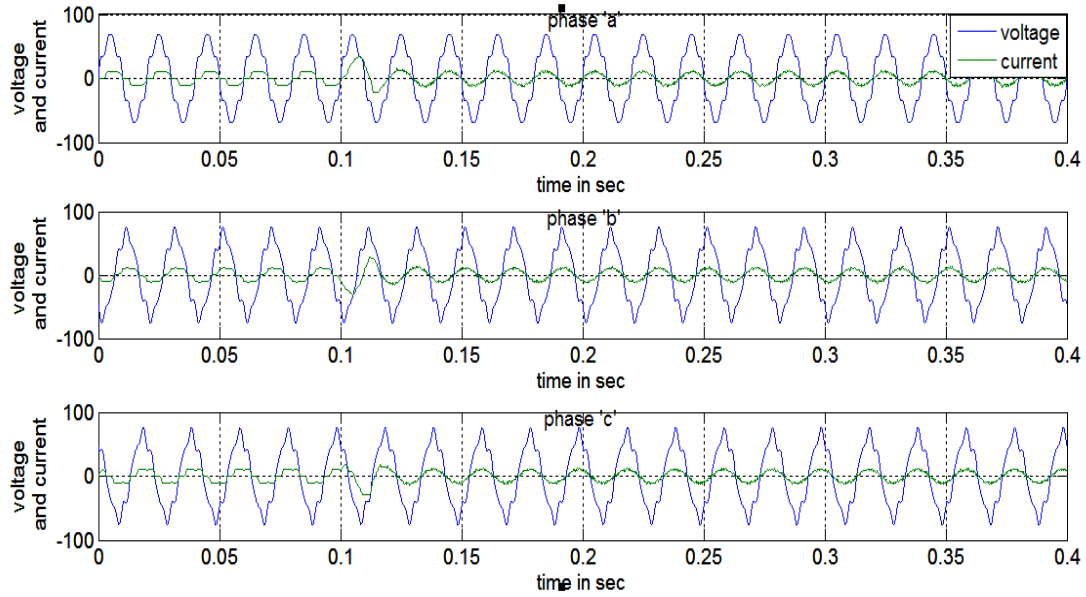

(c): Power factor

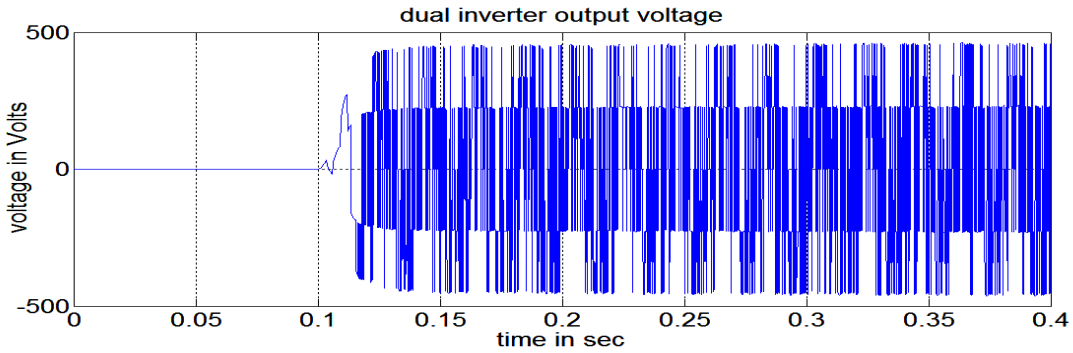

(d): Dual inverter phase voltage

Figure 4-29: Non-sinusoidal supply and non-linear load

Case (d): Non sinusoidal voltage and different non-linear loads. (Figure 4-30 (a) to (d))

Here too supply voltage is distorted with 5^{th} and 7^{th} harmonic components of voltages added to the fundamental. Initially the system runs without SAPF. The source current is equal to the load current. At t=0.1 sec, SAPF is added to the circuit. Now the source current becomes sinusoidal as shown in Figure 4-30(b) and the source current lies in phase with the source voltage as shown in Figure 4-30(c). At t=0.4 sec additional load is connected and the effect is seen in Figure 4-30(b) and (c). Still the system maintains unity pf. Figure 4-30(d) shows the dual inverter phase voltage.

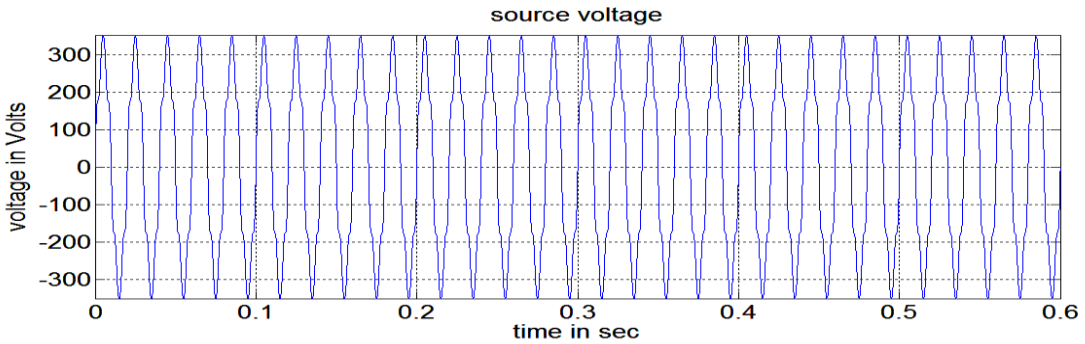

(a): Source phase voltage

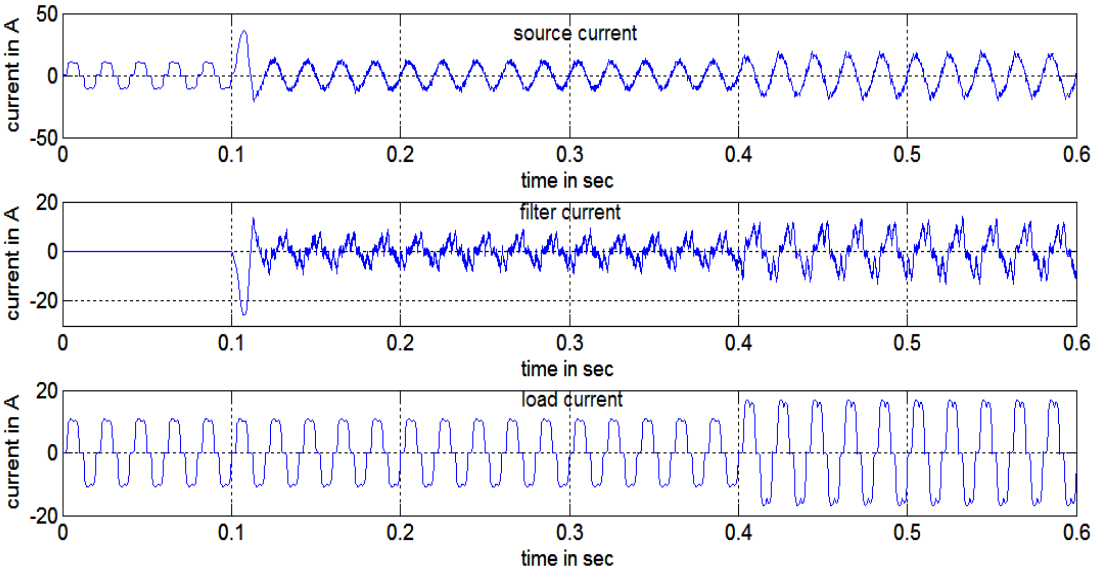

(b): Source, filter and load current

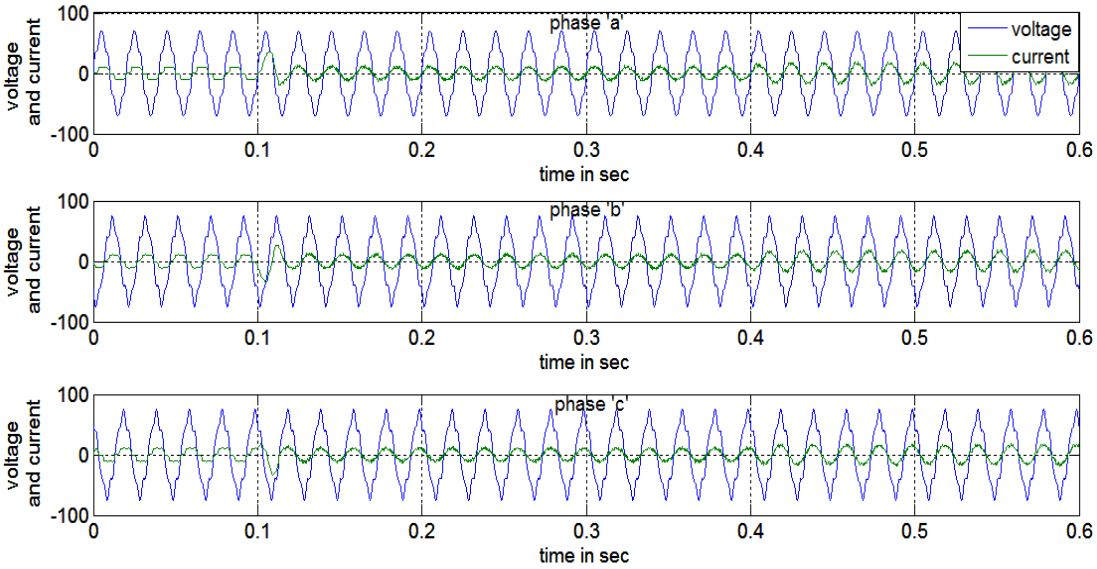

(c): Power factor

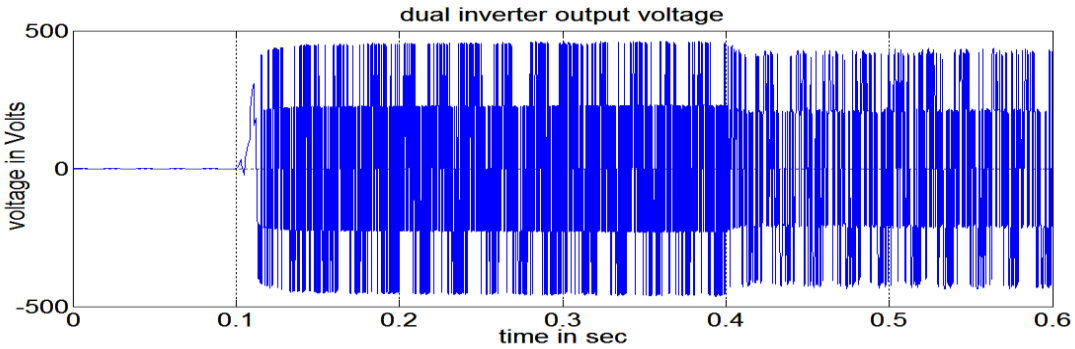

(d): Dual inverter phase voltage.

Figure 4-30: Non sinusoidal voltage and different non-linear loads

4.6: CONCLUSION

In this chapter, the modeling and simulation of a novel three-level topology for a shunt active power filter is presented. Initially the various control strategies used in SAPF are compared under balanced and unbalanced supply voltage conditions. An attempt is made here to introduce a dual inverter topology in SAPF. The reference current generation principle is simple. It is found that in both sinusoidal and non sinusoidal supply voltage conditions, the SAPF works very effectively keeping the source current near sinusoidal. Also the system power factor is kept near unity in all conditions. The system performance is also verified for different load conditions to check the dynamic behavior of the system. All the benefits of the multilevel inverter can be utilized here. Also the implementation through digital controller is simple as SVPWM technique is used to drive the dual inverter.

Chapter 5 : INTEGRATION OF GRID CONNECTED PV SYSTEM WITH POWER FILTERING FUNCTIONALITY

5.1 INTRODUCTION

The requirement of clean and green energy generation is the need of the hour. Grid – connected renewable power is the main path through which goal of reduction in carbon emission can be achieved. The distributed generation (DG) concept is becoming more and more popular as it can provide more reliability, reduced emissions and provide additional power quality benefits. Photovoltaic (PV) energy is one of the attractive sources of energy. Unfortunately, PV generation system suffers from disadvantages such as poor conversion efficiency, weather dependence and nonlinear I-V characteristics. Therefore it is very much essential to extract maximum available power from the PV array. Several maximum power point tracking (MPPT) algorithms are reported in the literature. When operated in grid connected mode the inverter is current controlled as the voltage at the point of common coupling (PCC) is imposed by the grid.

With the developments in Power Electronics devices, the non linear loads that consume non sinusoidal current have increased significantly e.g. VFD, electronic fan regulator, UPS, electronic choke fitted fluorescent lamps etc. These modern equipments behave as non linear loads and draw harmonic current from the power network. The increased use of power semiconductor devices in wide variety of loads has given birth to numerous power quality (PQ) problems in the electric power networks. The non sinusoidal voltage and/or current have adverse effect on the utilities and the load connected to it. Hence it has become very essential to pay attention to the power quality issues. Several power quality standards are defined in order to keep the harmonic distortion within the limits like IEEE-519-1992/IEC 61000. The various techniques used to suppress/eliminate harmonics include passive power filtering and active power filtering. Active power filtering uses either a current source inverter or a voltage source inverter which acts as a harmonic source to compensate for the load harmonics. APFs are capable enough to provide the solution related to harmonic compensation, reactive power compensation, balancing three-phase line currents, damping of oscillation in currents and voltage regulation. Shunt

APFs are connected in parallel with the load and they do not burden the source on account of displacement power factor and loading.

The use of APF requires additional cost. It is possible to integrate power quality functions by compensating the reactive power and the current harmonics drawn by the local non linear load into the grid - connected PV system just by modifying the control strategy to incorporate APF features. The idea is to integrate PV system with shunt APF capabilities. Here the PV array is connected to the grid system with its inverter performing the additional function of APF besides real power injection. This is achieved with suitable modifications in the control algorithm without any additional hardware or power circuit for making the existing inverter to act as APF too. Hence the overall cost of the system is reduced.

In the grid connected renewable sources the major issue of concern is the quality of current injected at PCC. This injected current also affects the grid current and hence it is required to inject current with minimum distortion. The quality of current can be improved if we can use multilevel voltage source inverters (VSI) at the conversion stage. Cascaded converter, together with the diode clamped and capacitor clamped converters, makes the three most common types of present multilevel topologies. Cascaded converters still receive large attention among these topologies, due to the simplicity of the power stage not requiring additional components such as diodes and capacitors. Cascaded topology provides the same number of output voltage levels using two yet simpler multilevel inverters instead of one complex inverter with large number of leg levels. In dual inverter topology, the two inverters are connected "in opposition" at two ends of the load in order to obtain output voltage as a difference of inverter's leg potentials. The benefit of dual inverter arises from the fact that use of components with lower voltage ratings enables bigger efficiency. The dual inverter configuration consists of the simple connection of two standard 2-level inverters to a three-phase open-winding load, and performs as a 3-level inverter. Although it is not scalable to get more voltage levels, it represents a viable solution to supply transformers and ac motors, especially when the dc source can be easily split in two insulated parts, as for batteries and PV panels.

In this chapter, a three-phase, grid- interactive PV system with dual inverter three-level VSI which also acts as SAPF to compensate for load harmonics and reactive power requirement so that the source current becomes sinusoidal and is in phase with the supply voltage is proposed. The idea is to integrate PV system such that the dual inverter feeds the open end primary of a three phase transformer which also acts as filter inductor. With this topology, more PV power is injected with two sources connected at the inputs of the two inverters. The three-phase, grid interactive PV system along with its MPPT algorithm and three-level dual inverter is modeled and simulated in MATLAB/Simulink environment. In the literature this type of multilevel topology is being used to drive induction motor namely open-end winding induction motor drive. Based on similar lines, a dual fed three phase transformer is used here in place of an induction motor. In the following section a brief description of the system is covered.

5.2 PRINCIPLE OF OPERATION

The system being studied is shown in Figure 5-1. It consists of a dual inverter feeding open end primary of a three phase transformer. The star connected secondary of this transformer is connected to PCC. Two PV sources are connected at the two inputs of the VSI's. They feed current into the grid and the local load through transformer inductance L which acts as filter inductance. The output DC voltage of PV cell is maintained constant by capacitor C_{dc} at the input of the inverter as the power output of the inverter oscillates at twice the line frequency. The two PV sources feed maximum power available at any particular instant into the grid due to MPPT circuits. The gate pulses for the generation of three level inverter output are generated based on dual inverter working principle which is already described in section 3.4.1. The reference current generation is based on direct power control. In this method the active power requirement of the load and available power from the two PV sources decides the source active power requirement. This principle is explained in detail in the next section.

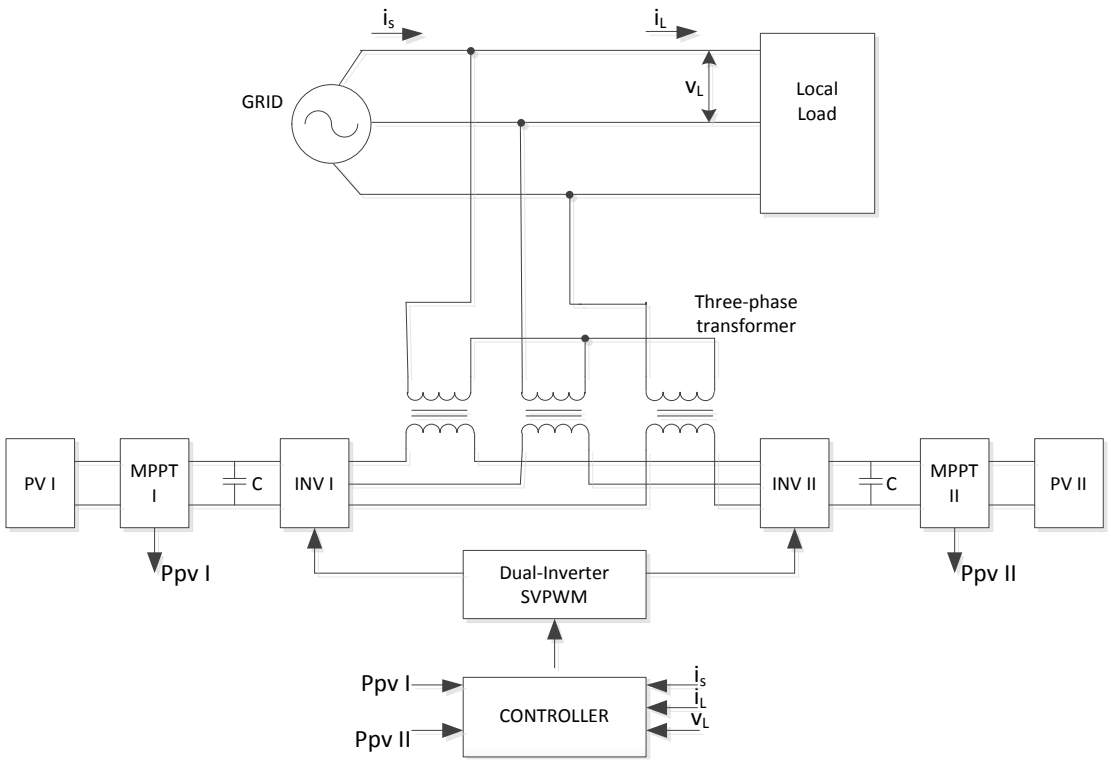

Figure 5-1: Grid connected PV system

5.3 ANALYTICAL STUDIES

The overall control circuit of proposed grid-interactive PV system, consisting of MPPT for PV array and an APF current controller with hysteresis band pulse width modulation (PWM), is shown in Figure 5-2. The system works in forward interconnected mode when both, PV array and grid, supply power to the load. It works in the reverse interconnected mode, when PV system supplies power to load as per load requirement and remaining power is injected into the grid. Also, it works in islanding mode, when the voltage interruption occurs on the grid. The AC-side voltages of APF inverter are controlled both in phase and magnitude to control the active and reactive power, respectively. The APF is controlled in a-b-c reference frame. In order to get the grid currents sinusoidal and in phase with the distorted grid voltages, the positive sequence components of the grid voltages are computed.

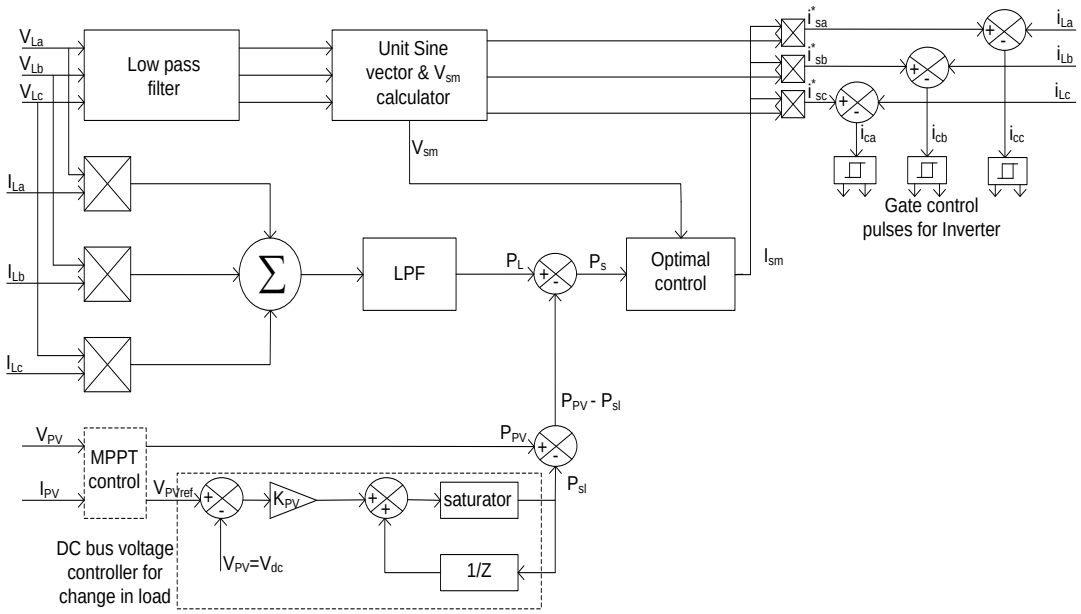

Figure 5-2: Overall control circuit of Grid-interactive PV system.

The proposed DC-bus voltage controller, as shown in Figure 5-2, is fed by two inputs, $V_{dc,ref} = V_{PV,ref}$ and $V_{dc} = V_{PV}$. $V_{dc,ref}$ is changed by MPPT subject to variation in atmospheric conditions imposed on PV array, while V_{dc} is changed due to variation in load. Hence, the controller generates the deficit power (*Psl*) under the variation of atmospheric condition as well as load.

The MPPT controller takes V_{pv} and I_{pv} as inputs to detect power slope and generates V_{ref} to track the maximum power point. This V_{ref} is then used to generate firing pulses for the DC-DC converter in closed loop system as shown in Figure 5-3.

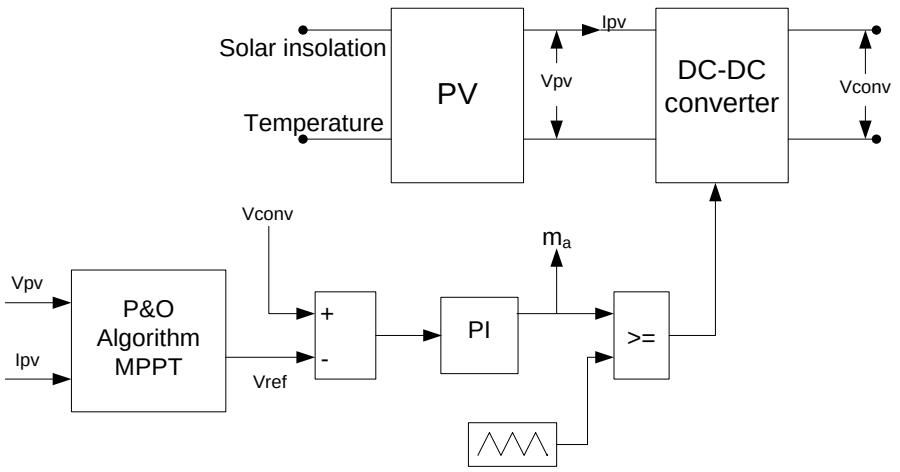

Figure 5-3: Control of DC-DC converter to obtain maximum power from PV system

Active Power Filter Control

In order to examine the overall control of the Grid-interactive PV system, let's assume that the instantaneous PCC voltage vector $V_L(t)$ and load current vector $i_L(t)$ consists of a set of harmonic components H which are expressed by equations (5.1) and (5.2) respectively, where $H = \{1, 2, 3\ldots, N\}$,

$$V_L(t) = \begin{bmatrix} V_{La} \\ V_{Lb} \\ V_{Lc} \end{bmatrix} = \begin{bmatrix} \sum_{\forall h \in H} V_{Lha} \sin\{h\omega t + \alpha_h\} \\ \sum_{\forall h \in H} V_{Lhb} \sin\{h(\omega t - \frac{2\pi}{3}) + \alpha_h\} \\ \sum_{\forall h \in H} V_{Lhc} \sin\{h(\omega t + \frac{2\pi}{3}) + \alpha_h\} \end{bmatrix} \qquad (5.1)$$

$$i_L(t) = \begin{bmatrix} i_{La} \\ i_{Lb} \\ i_{Lc} \end{bmatrix} = \begin{bmatrix} \sum_{\forall h \in H} I_{Lha} \sin\{h\omega t + \alpha_h - \phi_{ha}\} \\ \sum_{\forall h \in H} I_{Lhb} \sin\{h(\omega t - \frac{2\pi}{3}) + \alpha_h - \phi_{hb}\} \\ \sum_{\forall h \in H} I_{Lhc} \sin\{h(\omega t + \frac{2\pi}{3}) + \alpha_h - \phi_{hc}\} \end{bmatrix} \qquad (5.2)$$

V_{Lhx} and I_{Lhx} (with $x = a$, b, and c) are the peak values of three-phase PCC voltages and three-phase load currents corresponding to h^{th} order harmonics. α_h is the arbitrary angle of the grid voltage corresponding to h^{th} order harmonics. φ_{hx} (with $x = a$, b,and c) is the phase angle of three-phase load currents corresponding to h^{th} order harmonics.

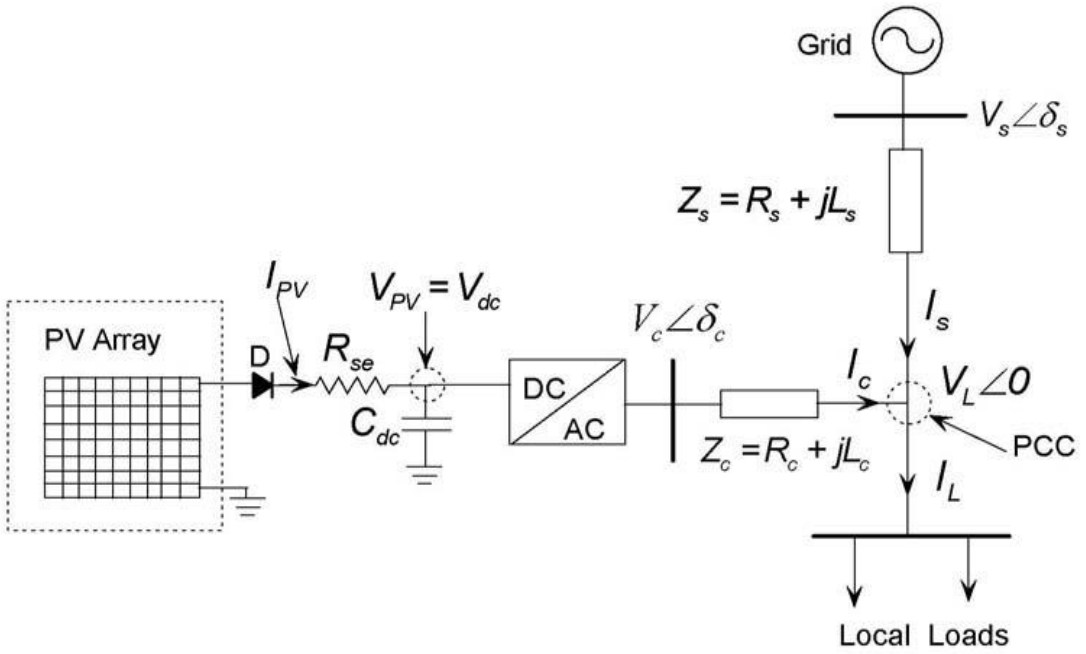

Figure 5-4: The single-line diagram of the Grid-interactive PV system.

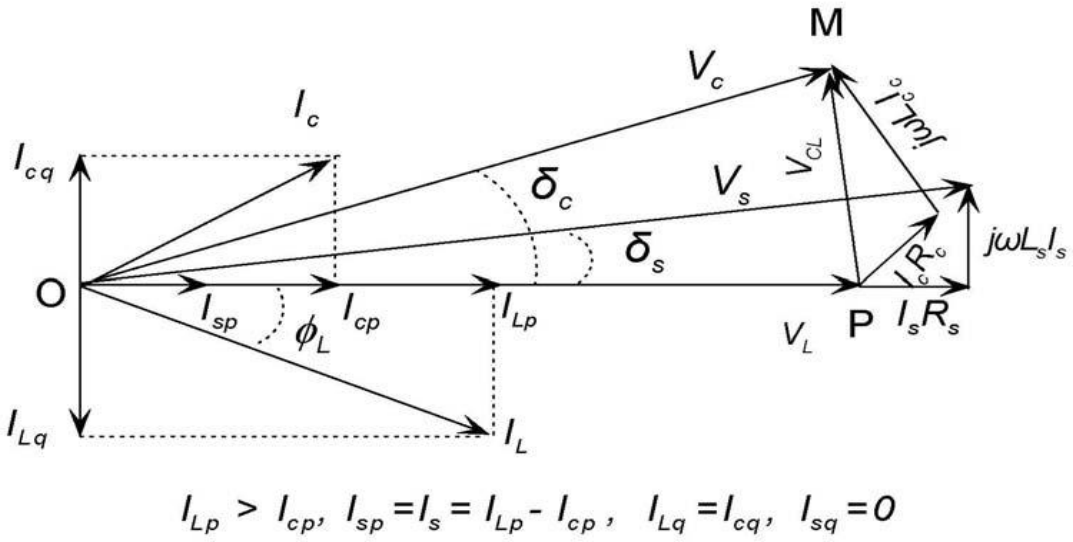

$$I_{Lp} > I_{cp},\ I_{sp} = I_s = I_{Lp} - I_{cp},\ I_{Lq} = I_{cq},\ I_{sq} = 0$$

Figure 5-5: Phasor diagram for forward interconnected mode.

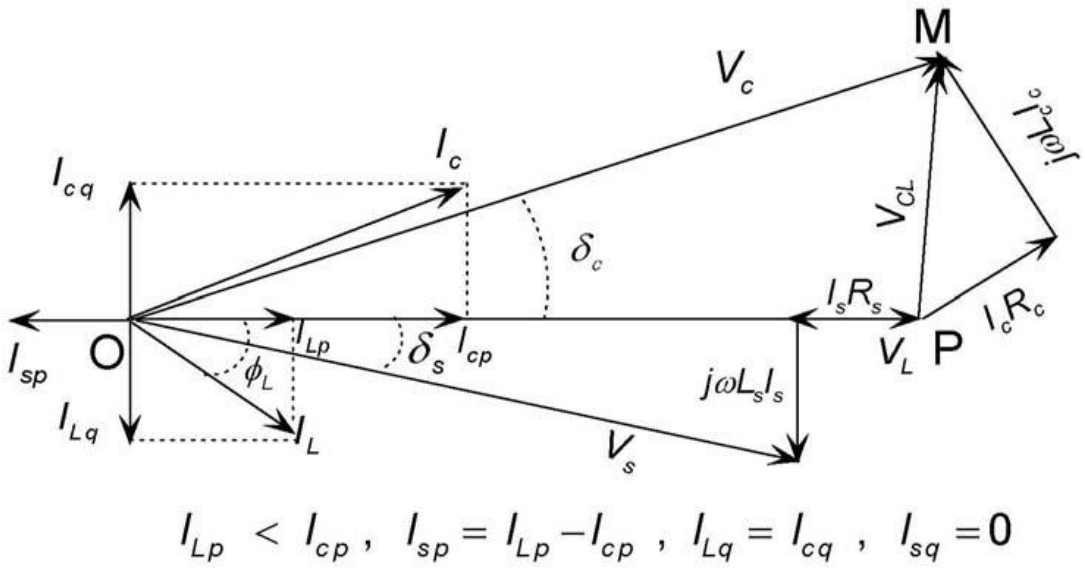

Figure 5-6: Phasor diagram for reverse interconnected mode.

A single line diagram of the proposed Grid-interactive PV system is shown in Figure 5-4, and the phasor diagram for forward and reversed interconnected mode of operation are represented in Figure 5-5 and Figure 5-6 respectively. In these figures, V_S, V_L and V_c are the rms values of fundamental component of voltages at grid, load and AC-side of VSI, respectively. I_S, I_L and I_c are the rms values of fundamental components of currents from grid, to load and from VSI, respectively. I_{sp}, I_{Lp} and I_{cp} are the fundamental active components while I_{sq}, I_{Lq} and I_{cq} are the fundamental reactive components of I_s, I_L and I_c, respectively. φ_L is the load power factor angle. δs is the angle between V_s and V_L. δ_c is the angle between V_c and V_L. From ΔOPM in Figure 5-5 and Figure 5-6, voltage V_{CL} across and current I_c through the filter inductor can be given by the following relations:

$$V_{CL}^2 = V_C^2 + V_L^2 - 2V_C V_L \cos\delta_C \tag{5.3}$$

$$I_C = \frac{V_{CL}}{R_C + j\omega L_C} \tag{5.4}$$

The R_c is very small as compared to ωL_c, and hence, can be neglected. Thus, the approximate value of I_c can be given as:

$$I_C \approx \frac{V_{CL}}{j\omega L_C} \tag{5.5}$$

Also, the following relation can be given with regard to ac and dc-side voltages of the PV/APF inverter as:

$$V_C = m_a V_{dc} \tag{5.6}$$

where, m_a is modulation index. Now, using (5.14), (5.16) and (5.17) the following expression is given:

$$I_C^2 = \frac{(m_a V_{dc})^2 + V_L^2 - 2(m_a V_{dc}) V_L \cos\delta_C}{(\omega L_C)^2} \tag{5.7}$$

The expression for active power (P_c) and reactive power (Q_c) controlled through PV/APF inverter can be given as:

$$P_C = \frac{V_L (m_a V_{dc})}{(\omega L_C)} \sin\delta_C \tag{5.8}$$

$$Q_C = \frac{(m_a V_{dc})}{(\omega L_C)} \{(m_a V_{dc}) - V_L \cos\delta_C\} \tag{5.9}$$

From equation (5.7) it evident, that the magnitude of I_c depends on the magnitude ($m_a V_{dc}$) of output voltage of the VSI and angle (δ_c) between V_c and V_L. For optimal control at unity power factor (cos φ_s=1) compensation, the active power $P_s(k)$ supplied by the source at k^{th} sampling instant is equal to source apparent power $S_s(k)$. Hence, the apparent power is minimized to obtain the peak value of desired source currents.

$$\mathrm{P}_s(k) = \mathrm{P}_{lavg}(k) + \mathrm{P}_{sl}(k) - \mathrm{P}_c(k) = \frac{3\mathrm{V}_{sm}(k)\mathrm{I}_{sm}(k)}{2} \tag{5.10}$$

where, $P_{lavg}(k)$, $P_{sl}(k)$, $P_c(k)$ are the average values of load active power, output power of DC-bus controller and AC-side active power of the inverter at k^{th} sampling instant respectively. $V_{sm}(k)$ and $I_{sm}(k)$ are the peak values of three-phase grid voltages assumed to be equal to PCC voltages and peak values of three-phase grid currents at

k^{th} sampling instant, respectively. In discrete system, these powers are given by the following relations (Petit *et a*l., 2007)

$$\mathrm{P}_{lavg}(k) = \frac{1}{NT_c} \sum_{n=k-N+1}^{k} \begin{bmatrix} V_{sa}(n) \\ V_{sb}(n) \\ V_{sc}(n) \end{bmatrix} \begin{bmatrix} i_{La}(n) \\ i_{Lb}(n) \\ i_{Lc}(n) \end{bmatrix}^T \tag{5.11}$$

$$\mathrm{P}_{sl}(k) = K_{pe}\{V_{PVref}(k) - V_{dc}(k)\} + P_{sl}(k-1) \tag{5.12}$$

$$V_{sm}(k) = \sqrt{\frac{2}{3}[V_{La}^2(k) + V_{Lb}^2(k) + V_{Lc}^2(k)]} \tag{5.13}$$

where, N and T_c correspond to number of samples per time period and sampling time of the signal, respectively whereas, K_{pe} is gain of the dc-bus voltage controller. Using equations (5.10)-(5.13) and $P_c(k) = P_{PV}(k)$, the desired peak value of grid currents can be obtained as:

$$I_{sm}(k) = \frac{2[\mathrm{P}_{lavg}(k) + P_{sl}(k) - P_c(k)]}{3\mathrm{V}_{sm}(k)} \tag{5.14}$$

Once, the I_{sm} is obtained, the instantaneous value of reference grid currents at k^{th} sampling instant can be obtained by multiplying I_{sm} with unit sine vectors, which are generated using phase lock loop (PLL) (Chang and Tai-Chang *et al*., 2004).

$$I_s(k) = \begin{bmatrix} i_{sa}^*(k) \\ i_{sb}^*(k) \\ i_{sc}^*(k) \end{bmatrix} = \begin{bmatrix} I_{sm}(k)\sin(\omega k) \\ I_{sm}(k)\sin(\omega k - \frac{2\pi}{3}) \\ I_{sm}(k)\sin(\omega k + \frac{2\pi}{3}) \end{bmatrix} \tag{5.15}$$

Further, the reference grid currents are compared with load currents to get inverter currents, expressed as:

$$I_c(k) = \begin{bmatrix} i_{ca}(k) \\ i_{cb}(k) \\ i_{cc}(k) \end{bmatrix} = \begin{bmatrix} i_{La}(k) \\ i_{Lb}(k) \\ i_{Lc}(k) \end{bmatrix} - \begin{bmatrix} i_{sa}^*(k) \\ i_{sb}^*(k) \\ i_{sc}^*(k) \end{bmatrix} \tag{5.16}$$

The inverter currents are given to hysteresis controllers to generate PWM signals to switch the devices used in VSI.

The performance of such a system can be always improved upon by replacing the interfacing voltage source inverter by a three level inverter. As the number of level increases the control circuitry complexity also increases. But as mentioned before, here a dual inverter based three level inverter topology is being proposed for this application. Its analysis is carried out by performing simulations under different conditions.

5.4 CONTROL METHOD

The generation of reference signal in this system is identical to the method already discussed in section 5.3. The only change is the generation of gate signals to the 2 two-level VSI's using SVPWM. The hysteresis comparator is now replaced by dual inverter SVPWM circuitry. The generation of gating signals using this method (dual inverter SVPWM) is already explained in section 3.4.1. The controller schematic is as shown in Figure 5-7.

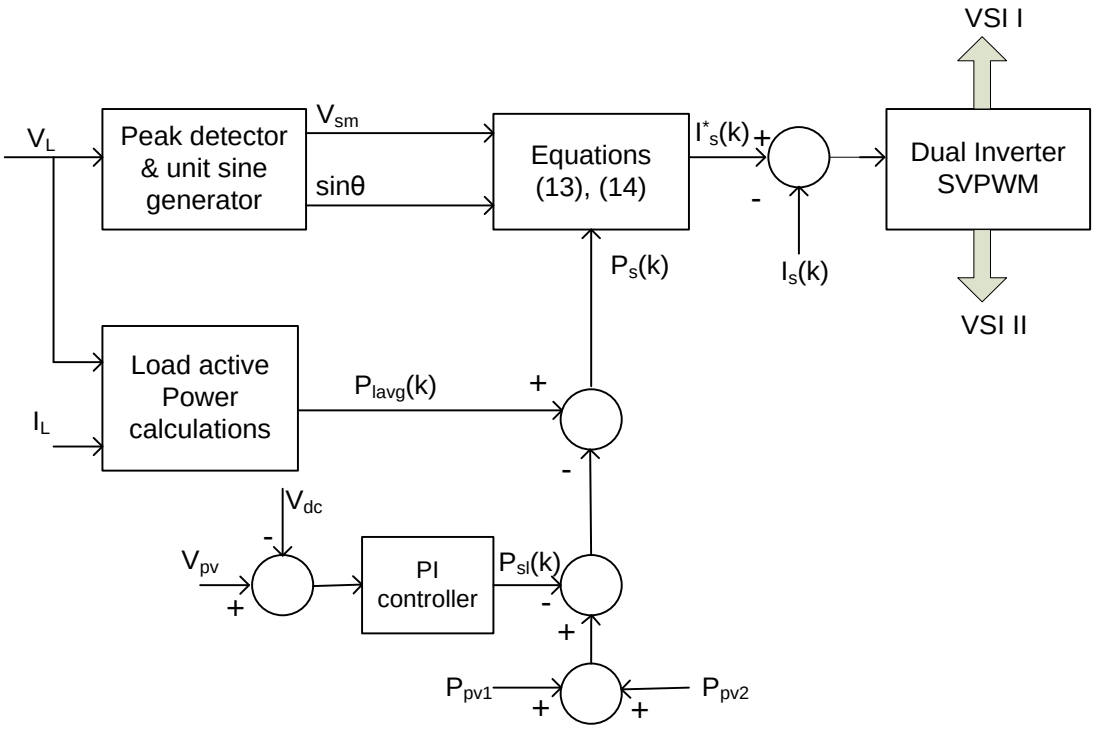

Figure 5-7: Controller schematic

5.5 RESULTS AND DISCUSSION

The various parameters used for simulation are given in Table 5-1.

Table 5-1: Simulation parameters

Location	Parameter	Value
PV	Total no of modules Maximum power generated by PV array	NsxNp=15x4=60 200x60 = 12000 W
Interconnecting Transformer	Open primary, star connected secondary	10kVA, 500V/500V
Grid	Grid voltage at 50 Hz	230 V
Load	Uncontrolled rectifier R-L load on DC side	5 kW+1kVAR

The operation of the system in different modes is summarized in the Table 5-2.

Table 5-2: Summary of operation

case	Time interval	Mode of operation	PV power injected
I	0 - 0.1sec	Without APF and PV	0
II	0.1 - 0.2sec	APF	0
III	0.2 - 0.3sec	APF+PV	$< P_L$
IV	0.3 - 0.4sec	APF+PV	$>P_L$

Case I: Here the system operates without APF/PV power injection. From Figure 5-8 it is clear that the source current is equal to load current. This can be seen from t=0 to t=0.1 sec. Figure 5-9 and Figure 5-10 show that real and reactive demand of the load is supplied by the grid. The grid current and its THD are shown in Figure 5-13.

Case II: at t=0.1sec, VSI is connected to the system with zero PV power generation. Now the VSI acts in pure APF mode. The reactive power demand of the load is supplied by the inverter as shown in Figure 5-10. Now the grid current is near sinusoidal as clear from Figure 5-8 and Figure 5-14. The corresponding grid, VSI and load active power are shown in Figure 5-9. There is slight increase in the grid active power demand as VSI draws fraction of active power to overcome inverter losses. The grid current and its THD are shown in Figure 5-14 for this mode of operation.

Case III: at t=0.2 sec, the PV system generates power less than load active power demand. Now the grid current is reduced as part of the load current is shared by the PV source. As seen from Figure 5-9, the grid active power is reduced by the same amount to that of the active power generated by the PV system. The remaining kVA capacity of the VSI is used to compensate for the reactive power demand of the load. Part of the reactive power is fed back to the grid due to line inductance. This result can be seen in Figure 5-10. The grid current remains near sinusoidal.

Case IV: at t=0.3 sec, the PV system generates power more than the load active power demand. The additional active power now is returned to the grid. This is

clear from the reverse direction of grid current at this instant. The reactive power requirement is still maintained.

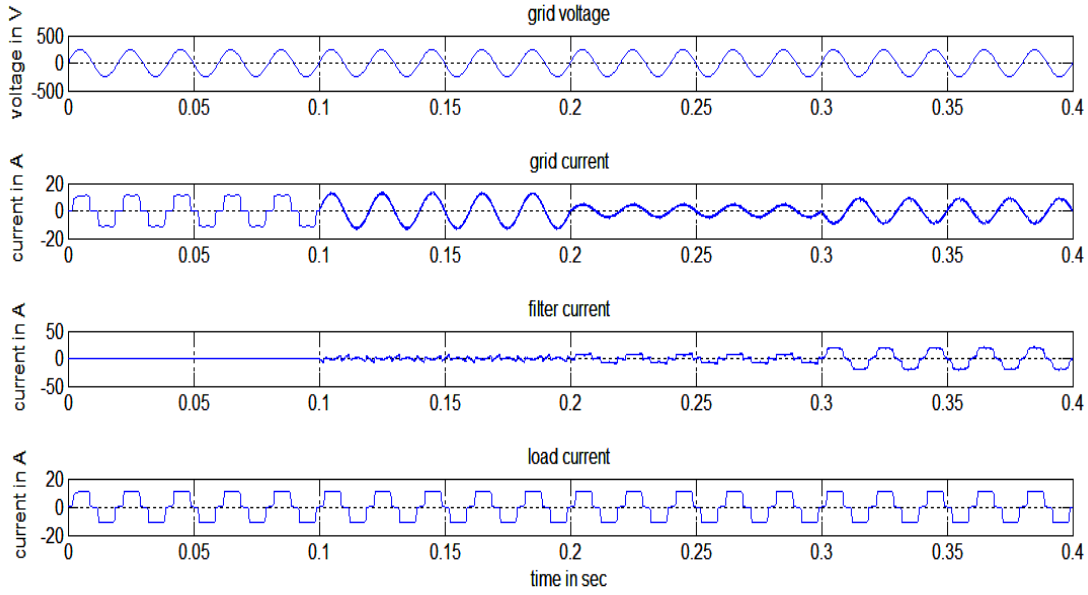

Figure 5-8: Currents at different points

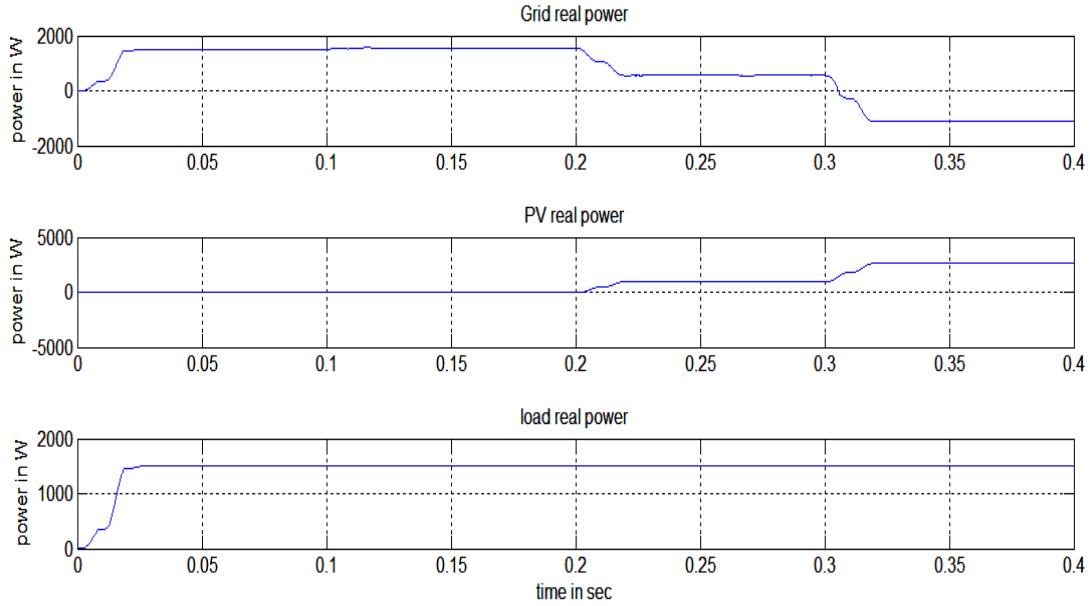

Figure 5-9: Active power distribution

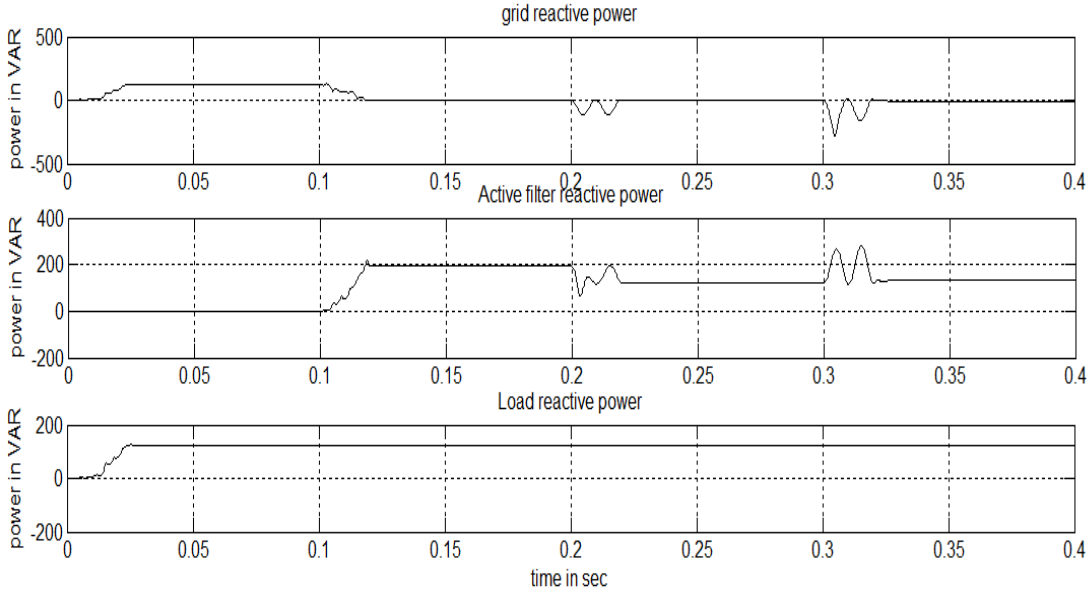

Figure 5-10: Reactive power distribution

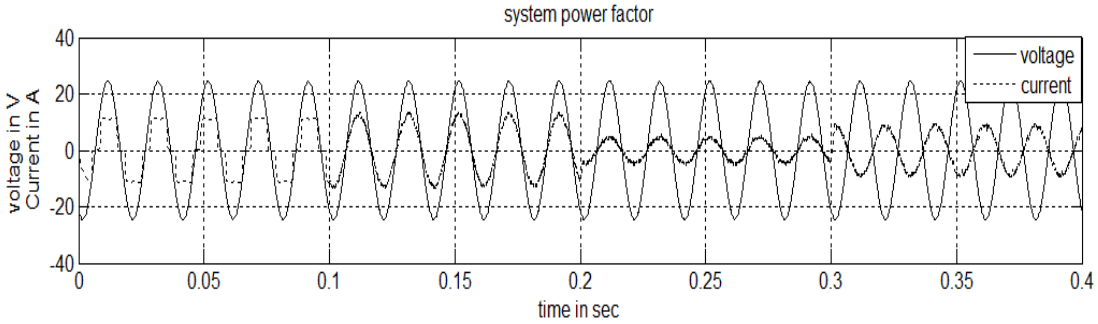

Figure 5-11: System power factor

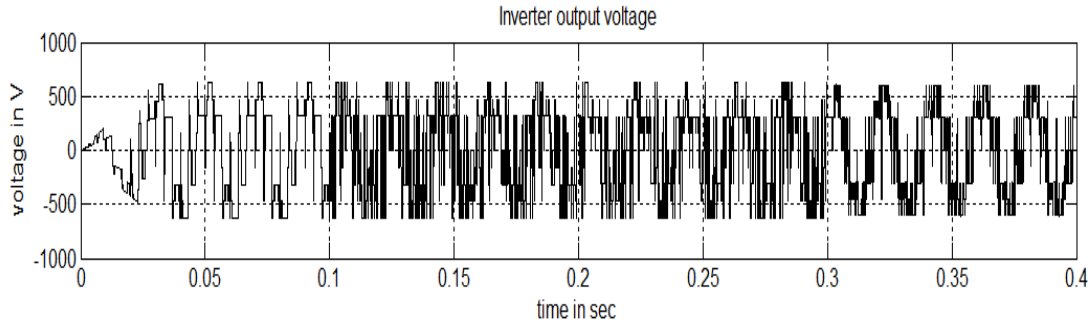

Figure 5-12: Dual-Inverter output phase-phase voltage

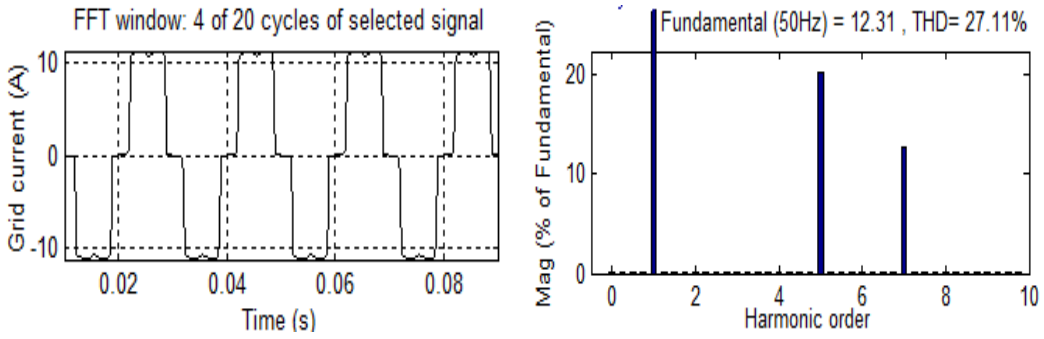

Figure 5-13: Grid current & its THD in case (i)

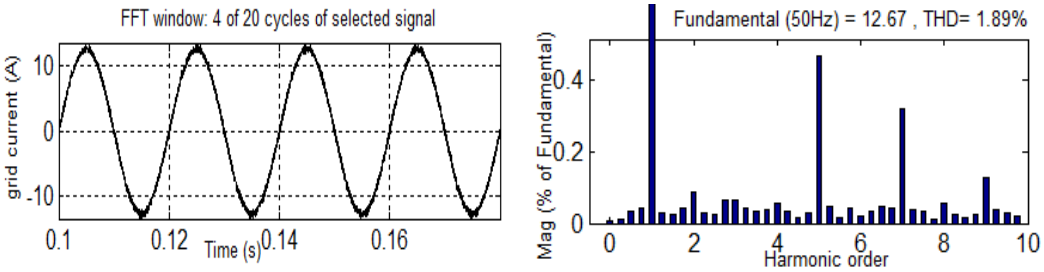

Figure 5-14: Grid current & its THD in case (ii)

5.6 CONCLUSION

The modelling and simulation of a grid connected PV system with APF functionality is presented in this chapter. The grid interfacing inverter also makes the grid current sinusoidal at unity power factor. The grid current is injected into the grid through a three-level dual inverter. The active power supplied by the PV system depending on environmental condition is injected into the grid. The local load active and reactive power is compensated by the PV system depending upon the PV power generated at the given instant. All the benefits of a multilevel inverter can be used in such a system. Also the control algorithm is very simple and easy to implement. Hence this system behaves as an integration of active power source and APF with minimum hardware (as same VSI is used for real and reactive power injection) and simple control algorithm. An attempt has been made to include three-level inverter as APF through a dual inverter topology. After compensation the grid current becomes sinusoidal and in phase with the voltage.

Chapter 6 : CONCLUSIONS AND FUTURE SCOPE OF WORK

In this thesis a grid connected PV system is integrated with active power filtering functionality. Initially a PV system along with a P&O MPPT method is modeled and simulated for its V-I and P-V characteristics. Then a PV system with a three level inverter is studied. Here a three level inverter is realized using a simpler topology of dual inverter. The PV current is injected into the grid through a three-level dual inverter. The active power supplied by the PV system depending on environmental condition is injected into the grid. The local load active power is compensated by the PV system depending upon the PV power generated at the given instant. All the benefits of a multilevel inverter can be used in such a system. Also the control algorithm is very simple and easy to implement.

In the next part, detailed study on the active power filtering is carried out. The commonly used control strategies in this field are simulated, analyzed and compared. Then the modeling and simulation of a novel three-level topology for a shunt active power filter is carried out. The reference current generation principle is simple. It is found that in both sinusoidal and non sinusoidal supply voltage conditions the SAPF works very effectively keeping the source current near sinusoidal. Also the system power factor is kept near unity in all conditions. The system performance is also verified for different load conditions to check the dynamic behavior of the system. All the benefits of the multilevel inverter can be utilized here. Also the implementation through digital controller is simple as SVPWM technique is used to drive the dual inverter.

Now the grid connected PV system is enhanced by adding the feature of active power filtering. The modelling and simulation of a grid connected PV system with APF functionality is presented. The grid interfacing inverter also makes the grid current sinusoidal at unity power factor. The grid current is injected into the grid through a three-level dual inverter. The active power supplied by the PV system depending on environmental condition is injected into the grid. The local load active and reactive power is compensated by the PV system depending upon the PV power generated at the given instant. All the benefits of a multilevel inverter can be used in

such a system. Also the control algorithm is very simple and easy to implement. Hence this system behaves as an integration of active power source and APF with minimum hardware (as same VSI is used for real and reactive power injection) and simple control algorithm. An attempt has been made to include three-level inverter as APF through a dual inverter topology. After compensation the grid current becomes sinusoidal and in phase with the voltage.

In the future scope of work it is required to experimentally verify the simulated results of the work mentioned in the three chapters viz. chapter 3, 4 & 5. The SVPWM algorithm for dual inverter can be realized using either microcontroller or DSP's. The overall control circuitry can also be realized using dSPACE controllers. At the second stage the SVPWM algorithm can be implemented using other algorithms like the sampled amplitudes of the reference phase voltage.

APPENDIX

Appendix-I

Table 1: Voltage Distortion Limits as per IEEE 519 standard

Voltage Distortion Limits		
Bus Voltage At PCC	**Individual Voltage Harmonic Distortion, %**	**Total Harmonic Distortion, %**
Below 69 kV	3.0	5.0
69 kV to 138 kV	1.5	2.5
138 kV and above	1.0	1.5

Table 2: Current Distortion Limits for General Distribution Systems (120 V through 69.0 kV)

Maximum Harmonic Current Distortion, % of I_L						
Individual Harmonic Order (Odd Harmonics)						
I_{SC} / I_L	**< 11**	**11 < h < 17**	**17 < h < 23**	**23 < h < 35**	**35 < h**	**TDD**
< 20*	4	2	1.5	0.6	0.3	5
20 < 50	7	3.5	2.5	1	0.5	8
50 < 100	10	4.5	4	1.5	0.7	12
100 < 1000	12	5.5	5	2	1	15
> 10000	15	7	6	2.5	1.4	20
Even harmonics are limited to 25 % of the odd harmonic limits above.						
Current distortions that result in a dc offset, e.g., half – wave converters, are not allowed.						
*All power generation equipment is limited to these values of current distortion, regardless of actual I_{SC} / I_L						
where I_{SC} = Maximum Short – circuit current at PCC I_L = Maximum demand load current (fundamental frequency component at PCC)						

Table 3: Current Distortion Limits for General Distribution Systems (69 kV through 161 kV)

Maximum Harmonic Current Distortion, % of I_L						
Individual Harmonic Order (Odd Harmonics)						
I_{SC} / I_L	**< 11**	**11 < h < 17**	**17 < h < 23**	**23 < h < 35**	**35 < h**	**TDD**
< 20*	2.0	1.0	0.75	0.3	0.15	5.0
20 < 50	3.5	1.75	1.25	0.5	0.25	8.0
50 < 100	5.0	2.25	2.0	0.75	0.25	12.0
100 < 1000	6.0	2.75	2.5	1.0	0.5	15.0
> 10000	7.5	3.5	3.0	1.25	0.7	20.0
Even harmonics are limited to 25 % of the odd harmonic limits above.						
Current distortions that result in a dc offset, e.g., half – wave converters, are not allowed.						
*All power generation equipment is limited to these values of current distortion, regardless of actual I_{SC} / I_L						
where I_{SC} = Maximum Short – circuit current at PCC I_L = Maximum demand load current (fundamental frequency component at PCC)						

Table 4: Current Distortion Limits for General Distribution Systems (>161 kV)
Dispersed
General and Cogeneration

Individual Harmonic Order (Odd Harmonics)						
I_{SC} / I_L	**< 11**	**11 < h < 17**	**17 < h < 23**	**23 < h < 35**	**35 < h**	**TDD**
< 50	2.0	1.0	0.75	0.3	0.5	2.5
≥ 50	3.0	1.5	1.15	0.45	0.22	3.75
Even harmonics are limited to 25 % of the odd harmonic limits above.						
Current distortions that result in a dc offset, e.g., half – wave converters, are not allowed.						
*All power generation equipment is limited to these values of current distortion, regardless of actual I_{SC} / I_L						
where I_{SC} = Maximum Short – circuit current at PCC I_L = Maximum demand load current (fundamental frequency component at PCC)						

Appendix –II

Design of Active Power Filter (APF) parameters

Assumptions:

(1) Source voltage is considered as sinusoidal.
(2) CC-VSI is assumed to be operated in linear modulation range.
(3) The filter resistance is neglected.
(4) The distortion in AC-side line current of the APF considered being 5%.
(5) Fixed reactive power compensation capability of APF.

1. Reference DC Voltage.

   It depends upon the reactive power compensation capacity of the APF. The reactive current is delivered by the APF only when output AC voltage of the inverter is more than the voltage at PCC. The upper limit of output AC voltage of the inverter is obtained on the basis of maximum compensation capacity of APF.

$$V_s \le V_{c1} \le 2V_s \qquad \text{AII.1}$$

   where, V_s is the RMS value of fundamental voltage at PCC; V_{c1} is the RMS value of fundamental component of output AC voltage of the inverter.

   Based on this the DC voltage reference is set as

$$V_{dc,ref} = 2\sqrt{2}V_{c1} \qquad \text{AII.2}$$

2. DC capacitance

   The main objective of an APF is to compensate total reactive and harmonic components of load that causes the DC-bus capacitor voltage fluctuations. The energy E_{dc} required to charge the DC-bus capacitor from actual voltage V_{dc} to the reference voltage $V_{dc,ref}$ can be given as

$$E_{dc} = \frac{1}{2}C_{dc}(V_{dc,ref}^2 - V_{dc}^2) \qquad \text{AII.3}$$

   Equating this to the total energy delivered by the source during load transition we obtain the expression for DC-bus capacitor as

$$C_{dc} = \frac{3V_s K_L I_c T}{(V_{dc,ref}^2 - V_{dc}^2)} \qquad \text{AII.4}$$

where, K_L is load factor; I_c is RMS value of harmonic and reactive load current; T is the supply voltage time period.

3. Filter Inductor

The instantaneous value of APF voltage and the current are the functions of the switching frequency. Hence the inductor plays a vital role in controlling the ripple current.

The filter inductor value is decided by using the following expression.

$$L_c = \frac{V_{dc}}{4 f_{sw} \Delta I_{sw,(p-p)}} \qquad \text{AII.5}$$

where, f_{sw} is the switching frequency; $\Delta I_{sw,(p\text{-}p)}$ is the peak to peak switching ripple current.

Appendix-III

PV-Modelling

Ideal Solar Cell

The ideal equivalent circuit of a solar cell is a current source in parallel with a single-diode.

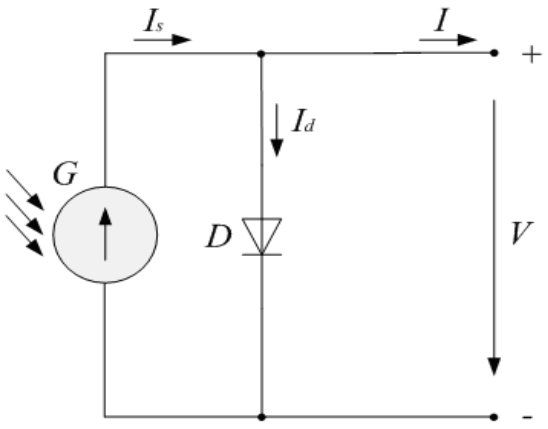

where, G is the solar radiance, I_s or I_{ph} is the photo generated current, Id is the diode current, I or I_c is the output current, and V or V_c is the terminal voltage.

The I-V characteristics of the ideal solar cell with single diode are given by:

$$I_c = I_{ph} - I_o(e^{\frac{qV}{akT}} - 1) \qquad \text{AIII.1}$$

where I_0 is the diode reverse bias saturation current, q is the electron charge, a is the diode ideality factor, k is the Boltzman's constant, and T is the cell temperature.

The short circuit current I_{sc} is given by:

$$I_{sc} = I = I_{ph} \quad \text{for} \quad V = 0 \qquad \text{AIII.2}$$

The open circuit voltage V_{oc} *is given by:*

$$V = Voc = \frac{akT}{q}\ln(1 + \frac{I_{sc}}{I_o}) \quad \text{for} \quad I = 0 \qquad \text{AIII.3}$$

Solar cell with series and parallel resistances

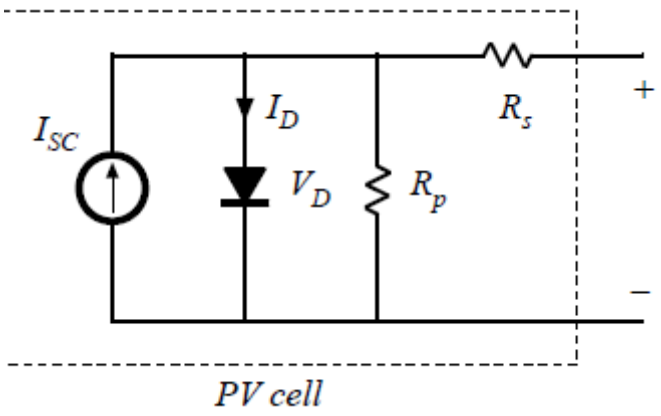

Now, the I-V characteristics are given by:

$$I_c = I_{ph} - I_o(e^{\frac{q(V+Ic*Rs)}{akT}} - 1) - \frac{V + I_c R_c}{R_p} \qquad \text{AIII.4}$$

The diode saturation current at the operating-cell temperature is given by:

$$I_o = I_o^* (\frac{T}{T_{nom}})^3 e^{\frac{E_g q}{ak}(\frac{1}{Tnom} - \frac{1}{T})} \qquad \text{AIII.5}$$

where I_o^* is the diode saturation current at STC, T is the p-n junction cell temperature, T_{nom} is the cell p-n junction temperature at STC, and E_g is the bandgap.

The PV cell photocurrent depends on the radiation and the temperature according to equation

$$I_{ph} = [I_{sc} + K_i(T - T_{nom})]\frac{Inso}{1000} \qquad \text{AIII.6}$$

where k_i = 0.017 A/^{o}K, short circuit temp coefficient.

The PV model can be represented by these equations and is shown in the simulink model shown below in figure AIII.1. The change in temperature and Insolation effect is incorporated in the figure AIII.2.

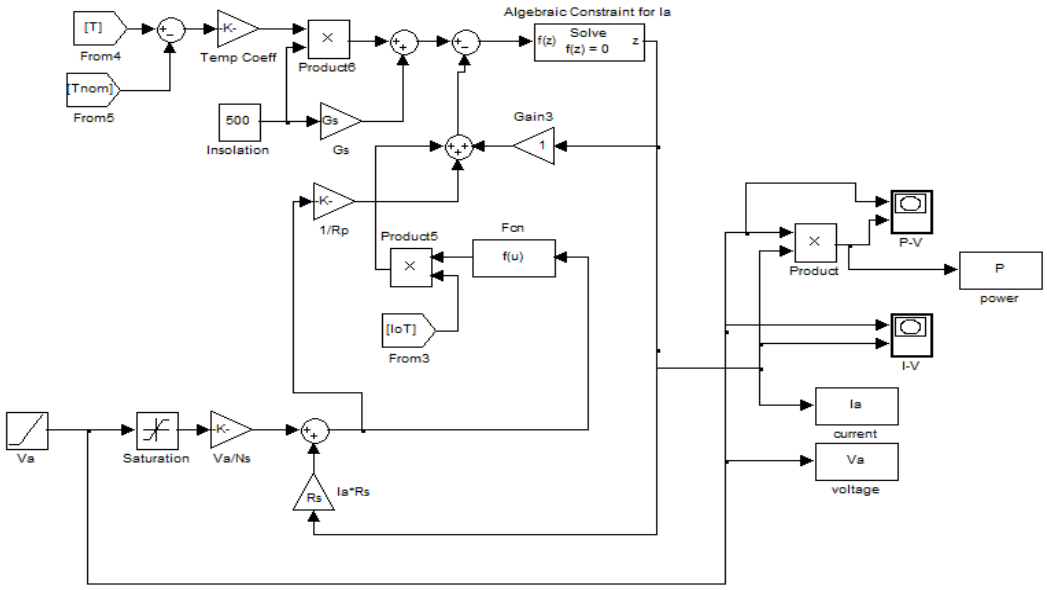

Figure AIII.1: simulink model of a PV module

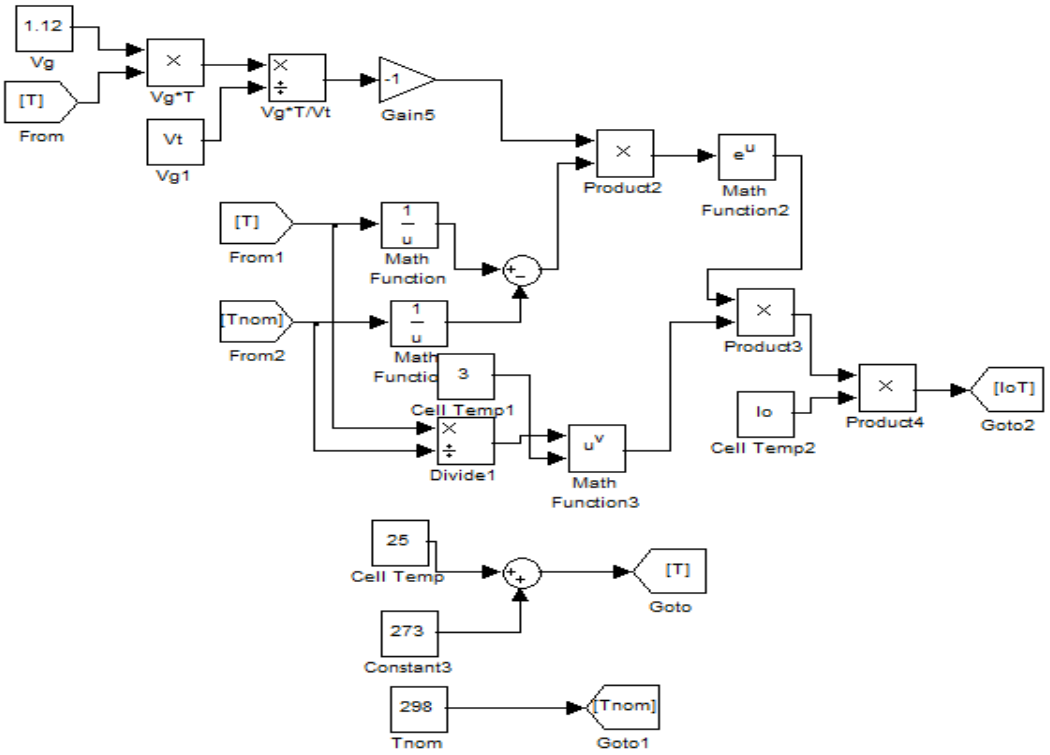

Figure AIII.2: Effect of Temperature and Insolation

REFERENCES

Abouzahr I. and Ramakumar R. (1993). "An approach to assess the performance of utility-interactive photovoltaic systems." *IEEE Transactions on Energy Conversion*, (8), 2, 145-153.

***Active Filters**: Technical Document.* (1989). *2100/1100 Series, Mitsubishi Electric Corp*., Tokyo, Japan, 1–36.

Ahmed, N.A. and Miyatake, M. (2008). "A novel maximum power point tracking for photovoltaic applications under partially shaded insolation conditions." *Electric Power Systems Research,* (78), 777–784.

Ajami, A. (2011). "Active power filter based on cascaded transformer multilevel inverter." *(IJAEST) international journal of advanced engineering sciences and technologies,* (7), 2, 313 - 318.

Akagi, H. (1996). "New trends in active filters for improving power quality." *Proceedings PEDES Conference Record*.

Akagi, H. (1996). "New trends in active filters for power conditioning." *IEEE Transactions on Industrial Applications,* (3), 6, 1312-1322.

Akagi, H., (1994). "Trends in active power line conditioners." *IEEE Transaction on Power Electron*ics, (9), 3, 283-268.

Akagi, H., Kanazawa, Y. and Nabae, A. (1984). "Instantaneous reactive power compensators comprising switching devices without energy storage components." *IEEE Transactions Industrial Applications,* (IA-20), 3, 625-630.

Alepuz S., Busquets-Monge, S., Bordonau, J., Gago,J., Gonzalez, D. and Balcells, J. (2006). "Interfacing renewable energy sources to the utility grid using a three-level inverter." *IEEE Transactions Industrial Electronics,* (53), 5, 1504-1511.

Alonso, O., Sanchis, P., Gubia, E. and Marroyo, L. (2003). "Cascaded H-Bridge Multilevel Converter for Grid Connected Photovoltaic Generators with Independent Maximum Power Point Tracking of each Solar Array." *IEEE 34th Annual Power Electronics Specialist Conference, 2003. PESC '03,* (2), 731-735.

Amini, J., Talebi, N., Akbarzadeh, A. (2011). "Damping of low frequency oscillations in power system with Neuro-Fuzzy UPFC controller." *10th International Conference on, Environment and Electrical Engineering (EEEIC),* 1-5.

Amoli, M. E. and Florence, T. (1990). "Voltage, current harmonic control of a utility system—A summary of 1120 test measurements." *IEEE Transactions on Power Delivery,* (5), 1552-1557.

Angrist, S. W. (1982). "*Direct Energy Conversion*" Allyn and Bacon, Inc., 4th edition, 177-227.

Armstrong, S. and Hurley, W.G. (2004). "Self-regulating maximum power point tracking for solar energy systems." *Proceeding of the 39th International Universities Power Engineering Conference,* University of the West of England (UWE), Bristol, UK, 1339-1350.

Baghzouz, Y. (1991). "Effects of non-linear loads on optimal capacitor placement in radial feeders." *IEEE Transactions on Power Delivery,* (6), 1, 245-251.

Baghzouz, Y. and Cox, M. D. (1991) "Optimal shunt compensation for unbalanced linear loads with non-sinusoidal supply voltages." *Electric Machines and Power Systems,* (19), 171-183.

Baiju, M. R., Mohapatra, K. K., Kanchan, R. S. and Gopakumar, K. (2004). "A dual two-level inverter scheme with common mode voltage elimination for an induction motor drive." *IEEE Transactions Power Electronics*, (19), 3, 794-805.

Baiju, M. R.., Mohapatra, K. K., Kanchan, R. S. Gopakumar, K. (2004). "A dual two-level inverter scheme with common mode voltage elimination for an induction motor drive" *IEEE Transactions on Power Electronics*, (19), 3, 794- 805.

Barker, P. P. ; Burke, J.J. ; Mancao, R.T. ; Short, T. A. ; Warren, C. A. ; Burns, C.W. ; Siewierski, J.J. (1994). "Power quality monitoring of a distribution system." *IEEE Transactions on Power Delivery*, (9), 2, 1136-1142.

Bekker, B. and Beukes H. J. (2004). "Finding an optimal PV panel maximum power point tracking method." *Proceedings 7th AFRICON Conference Africa*,1125-1129.

Best R. A., and De La Parra, H. Z. (1996). "Transient response of a static VAR shunt compensator," *IEEE Transactions on Power Electronics*, (11), 3, 489-494.

Bhattacharya, S. and Divan, D. (1995). "Synchronous frame based controller implementation for a hybrid series active filter system." *Conference Recordings IEEE-IAS Annual Meeting*, 2531–2540.

Bhattacharya, S., Divan, D. M. and Banerjee, B. B. (1993). "Control, reduction of terminal voltage total harmonic distortion (THD) in a hybrid series active, parallel passive filter system." *Proceedings IEEE PESC'93*, 779-786.

Bhattacharya, S., Divan, D. M. and Banerjee, B. B. (1993). "Control, reduction of terminal voltage total harmonic distortion (THD) in a hybrid series active, parallel passive filter system." *Proceedings IEEE PESC'93*, 779-786.

Bhattacharya, S., Divan, D. M., and Banerjee, B. B. (1995). "Active filter solutions for utility interface." *Proceedings IEEE ISIE'95*, 1–11.

Bhuvaneswari, G. and Nair, M. G. (2008). "Design, simulation, and analog circuit implementation of a three-phase shunt active filter using the Icosϕ algorithm." *IEEE Transactions on Power Delivery*, (23), 2, 1222-1235.

Bodur, M. and Ermis, M., (1994). "Maximum power point tracking for low power photovoltaic solar panels." *Proceedings 7th Mediterranean Electrotechnical Conference*, 758-761.

Boehringer, A. F. (1968). "Self-adapting dc converter for solar spacecraft power supply." *IEEE Transactions on Aerospace Electronics System,* (AES-4), 1, 102-111.

Borle, L., Dymond, M., Nayar, C. (1997). "Development and testing of a 20-kW grid interactive photovoltaic power conditioning system in Western Australia." *IEEE Transaction Industrial Applications,* (33), 2, 502–508.

Brambilla, A., Gambarara, M., Garutti, A. and Ronchi, F. (1999). "New approach to photovoltaic arrays maximum power point tracking." P*roceedings 30th Annual IEEE Power Electronics Special Conference,* 632-637.

Buciarelli, L. L., Grossman,B. L., Lyon, E. F., and Rasmussen, N. E. (1980). "The energy balance associated with the use of a MPPT in a 100 kW peak power system." *IEEE Photovoltaic Special Conference,* 523-527.

Buresch, M. (1983). "*Photovoltaic Energy System Design and Installations*." MGraw-Hill, New York.

Buresch, M. (1983). *Photovoltaic Energy Systems*. New York: McGraw Hill.

Buso, S., Malesani, L., and Mattavelli, P. (1998). "Comparison of current control techniques for active filter applications." *IEEE Transactions on Industrial Electronics,* (45), 5, 722-729.

Bzura, J. J. (1990). "The New England electric photovoltaic systems research and demonstration project." *IEEE Transactions on Energy Conversion*, (5), 2, 284-289.

Bzura, J. J. (1992). "Performance of grid-connected photovoltaic systems on residences and commercial buildings in New England." *IEEE Transactions on Energy Conversion*, (7), 1, 79-82.

Calais, M., Agelidis, V.G., and Chen, J.Y. (1998). "A Five-Level Zero Average Current Error Controlled Single-phase Grid-Interactive Inverter." *Proceedings 1998 International Conference on Power Electronic Drives and Energy Systems for Industrial Growth*, (1), 50-55.

Calais, M.,. Agelidis, V.G., Borle, L.J. and Dymond, M.S. (2000). "A Transformerless Five Level Cascaded Inverter Based Single Phase Photovoltaic System." *IEEE 31st Annual Power Electronics Specialists Conference, 2000*. (3), 1173-1178.

Chandra, A., Singh, B., Singh, B. N., and Al-Haddad, K. (2000). "An improved control algorithm of shunt active filter for voltage regulation, harmonics elimination, power-factor correction and balancing of non-linear loads." *IEEE Transactions on Power Electronics*, (15), 3, 495-507.

Chang, G. W. (2006). "A new approach for optimal shunt active power filter control considering alternative performance indices." *IEEE Transactions on Power Delivery*, (21), 1, 406-413.

Chang, G. W. and Chen, W. C. (2006). "A new reference compensation voltage strategy for series active power filter control." *IEEE Transactions on Power Delivery*, (21), 3, 754-1756.

Chang, G. W., Tai-Chang, S. (2004). "A novel reference compensation current strategy for shunt active power filter control." . *IEEE Transactions on Power Electronics* , 1751-1757.

Cheng, P. T., Bhattacharya, S., and Divan, D. M. (1996). "Hybrid solutions for improving passive filter performance in high power applications." P*roceedings IEEE APEC'96*, 911–917.

Chu, R. F., Wang, J., Chiang, H. (1994). "Strategic planning of LC compensators in non-sinusoidal distribution systems." *IEEE Transactions on Power Delivery*, (9), 3, 1558-1563.

Chu, R. F., Wang, J., Chiang, H., (1994). "Strategic planning of LC compensators in non-sinusoidal distribution systems," *IEEE Transactions on Power Delivery*, (9), 3, 1558-1563.

Costogue, E. N. and Lindena, S. (1976). "Comparison of candidate solar array maximum power utilization approaches." *Intersociety Energy Conversion Engineering Conference*, 1449-1456.

Dixon, J. W., Venegas, G., and Moran, L. A. (1997). "A series active power filter based on a sinusoidal current-controlled voltage-source inverter." *IEEE Transactions on Industrial Electronics,* (44), 5, 612-619.

Duffey, C. K. and Stratford, R. P. (1989). "Update of harmonic standard IEEE- 519: IEEE recommended practices, requirements for harmonic control in electric power systems," *IEEE Transactions on Industrial Applications,* (25), 1025-1034.

Dugan, R. C., Mcranaghan, M. F., Santoso, S., and Beaty, H. W. (2004). "*Electrical power systems quality*", Second Edition, McGraw-Hill.

Eichert, K., Mangold, T., Weinhold, M. (1999). "Power quality issues and their solutions." *VII Seminario de Electrónica de Potencia*, Valparaíso, Chile.

Femia, N., Petrone, G., Spagnuolo, G. and Vitelli, M. (2005). "Optimization of perturb and observe maximum power point tracking method." *IEEE Transactions on Power Electronics*, (20), 4, 963-973.

Femia, N., Petrone, G., Spagnuolo, G., and Vitelli, M. (2005). "Optimization of perturb and observe maximum power point tracking method." *IEEE Transaction Power Electronics*, (20), 4, 963-973.

George, S. and Agarwal, V. (2007). "A DSP-based optimal algorithm for shunt active filter under non sinusoidal supply and unbalanced load conditions." *IEEE Transactions on Power Electronics*, (22), 2, 593-601.

Gow, J. A. and Manning, C. D. (1999). "Development of a photovoltaic array model for use in power-electronics simulation studies." *IEE Proceedings- Electric Power Applications*, (146), 2, 193-199.

Guojun, T., Xuanqin, W., Hao, L., Meng, L. (2010). "Novel control strategy for multilevel active power filter without phase-locked-loop." *Energy and Power Engineering*,(2), 262-270.

Gupta, A. K. and Khambadkone, A. M. (2006). "A space vector pwm scheme to reduce common mode voltage for a cascaded multilevel inverter." Proceedings of 37th *IEEE PESC* '06, 1-7.

Gupta, A. K. and Khambadkone, A.M. (2006). "A space vector pwm scheme for multilevel inverters based on two level space vector PWM." *IEEE Transaction Industrial Electronics*, 1631–1639.

Gupta, A., Khambadkone, A. M. (2007). "A General Space Vector PWM Algorithm for Multilevel Inverters, Including Operation in Overmodulation Range." *IEEE transactions on power electronics*, (22), 2, 517-526.

Gyugyi, L. (1979). "Reactive power generation, control by thyristor circuits." *IEEE Transactions on Industry Applications*, (5), 5, 521-532.

Gyugyi, L. (1979). "Reactive power generation, control by thyristor circuits." *IEEE Transactions on Industry Applications,* (5), 5, 521-532.

Gyugyi, L. (1988). "Power electronics in electric utilities: Static Var compensators." *IEEE Proceedings*, (76), 4, 483-494.

Gyugyi, L. (1988). "Power electronics in electric utilities: Static Var compensators." *IEEE Proceedings*, (76), 4, 483-494.

Gyugyi, L., Otta, R. A. and Putman, T. H. (1978). "Principles, applications of static, thyristor controlled shunt compensators." *IEEE Transaction on PAS*, (97), 5, 1935-1945.

Gyugyi, L., Otta, R. A. and Putman, T. H. (1978). "Principles, applications of static, thyristor controlled shunt compensators," *IEEE Transaction on PAS*, (97), 5, 1935-1945.

Hamrouni, N. and Chérif, A. (2007). "Modeling and control of a grid connected photovoltaic system", *Revue des Energies Renouvelables*, (10), 3, 335-344.

Harada, J. and Zhao, G. (1989). "Controlled power-interface between solar cells and ac sources." *IEEE Telecommunication and Power Conference*, 22.1/1–22.1/7.

Hart, G. W., Branz, H. M., and Cox, C. H. (1984). "Experimental tests of open loop maximum-power-point tracking techniques." *Solar Cells*, (13), 185-195.

Hashimoto, O., Shimizu, T., and Kimura, G. (2000). "A novel high performance utility interactive photovoltaic inverter system." *Conference Record 2000 IEEE Industrial Applications Conference*, 2255-2260.

Hiyama, T., Hammam, M. S. A. A. and Ortmeyer, T. H. (1989). "Distribution system modeling with distributed harmonic sources." *IEEE Transactions on Power Delivery*, (4), 2, 1297-1304.

Hu, H., Yao. W., Lu, Z. (2007). "Design and implementation of three-level SVPWM IP core for FPGAs." *IEEE Transaction Power Electronics*, 2234-44.

Hua, C. and Lin, J. R. (1996). "DSP-based controller application in battery storage of photovoltaic system." *Proceedings of IEEE IECON 22nd International Conference on Industrial Electronics, Control and Instrumentation*, 1705–1710.

Hua, C. C. and Shen, C. M. (1998). "Study of maximum power tracking techniques and control of dc-dc converters for photovoltaic power system." *Proceedings of 29th annual IEEE Power Electronics Specialists Conference*, (1), 86-93.

Huang, S. J. and Wu, J. C. (1999). "A control algorithm for three-phase three-wired active power filters under non ideal mains voltages." *IEEE Transactions on Power Electronics*, (14), 4,753-760.

Hussein, A., Hirasawa, K., Hu, J., and Murata, J. (2002). "The dynamic performance of photovoltaic supplied dc motor fed from DC–DC converter and controlled by neural networks." *Proceedings International Joint Conference Neural Network*, 607-612.

Hussein, K. H. and Mota, I. (1995). "Maximum photovoltaic power tracking: An algorithm for rapidly changing atmospheric conditions." *IEE Proceedings on Generation Transmission Distribution*, 59–64.

IEEE std. 1036-1992 *IEEE guide for application of shunt capacitors*.

IEEE std. C57.110-1998, *IEEE Recommended practice for establishing transformer capability when supplying non-sinusoidal load currents*.

IEEE std.1100-1992 *IEEE Recommended Practice for Powering and Grounding Sensitive Electronic Equipments*.

IEEE std.141-1993 *IEEE Recommended Practice for Electric Power Distribution for Industrial Plants.*

IEEE Task force on the effects of harmonics on equipment. (1993) "Effects of harmonics on equipment," *IEEE Transactions on Power Delivery*, (8), 2.

IEEE Working Group on Power System Harmonics, (1983). "Power system harmonics: an overview," *IEEE Transaction PAS*, (102), 2455-2460.

IEEE Working Group on Power System Harmonics. (1983). "Power system harmonics: An overview," *IEEE Transactions on PAS*, (102), 2455-2460.

Jain, S. K., Agarwal, P., and Gupta, H. O. (2004). "A control algorithm for compensation of customer-generated harmonics and reactive power." *IEEE Transactions on Power Delivery*, (19), 1, 357-366.

Jain, S. K., Agarwal, P., and Gupta, H.O. (2006). "Neutral current compensation and load balancing with fuzzy logic controlled active power filter." *Proceedings of IEEE International Symposium of Industrial Electronics*, (2), 1311-1316.

Jinn-Chang, W., Kuen-Der, W., Hurng-Liang, J., Shun-Tian, X. (2011). "Diode clamped multi-level power converter with a zero-sequence current loop for three-phase three wire hybrid power filter." *Electric Power Systems Research*, (81), 2, 263-270.

Jinn-Chang, W., Kuen-Der, W., Hurng-Liang, J., Shun-Tian, X. (2011). "Diode clamped multi-level power converter with a zero-sequence current loop for three-phase three wire hybrid power filter." *Electric Power Systems Research*, (81), 2, 263-270.

Jou, H. L., Wu, J. C., Chang, Y. J., and Feng, Y. T. (2005). "A novel active power filter for harmonic suppression." *IEEE Transactions on Power Delivery*, (20), 2, 1507-1513.

Jou, H. L., Wu, J. C., Chang, Y. J., Feng, Y. T., and Hsu, W. P. (2006). "New active power filter and control method." *IEE Proceedings on Electric Power Applications*, (152), 2, 175-181.

Jou, H. L., Wu, K. D., Wu, J. C., and Chiang, W. J. (2008). "A three-phase four-wire power filter comprising a three-phase three-wire active power filter and a zig-zag transformer." *IEEE Transactions on Power Electronics*, (23), 1, 252-259.

Kale, M. and Ozdemir, E. (2005). "An adaptive hysteresis band current controller for shunt active power filters." *Electric Power Systems Research*, (72), 113-119.

Kanchan, R. S., Baiju, M. R., Mohapatra, K., Ouseph, P., Gopakumar, K. (2005). "Space-vector PWM signal generation for multilevel inverters using only the sampled amplitudes of reference phase voltage". *IEE Proceedings Electric Power Applications,* 297–309.

Kanchan, R. S., Gopakumar, K., Kennel, R. (2007). "Synchronised carrier-based SVPWM signal generation scheme for the entire modulation range extending up to six-step mode using the sampled amplitudes of reference phase voltages." *IET Electric Power Applications,* (1), 3, 407-415.

Kang, D.-W., Lee, B.-K., Jeon, J.-H., Kim, T.-J. and Hyun, D.-S. (2005). "A symmetric carrier technique of CRPWM for voltage balance method of flying

capacitor multilevel inverter." *IEEE Transactions Industrial Electronics,* (52), 3, 879-888.

Karuppanan, P., and Mahapatra, K. (2010). "A novel SRF based Cascaded multi-level active filter for power line conditioners." *2010 Annual IEEE India Conference (INDICON).* 1-4.

Khaehintung, N., Pramotung, K., Tuvirat, B., and Sirisuk, P. (2004), "RISC microcontroller built in fuzzy logic controller of maximum power point tracking for solar-powered light-flasher applications." *Proceedings of 30th Annual Conference IEEE Industrial Electronics Society,* 2673-2678.

Khomfoi, S., Praisuwanna, N. and Tolbert, L. M. (2010). "A Hybrid Cascaded Multilevel Inverter Application for Renewable Energy Resources Including a Reconfiguration Technique." *2010 IEEE Energy Conversion Congress and Exposition (ECCE),* 3998-4005.

Kikuchi, A. H. (1992). "Active power filters," *Toshiba GTR Module (IGBT) Application Notes, Toshiba Corp.*, Tokyo, Japan, 44–45.

Kim, S. and Enjeti, P. N. (2002). "A new hybrid active power filters (APF) topology, "*IEEE Transactions on Power Electronics,* (17), 1, 48-54.

Kim, Y., Jo, H., and Kim, D. (1996). "A new peak power tracker for cost-effective photovoltaic power system." *Proceedings of 31st Intersociety Energy Conversion Engineering Conference,* 1673-1678.

Kitano, T., Matsui, M., and Xu, D.-h. (2001) "Power sensor-less MPPT control scheme utilizing power balance at DC link-system design to ensure stability and response." *Proceedings 27th Annual Conference IEEE Industrial Electronics Society,*1309-1314.

Kou, X., Corzine, K. and Wielebski, M. (2006). "Overdistention operation of cascaded multilevel inverters." *IEEE Transactions Industrial Applications*, (42), 3, 817-824.

Koutroulis, E., Kalaitzakis, K., and Voulgaris, N. C. (2001). "Development of a microcontroller-based, photovoltaic maximum power point tracking control system." *IEEE Transactions on Power Electronics*, (16), 21, 46-54.

Koutroulis, E., Kalaitzakis, K., and Voulgaris, N. C. (2001). "Development of a microcontroller-based photovoltaic MPPT control system." *IEEE Transaction Power Electronics*, (16), 1, 46-54.

Kyoungsoo R. and Rahman, S. (1998). "Two-loop controller for maximizing performance of a grid-connected photovoltaic-fuel cell hybrid power plant." *IEEE Transactions on Energy Conversions*, (13), 3, 276-281.

Lancarotte, M. S. and Penteado, A. D. A. (2001). "Estimation of core losses under sinusoidal or non-sinusoidal induction by analysis of magnetization rate." *IEEE Transactions on Energy Conversion*, (16), 2, 174-179.

Ledwich, G.F., Hosseini, S. H. and Shannon, G. F. (1992). "Voltage balancing using switched capacitors," *Electric Power Systems Research*, (24), 85-90.

Lee, C. Y. and Lee, W. J. (1999). "Effects of non-sinusoidal voltage on the operation performance of a three-phase induction motor." *IEEE Transactions on Energy Conversion*, (14), 2, 193-201.

Li, H., Zhuo, F., Wang Z., Lei W., and Wu, L. (2005). "A novel time-domain current-detection algorithm for shunt active power filters." *IEEE Transactions on Power Systems*, (20), 2, 644-651.

Lin, B.-R. and Huang, C.-H. (2006) "Implementation of a three-phase capacitor clamped active power filter under unbalanced condition." *IEEE Transaction Industrial Electronics*, (53), 5, 1621-1630.

Mansoor, A., Grady, W. M., Staats, P. T., Thallam, R. S. (1994). "Predicting the net harmonic currents produced by large numbers of distributed single-phase computer loads." *IEEE Transactions on Power Delivery*, (10), 2001-2006.

Marchesoni, M., Mazzucchelli, M. and Tenconi, S. (1998). "A non conventional power converter for plasma stabilization." *Proceedings IEEE Power Electronics, Special Conference*, 122–129.

Masoum, M. A. S., Dehbonei, H., and Fuchs, E. F. (2002). "Theoretical and experimental analysis of photovoltaic systems with voltage and current-based maximum power-point tracking." *IEEE Transactions on Energy Conversions*, (17), 4, 514-522.

Massoud, A. M., Finney S. J., Cruden A. J., and Williams B. W. (2007). "Three-phase, three-wire, five-level cascaded shunt active filter for power conditioning, using two different space vector modulation techniques." *IEEE Transactions on Power Delivery*, (22), 4, 2349-2361.

Massoud, A. M., Finney, S. J., and Williams, B. W. (2003). "Control techniques for multilevel voltage source inverters." *Proceedings Power Electronics Special conference*,(1), 171–176.

Mastromauro, R. A., Kerekes, T. and Dell'Aquila, A. (2009). "A Single-Phase Voltage-Controlled Grid-Connected Photovoltaic System With Power Quality Conditioner Functionality." IEEE Transactions on Industrial Electronics, (56), 11, 4436-4444.

Matsui, M., Kitano, T., Xu, D.-h., and Yang, Z.-q. (1999). "A new maximum photovoltaic power tracking control scheme based on power equilibrium at DC link." *Conference Record 1999 IEEE Industrial Application Conference*, 804-809.

Mattavelli, P. (2001). "A closed-loop selective harmonic compensation for active filters." *IEEE Transactions on Industry Applications*, (37), 1, 81-89.

Meynard, T. and Foch, H. (1992). "Multi-level choppers for high voltage applications." *European Power Electronics Journal*, (2), 1, 45-50.

Midya, P., Krein, P. T., Turnbull, R. J., Reppa, R., and Kimball, J. (1996). "Dynamic maximum power point tracker for photovoltaic applications." *Proceedings 27th Annual IEEE Power Electronics Special Conference*, 1710-1716.

Mohapatra, K. K., Gopakumar, K., Somasakhar, V. T., and Umanand, L. (2003). "A harmonic elimination and suppression scheme for an open-end winding induction motor drive." *IEEE Transaction Industrial Electronics*, (50), 6, 1187-1198.

Mutoh, N., Matuo, T., Okada, K., and Sakai, M. (2002). "Prediction-data-based maximum-power-point-tracking method for photovoltaic power generation systems." P*roceedings of 33rd Annual IEEE Power Electronics Special Conference*, 1489-1494.

Nabae, A. and Akagi, H. (1981). "A new neutral-point clamped PWM inverter," *IEEE Transactions Industrial Applications*, (IA-17), 5, 518-523.

Nabae, A. and Tanaka, T. (1996). "A new definition of instantaneous active-reactive current and a power based on instantaneous space vectors on polar coordinates in three phase circuits." *IEEE Tran. Power Delivery*, (11), 3, 1238-1243.

Nabae, A. and Tanaka, T. (1996). "A new definition of instantaneous active-reactive current and a power based on instantaneous space vectors on polar coordinates in three phase circuits," *IEEE Transactions Power Delivery*, (11), 3, 1238-1243.

Neves, P., Gonçalves, D., Pinto, J. G., Alves, R., Afonso, J.L. (2009). "Single-Phase Shunt Active Filter Interfacing Renewable Energy Sources with the Power Grid." *IEEE 35th Annual Conference of Industrial Electronics, 2009 IECON'09*, 3264-3269.

Noguchi, T., Togashi S., and Nakamoto, R. (2000). "Short-current pulse based adaptive maximum-power-point tracking for photovoltaic power generation system." P*roceedings of 2000 IEEE International Symposium Industrilal Electronics*, 157-162.

Ortmeyer, T. H. and Hiyama, T., (1996), "Distribution system harmonic filter planning." *IEEE Transactions on Power Delivery*, (11), 4, 2005-2012.

Ortmeyer, T. H. and Zeher, K. (1991). "Distribution system harmonic design." *IEEE Transactions on Power Delivery*, (6), 1, 289-294.

Ortmeyer, T. H., Hammam, M. S. A. A., Hiyama, T. and Webb, D. B. (1988). "Measurement of the harmonic characteristics of radial distribution systems." *Power Engineering Journal (IEE*), (2), 3, 163-172.

Packebush, P. and Enjeti, P. (1994) "A survey of neutral current harmonics in campus buildings, suggested remedies." *Proceedings Power Quality Conference*, 194-205.

Packebush, P. and Enjeti, P. (1994). "A survey of neutral current harmonics in campus buildings, suggested remedies." *Proceeding Power Quality Conference*, 194-205.

Patcharaprakiti, N. and Premrudeepreechacharn, S. (2002). "Maximum power point tracking using adaptive fuzzy logic control for grid-connected photovoltaic system." *IEEE Power Engineering Society Winter Meet*, 372-377.

Patel, H. and Agarwal, V. (2006). "PV Based Distributed Generation with Compensation Feature Under Unbalanced and Non-linear Load Conditions for a 3-phase, 4 Wire System." *IEEE International Conference on Industrial Technology, ICIT 2006*, 322-327.

Patel, H. and Agarwal, V. (2010). "Investigations into the performance of photovoltaic-based active filter configurations and their control schemes under uniform and non-uniform radiation conditions." *IET Renewable Power Generation,* (4), 1, 12–22.

Patidar, R. D., Singh, S. P., Rathod, D. K. (2010). "Single-phase single-stage grid-interactive Photovoltaic system with active filter functions." *IEEE conference on Power and Energy Society General Meeting*, 1-7.

Patterson, D. J. (1990). "Electrical system design for a solar powered vehicle." *Proceedings of 21st Annual IEEE Power Electronics Special Conference*, 618-622.

Petit, J. F., Robles, G., Amaris, H. (2007). "Current reference control for shunt active power filters under nonsinusoidal voltage conditions." *IEEE Transactions on Power Delivery,* 2254-2261.

Phang, J. C. H., Chan, D. S. H., and Philips, J. R. (1984). "Accurate analytical method for the extraction of solar cell model parameters," *Electronics Letters*, (20), 10, 406-408.

Phipps, J. K., Nelson, J. P., and Sen, P. K. (1994). "Power quality and harmonic distortion on distribution systems." *IEEE Transactions on Industry Applications*, (30), 2, 176-184.

Phipps, J. K., Nelson, J. P., Sen, P. K. (1994). "Power quality and harmonic distortion on distribution systems." *IEEE Transactions on Industrial Appl*ications, (30), 2, 176-184.

Pottker, F., Barbi, I. (2000). "Single phase active power filters for distributed power factor correction." *IEEE Power Electronics Specialists Conference Record*, 500–505.

Pou, J., Pindado, R., and Boroyevich, D. (2005). "Voltage-balance limits in four level diode-clamped converters with passive front ends." *IEEE Transactions Industrial Electronics*, (52), 1, 190–196.

Pouresmaeil, E., Gomis-Bellmunt, O., Montesinos-Miracle, D., Bergas-Jané, J. (2011). "Multilevel converters control for renewable energy integration to the power grid." *Energy*, 36, 950-963.

Purkait, P. and Sriramakavacham, S. (2006). "A new generalized space vector modulation algorithm for neutral-point-clamped multilevel converters." *Proceedings of progress in electromagnetics research symposium, Cambridge (USA)*, 330-335.

Rahmani, M., Arora, A., Pfister, R., Huencho, P. (1999). "State of the Art power quality devices and innovative concepts." *VII Seminario de Electrónica de Potencia*, Valparaíso, Chile.

Report by load characteristics task force and effects of harmonics task force. (1998). "The effects of power system harmonics on power system equipment and loads," *IEEE Transaction on PAS*, (104), 9.

Richards, C. G., Klinkhachorn, P., Tan, O. P. and Hartana, R. H. (1989). "Optimal LC compensators for non-linear loads with uncertain non-sinusoidal source, load characteristics." *IEEE Transactions on Power Systems*, (4), 1, 30-36.

Rodriguez, J., Hammond, P., Pontt, J., Musalem, R., Lezana, P., and Escobar, M. (2005). "Operation of a medium-voltage drive under faulty conditions." *IEEE Transactions Industrial Electronics*, (52), 4, 1080-1085.

Ropp, M.E. and Gonzalez, S. (2009). "Development of a MATLAB/simulink model of a single-phase grid connected photovoltaic system." IEEE Transactions on Energy Conversions." (24), 195-202.

Routimo, M., Salo, M., and Tuusa, H. (2003). "A novel control method for wideband harmonic compensation," *Proceedings of the IEEE International Conference on Power Electronics and Drive Systems (PEDS)*, 799-804.

Saad, S., Zellouma, L., (2009). "Fuzzy logic controller for three-level shunt active filter compensating harmonics and reactive power." *Electric Power Systems Research*, (79), 1337-1341.

Sankaran, C. (2002). "*Power Quality*," CRC Press LLC.

Schoeman, J. J. and vanWyk, J. D. (1982). "A simplified maximal power controller for terrestrial photovoltaic panel arrays." *Proceedings of 13th Annual IEEE Power Electronics Special Conference*, 361-367.

Selvaraj, J. and Rahim, N. A. (2009). "Multilevel Inverter for Grid-Connected PV System Employing Digital PI Controller." *IEEE Transactions Industrial Electronics* , (*56)*, 1,149-158.

Shivakumar, E. G., Gopakumar, K., Sinha, S. K., Pittet ,A., and Ranganathan, V. T. (2002). "Space vector control of dual inverter fed open end winding induction motor drive." *EPE Journal*, (12), 1, 9-18.

Shivakumar, E. G., Gopakumar, K., Sinha, S. K., Pittet, A., and Ranganathan, V. T. (2002). "Space vector control of dual inverter fed open-end winding induction motor drive', *European Power Electronics Journal*,(12), 1, 9-18.

Shmilovitz, D. (2005). "On the control of photovoltaic maximum power point tracker via output parameters." *IEE Proceedings Electric Power Applications*, 239-248.

Singh, B., Al-Haddad, K. and Chandra, A. (1998). "A New control approach to three-phase active filter for harmonics and reactive power compensation" *IEEE Transactions on Power Systems*, (13), 1.

Singh, B., Al-Haddad, K. and Chandra, A. (1999). "A review of active filters for power quality improvement." *IEEE, Transaction on Industrial Electronics*," (46), 5, 960-971.

Singh, B., and Verma, V. (2006). "An indirect current control of hybrid power filter for varying loads." *IEEE Transactions on Power Delivery*, (21), 1, 178-184.

Singh, B., Chandra, A., Al-Haddad, K. (1999). "Computer-aided modeling and simulation of active power filters." *Taylor & Francis, Inc. Electrical Machine and Power Systems*, (27), 1227-1241.

Singh, B., Verma, V. and Solanki, J. (2007). "Neural network based selective compensation of current quality problems in distribution system." *IEEE Transactions on Industrial Electronics*, (54), 1, 53-60.

Singh, B., Verma, V., Chandra, A., Al-Haddad, K. (2005). "Hybrid filters for power quality improvement." *IEE-Proceeding-Generation, Transmission and distribution*, (152), 3, 365-378.

Singh, G. K. (2007). "Power system harmonics research: a survey," *European Transactions on Electrical Power*, (19), 2,151-340.

Somasekhar, V. T. and Srinivas, S. (2004). "Switching algorithms for a dual inverter fed open-end winding induction motor drive." *Proceedings IEEE IICPE*, Mumbai, India. [CD-ROM].

Somasekhar, V. T., Baiju, M. R., and Gopakumar, K. (2004). "Dual two level inverter scheme for an open end winding induction motor drive with a single DC power supply and improved DC bus utilization." *IEE Proceedings, Electric Power Applications*, (151), 2, 230-238.

Somasekhar, V. T., Srinivas, S., Kumar, K. K. (2008). "Effect of Zero-Vector Placement in a Dual-Inverter Fed Open-End Winding Induction-Motor Drive With a Decoupled Space-Vector PWM Strategy." *IEEE Transaction Industrial Electronics*, (55), 6, 2497- 2505.

Somasekhar, V. T., Srinivas, S., Prakash Reddy, B., Nagarjuna Reddy, Ch. and Sivakumar, K. (2007). "Pulse width-modulated switching strategy for the dynamic balancing of zero-sequence current for a dual-inverter fed openend winding induction motor drive." *IET Electric Power Applications*, (1), 4, 591- 600.

Steeper, D. E. and Stratford, R. P. (1976). "Reactive compensation, harmonic suppression for industrial power systems using thyristor converters." *IEEE Transactions on Industrial Applications*, (12), 3, 232-254.

Steeper, D. E. and Stratford, R. P. (1976). "Reactive compensation, harmonic suppression for industrial power systems using thyristor converters." *IEEE Transactions on Industrial Applications*, (12), 3, 232-254.

Stemmler, H., and Geggenbach, P. (1993). "Configurations of high power voltage source inverter drives." *Proceedings EPE Conference*, Brighton, UK, 7–14.

Subjak, J. S. and Mcquilkin, J. S., (1990). "Harmonics-causes, effects, measurements, analysis: An update," *IEEE Transactions on Industrial Appl*ications, (26), 1034-1042.

Sun, X., Wu, W., Li, X., and Zhao, Q. (2002). "A research on photovoltaic energy controlling system with maximum power point tracking." *Proceedings of Power Conversion Conference,* 822-826.

Teulings, W. J. A., Marpinard, J. C., Capel, A. and O'Sullivan, D. (1993). "A new maximum power point tracking system." *Proceedings of 24th Annual IEEE Power Electronics Special Conference,* 833-838.

Tey, L. H., So, P. L., Chu, Y. C. (2004). "Unified power quality conditioner for improving power quality using ANN with hysteresis control." *International conference on power system-POWERCON* 2004, 1441-1446.

Theocharis, A.D., Menti, A. J., Milias-Argitis and Zacharias,T. (2005). "Modeling and simulation of a single-phase residential photovoltaic system." *Proceeding of the IEEE Russia Power Tech*, IEEE Computer Society, St. Petersburg, 1-7.

Tsengenes, G., Adamidis, G. (2011). "A multi-function grid connected PV system with three level NPC inverter and voltage oriented control." *Solar Energy*, (85), 2595–2610.

Veerachary, M., Senjyu T., and Uezato, K. (2001). "Maximum power point tracking control of IDB converter supplied PV system." *IEE Proceedings Electric Power Applications*, 494-502.

Veerachary, M., Senjyu, T., and Uezato, K. (2003). "Neural network based maximum power point tracking of coupled inductor interleaved boost converter supplied PV system using fuzzy controller." *IEEE Transactions on Industrial Electronics*, (50), 4, 749-758.

Verne, S. A., Valla, M. I., (2009). "Active power filter with predictive current control of a Diode clamped Multilevel inverter," *35th Annual Conference of IEEE Industrial Electronics*, IECON '09, 3211 – 3216.

Villalva, M.G., Gazoli, J.R. and Filho, E.R. (2009). "Modeling and circuit-based simulation of photovoltaic arrays." IEEE Transactions on Power Electronics, (25), 1198-1208.

Villanueva, E., Correa, P., Rodríguez, J. and Pacas, M. (2009). "Control of a Single-Phase Cascaded H-Bridge Multilevel Inverter for Grid-Connected Photovoltaic Systems." *IEEE Transactions on Industrial Electronics,* (56), 11, 4399-4406.

Wang, Z., Wang, Q., Yao, W., and Liu, J. (2001). "A series active power filter adopting hybrid control approach." *IEEE Transactions on Power Electronics*, (16), 3, 301-310.

Wasynczuk, O. (1983). "Dynamic behavior of a class of photovoltaic power systems." *IEEE Transactions on Power Apparatus and Systems*, (PAS-102), 9, 3031-3037.

Wasynczuk, O. (1983). "Dynamic behavior of a class of photovoltaic power systems." *IEEE Transactions on Power Application Systems*, (102), 9, 3031-3037.

Wasynczuk, O. (1989). "Modeling and dynamic performance of a line commutated photovoltaic inverter system." *IEEE Transactions on Energy Conversion*, (4), 3, 337-343.

Wilamowski B. M. and Li X. (2002). "Fuzzy system based maximum power point tracking for PV system." *Proceedings 28th Annual Conference IEEE Industrial Electronics Society,* 3280-3284.

Xiao, W. and Dunford, W. G. (2004). "A modified adaptive hill climbing MPPT method for photovoltaic power systems." *Proceedings of 35th Annual IEEE Power Electronics Special Conference,* 1957-1963.

Yuvarajan, S. and Xu, S. (2003). "Photo-voltaic power converter with a simple maximum-power-point-tracker." *Proceedings 2003 International Symposium Circuits Systems,* III-399–III-402.

Zeng, J., Yu, C., Qi, Q., Yan, Z., Ni, Y., Zhang, B. L., Chen, S. and Wu, F. F. (2004). "A novel hysteresis current control for active power filter with constant frequency." *Electric Power Systems Research,* (68), 75-82.

Zhang, L., Bai, Y. and Al-Amoudi, A. (2002). "GA-RBF neural network based maximum power point tracking for grid-connected photovoltaic systems." *Proceedings International Conference Power Electronics, Machines and Drives*, 18-23.

Zhou, G., Wu, B., Xu, D. (2004). "Direct power control of a multilevel inverter based active power filter." 2004 *IEEE International Conference on Industrial Technology* (ICIT). 498-503.

PUBLICATIONS

- **Anant Naik, Udaykumar Yaragatti**, ”A novel MPPT controlled grid connected photovoltaic system with dual functionality of active power injection and reactive power compensation in a single phase system”, Journal of Electrical Engineering, Romania, “Politechnica” publishing house, volume 12/2012-edition:2, pp-165-172.

- **Anant Naik, Udaykumar Yaragatti,** “Modelling of a Grid Connected PV systems with Perturb and Observe based Maximum Power Point Tracking”, International journal of Distributed Generation and Alternative Energy, **Taylor & Francis**, vol 28(4) 2013, pp-49-72.

- **Anant Naik, Udaykumar Yaragatti**, “Comparison of Three Popular Control Strategies Used in Shunt Active Power Filters”, **IEEE** Asia-Pacific Post Graduate Research in Microelectronics & Elecctronics (**PRIME-ASIA**) conference held at BITS PILANI Hyderabad, Dec-2012.

- **Anant Naik, Vinayak Kole, Udaykumar Yaragatti**, “Power Management of a Hybrid Fuel Cell and Photovoltaic with Ultracapacitor for Grid Connected/Isolated Operation”, **IEEE** International Conference on Power Electronics, Drives and Energy Systems (**PEDES 2012**) held at IISC- Bangalore Dec-2012

CURRICULUM VITAE

Shri Naik Anant Jaivant is a research scholar in the Department of Electrical & Electronics Engineering, National Institute of Technology Karnataka (NITK), Surathkal, Mangalore, INDIA. He graduated in B.E.(Electrical) from Goa University, Goa in the year 1994. He completed his post graduation M. Tech (Power and Energy Systems) from NITK, Surathkal in the year 2004. He is in teaching profession since year 1997. Presently he is working as Associate Professor in EEE Department of Goa Engineering College, Goa. His fields of interest are Renewable Energy, Application of Power Electronics in Renewable Energy field and Artificial Intelligence.

Address:

Shri Naik Anant Jaivant,

Associate Professor,

Department of Electrical & Electronics Engineering,

Goa College of Engineering, Farmagudi Ponda-403401, Goa INDIA.

Phone:+918322336332

Email: ajn@gec.ac.in